Spring 2012

Nano-particles induced oxidative stress in immortalized human brain endothelial cells

Xinsheng Zhang

Department: Chemistry

NANO-PARTICLES INDUCED OXIDATIVE STRESS IN IMMORTALIZED HUMAN BRAIN ENDOTHELIAL CELLS

by

XINSHENG ZHANG

A DISSERTATION

Presented to the Faculty of the Graduate School of the

MISSOURI UNIVERSITY OF SCIENCE AND TECHNOLOGY

In Partial Fulfillment of the Requirements for the Degree

DOCTOR OF PHILOSOPHY

in

CHEMISTRY

2012

Approved

Nuran Ercal, Advisor

Philip D. Whitefield

Yinfa Ma

Paul Nam

Katie Shannon

ABSTRACT

Nanoparticles are engineered structure with at least one dimension of 100 nanometers or less. These materials are increasingly being used for commercial purposes such as catalyst, semiconductor, cosmetics, microelectronic, and drug carrier. However, the toxicological impact of these materials has not yet been studied in detail, thereby limiting their use. In our present study, we use human brain endothelial cell line as a blood-brain barrier (BBB)model to investigate if two kinds of nanoparticles [1). Diesel exhaust particles (DEPs) and 2). single wall carbon nanotube (CNT)] induced oxidative stress in cell model. Our studies showed that DEPs or CNT significantly decreased the levels of intracellular glutathione (GSH) and glutathione peroxidase (GPx). Malondialdehyde (MDA) levels increased dramatically after DEPs or CNT treatment, and generation of reactive oxygen species (ROS) increased after DEPs or CNT exposure as well. In order to determine whether DEPs/CNT-induced oxidative stress in BBB cells alters BBB integrity, permeability and trans-endothelial electrical resistance (TEER) tests were performed. Cells exposed to DEPs or CNT showed significant increases in cell permeability and significant decreases in TEER compared to those of control. These results strongly suggest that DEPs or CNT induce oxidative stress in human brain endothelial cells and disrupt the integrity of the BBB. We hypothesize that nano material such as DEPs or CNT induced oxidative damage may contribute to the increase incidences of neurodegenerative diseases. Therefore, an antioxidant should be recommended in the areas with nanoparticle exposure related disease.

ACKNOWLEDGEMENTS

I would like to express my sincere gratitude to my advisor Dr. Nuran Ercal for her trust, support and guidance throughout my graduate studies at Missouri S&T. Without her help, my dissertation would never have been completed.

Secondly, I would like to thank my Ph.D. Advisory Committee Members: Dr. Philip Whitefield, Dr. Yinfa Ma, Dr. Paul Nam, and Dr. Katie Shannon for the time and help which they gave me in preparing this dissertation.

I greatly appreciated the assistance and support from my laboratory group members: Josh, Weili, Hsiu-Jen, Shakila, Tulin, Linu, Kalyan and Atrayee, all of whom gave me a lot helpful advice on my experiments. Thanks also to other graduate students, in the Chemistry Department at Missouri University of Science & Technology for their support. I would like to thank Barbara Harris for editing the manuscript.

Finally, I would also like to thank my parents, Jinxian Zhang and Yuzheng Liu, and my mother in law, Jiangsheng Li, for their long-term encouragement and support of my graduate study. I want to thank my wife, Youyou Zheng, and my son Benjamin for their support and constant encouragement. Without their love and support, I could not have completed my graduate study in the U.S.A.

TABLE OF CONTENTS

Page

ABSTRACT---------- iii

ACKNOWLEDGEMENTS---------- iv

LIST OF ILLUSTRATIONS ---------- ix

LIST OF TABLES---------- x

SECTION

1. INTRODUCTION---------- 1

1.1. REVIEW OF LITERATURE----------3

1.1.1. Introduction of Free Radicals ---------- 3

1.1.2. Oxidative Stress in the Nervous System ---------- 4

1.1.3. Blood-Brain Barrier ----------6

1.1.4. Antioxidant System ---------- 7

1.1.5. Introduction of Diesel Exhaust Particles ----------7

1.1.6. Introduction of Carbon Nanotubes ----------10

1.2. PROJECT SUMMARY---------- 15

2. DIESEL EXHAUST PARTICLES INDUCED OXIDATIVE STRESS IN HUMAN BRAIN ENDOTHELIAL CELLS----------16

2.1. EXPERIMENTAL DESIGN---------- 17

2.1.1. Thiol Levels after DEPs Treatment of HBMVEC Cells---------- 17

2.1.2. Cytotoxicity Studies---------- 17

2.1.3. Oxidative Stress Studies ---------- 17

2.1.4. Functional Endopoint Assay---------- 18

2.1.5. Mitochondrial Damage Studies ---------- 18

2.2. MATERIALS AND METHODS---------- 19

2.2.1. Materials---------- 19

2.2.2. Culture of Human Brain Microvascular Endothelial Cells ---------- 19

2.2.3. Cell Viability Assay---------- 19

2.2.4. Intracellular ROS Measurement----------20

2.2.5. Determination of Glutathione (GSH) ----------20

2.2.6. Determination of Malondialdehyde (MDA) ---------- 21

2.2.7. Glutathione Peroxidase (GPx) Activity Assay ---------- 22

2.2.8. Fluorescent Mitochondria Potential Staining----------22

2.2.9. Dextran Permeability Study ---------- 23

2.2.10. Trans-Endothelial Electric Resistance (TEER) Measurement -------- 23

2.2.11. Determination of Protein ---------- 24

2.2.12. Statistical Analysis---------- 24

2.3. RESULTS---------- 24

2.3.1. Effect of DEPs on Cell Viabili ---------- 24

2.3.2. Effect of DEPs on Intracellular ROS Levels ---------- 26

2.3.3. Effect of DEPs on Intracellular GSH and GPx Activity ----------26

2.3.4. Effect of DEPs on Lipid peroxidation Byproduct MDA ---------- 30

2.3.5. TEER and Cell Permeability Assay ---------- 30

2.3.6. Dissipation of Mitochondrial Membrane Potential ($\Delta\Psi m$)---------- 33

2.4. DISCUSSIONS---------- 35

2.5. CONCLUSION---------- 39

3. SINGLE WALL CARBON NANOTUBE INDUCED OXIDATIVE STRESS IN HUMAN BRAIN ENDOTHELIAL CELLS ---------- 40

3.1. EXPERIMENTAL DESIGN---------- 40

3.2. MATERIALS AND METHODS---------- 42

3.2.1. Materials---------- 42

3.2.2. Culture of Human Brain Microvascular Endothelial Cells ---------- 42

3.2.3. Cell Viability Assay---------- 43

3.2.4. Determination of Glutathione (GSH) ----------43

3.2.5. Determination of Malondialdehyde (MDA) ---------- 44

3.2.6. Intracellular ROS Measurement ----------45

3.2.7. Catalase (CAT) Activity Assay---------- 45

3.2.8. Permeability Study ---------- 45

3.2.9. Trans-Endothelial Electric Resistance (TEER) Measurement -------- 46

3.2.10. Determination of Protein ---------- 46

3.2.11. Statistical Analysis---------- 47

3.3. RESULTS---------- 47

3.3.1. Characterization of Single Wall Carbon Nanotubes ---------- 47

3.3.2. Effect of SWCNTs on Cell Viability ---------- 47

3.3.3. Effect of SWCNTs on Intracellular GSH and CAT Activity---------- 50

3.3.4. Effect of SWCNTs on Intracellular ROS Levels ----------50

3.3.5. Effect of SWCNTs on Lipid Peroxidation Byproduct MDA ---------- 54

3.3.6. TEER and Cell Permeability Assay ---------- 54

3.4. DISCUSSIONS---------- 58

3.5. CONCLUSION---------- 60

APPENDIX---------- 62

BIBLIOGRAPHY ---------- 96

VITA ----------104

LIST OF ILLUSTRATIONS

Figure Page

1.1. The reactions of free radicals ---------- 4

1.2. Structures of (a) SWCNT and (b) MWCNT ---------- 11

1.3. 3D structure of single wall carbon nanotubes---------- 12

2.1. Cytotoxicity of DEPs on HBMVEC cells ---------- 25

2.2. Effect of DEPs-induced intracellular ROS levels ---------- 27

2.3. Effect of DEPs on intracellular GSH levels in HBMVEC cells ---------- 28

2.4. Effects of DEPs on FITC-Dextran permeability in HBMVEC cells ---------- 31

2.5. Effects of DEPs on TEER in HBMVEC cells ---------- 32

2.6. Effects of DEPs on mitochondrial membrane damage in HBMVEC cells ---------- 34

3.1.SEM images of (a) SWCNTs and (b) MWCNTs ---------- 48

3.2. Cytotoxicity of SWCNTs on HBMVEC cells ---------- 49

3.3. Effects of SWCNTs on intracellular GSH levels in HBMVEC cells---------- 51

3.4. Effects of SWCNTs-induced CAT activity ---------- 52

3.5. Effects of SWCNTs-induced intracellular ROS levels ---------- 55

3.6. Effects of SWCNTs on FITC-Dextran permeability in HBMVEC cells ---------- 56

3.7. Effects of SWCNTs on TEER in HBMVEC cells ---------- 57

LIST OF TABLES

Table Page

2.1. Effects of DEPs on the activity of GPx and MDA levels ---------- 29

3.1. Effects of SWCNTs on intracellular MDA levels in HBMVEC cells ---------- 53

1. INTRODUCTION

The properties of nanoparticles differ from those of bulk materials of the same composition, allowing them to execute novel activities. A possible downside of these capabilities is harmful interactions with biological systems, with the potential to generate toxicity. Due to the large surface areas of nanoparticles, they are highly reactive and induce oxidative stress.

Oxidative stress is an imbalance between the production of reactive oxygen species (ROS) and a biological system's ability to readily detoxify the reactive species or easily repair the resulting damage; it also called "antioxidant system". Oxidative damage is evidenced by increases in the oxidative products of DNA, proteins, and lipids (Halliwell 2004,). These kinds of oxidative damage can be detected in all organs in humans, but the brain is considered to be more susceptible to oxidative damage. The human brain is 2% of body weight, but it consumes about 20% of the O_2 utilized by body, which is why the brain is so susceptible to oxidative damage (Dringen, 2000).

All kinds of nanoparticles are used in industry worldwide, which increase the risk of environmental exposure to nanoparticles. The single-walled carbon nanotubes (SWCNT) are one of the most attractive nanoparticles due to their unique chemical and physical properties, including small size (usually 1-10nm), large surface area, and strength (Sun, 2002).

Application of SWCNT was found in the field of biotechnology, i.e. it can be used as biosensor or drug delivery, therefore, it is necessary to carefully evaluate the toxicological studies of cell or animal models. A recent study showed that SWCNT

induced oxidative stress in rat lung epithelial cells (Sharma, 2007). Another *in vivo* study also showed that inhalable SWCNT induced oxidative stress in mice and may become one of the important environmental risk factors for allergic airway inflammatory disorders such as bronchial asthma (Inoue, 2010)

Diesel exhaust particles (DEPs) are an important source of air pollution, which has been associated with an increased incidence of cardiovascular and respiratory diseases. Incidences of neurodegenerative diseases are also increasing, as the population increases (Tansey et al., 2007) and air pollution becomes an important risk factor for these diseases. However, there have been no studies to indicate that DEPs can affect the blood-brain barrier (BBB) function, which might lead to neurodegenerative diseases. DEPs contain a large portion of the polycyclic aromatic hydrocarbons (PAHs) found in diesel exhaust. It also has small amounts of transition metal and quinonones (Li, 2003), all of which can generate ROS through redox chemistry. DEP was also found to lodge in mitochondria, causing damage to the mitochondrial function, which can also generate ROS, which finally induces oxidative stress. Several *in vitro* and *in vivo* experiments also showed that DEP induced oxidative stress by generating ROS and antioxidant can reverse this effect (Banerjee, 2009).

An approach to assessing the safety of nanomaterials is urgently required. Our purpose in this study is to analyze how diesel exhaust nanoparticles and single wall carbon nanotubes induce oxidative stress and cytotoxicity on immortalized human brain microvascular endothelial cells (HBMVEC). We are interested in using an endothelial cell model to study these nanoparticles because results of previous studies in this area are incomplete and controversial. (Schrand et al., 2007; Yang et al., 2007; Pancrazio, 2008).

These investigations indicated that the purity and functionality of SWCNT did not affect their toxicity. Another reason is that the brain is more vulnerable to oxidative stress, which might lead to many neurodegenerative diseases, such as Parkinson's and Alzheimer's. Because the HBMVEC cells can mimic the blood-brain barrier, it is a good cell model to study central nervous system (CNS) related diseases. In summary, it has been demonstrated that SWCNTs and DEPs are both toxic and induced oxidative stress in HBMVEC cell.

1.1. REVIEW OF LITERATURE

1.1.1. Introduction of Free Radicals. Free radicals are any species capable of independent existence that contain one or more unpaired electrons (Halliwell et al., 2007). The presence of one or more unpaired electrons usually causes free radicals to be slightly attracted to a magnetic field, which makes them highly reactive. These reactive molecules with unpaired electrons can generate highly reactive oxygen species (ROS). ROS and other free radicals are essential for life, because they are important in cell signaling and they are used by phagocytes to fight against bacteria. Highly reactive radicals can oxidize DNA, lipids, and proteins in the human body, causing cell membrane damage, protein modification, DNA damage, and cell death.

A major family of free radicals is the reactive oxygen species (ROS), derived metabolically from molecular oxygen via superoxide anions ($O_2^{\cdot -}$) as shown in Figure 1.1. The most common ROS include: singlet oxygen (O_2), hydroxyl radical ($\cdot OH$), superoxide anion, and hydrogen peroxide (H_2O_2). Superoxide anion radical is formed by addition of one electron to molecular oxygen and is not a very reactive species. Its chemical

reactivity depends on its site of generation in the cell as well as the possibility of being protonated to a stronger oxidant (perhydroxyl radical). On the other hand, hydrogen peroxide can be formed upon two-electron reduction of molecular oxygen or one-electron reduction of superoxide anion. Although hydrogen peroxide is little reactive, it can diffuse long distances crossing membranes and can react with transition metals by a homolytic cleavage yielding the highly reactive hydroxyl radical. Hydroxyl radical is the most powerful oxidant and unlike superoxide anion and hydrogen peroxide, it indiscriminately reacts with almost all biological compounds.

$$O_2 + e \rightarrow O_2^{\cdot -}$$

$$2H^+ + O_2^{\cdot -} + e \rightarrow H_2O_2$$

$$H_2O_2 + e \rightarrow {}^{\cdot}OH + {}^{-}OH$$

$${}^{\cdot}OH + {}^{-}OH + e \rightarrow H_2O + O_2$$

Figure 1.1. The reactions of free radicals.

1.1.2. Oxidative Stress in the Nervous System. Oxidative stress is caused by an imbalance between the production of reactive oxygen and a biological system's ability to readily detoxify the reactive intermediates or easily repair the resulting damage. All forms of life maintain a reducing environment within their cells. This reducing environment is preserved by enzymes that maintain the reduced state through a constant input of metabolic energy. Disturbances in this normal redox state can cause toxic effects

through the production of peroxides and free radicals that damage all components of the cell, including proteins, lipids, and DNA. Free radicals, such as ROS, are formed during a variety of biochemical reactions and cellular functions (such as mitochondria metabolism). The steady-state formation of pro-oxidants (free radicals) is normally balanced by a similar rate of consumption by antioxidants. Free radical formation and the effect of these toxic molecules on cell function (which can result in cell death) are collectively called "oxidative stress", which results from an imbalance between formation and neutralization of pro-oxidants. Various pathologic processes disrupt this balance by increasing the formation of free radicals in proportion to the available antioxidants (thus, oxidative stress). These free radicals are highly reactive, unstable molecules that have an unpaired electron in their outer shells. They react with (oxidize) various cellular components, including DNA, proteins, and lipids/fatty acids. These reactions between cellular components and free radicals lead to DNA damage, mitochondrial malfunction, cell membrane damage and eventually cell death.

Oxidative damage to lipids: Unsaturated fatty acids are highly susceptible to free radical attack, and lipid peroxidation is a sensitive biomarker for oxidative stress. Lipid peroxidation is a chain reaction which provides a continuous supply of free radicals in the presence of oxygen. It initiates further peroxidation that results in the destruction of the membrane lipids and may ultimately lead to alterations in membrane permeability and function. Polyunsaturated fatty acids are attacked by free radicals to form lipid peroxides which decompose to yield toxic products such as 4-hydroxy-2,3-nonenal (4-HNE), acrolein, malondialdehyde (MDA), etc.

Oxidative damage to proteins: Protein oxidation is defined as the covalent modification of a protein induced either directly by reactive oxygen species or indirectly by reaction with secondary by-products of oxidative stress. Oxidative damage of intracellular proteins plays an important role in the biological system because those damaged proteins often lose catalytic function and undergo degradation. Lose of a protein thiol group can be induced by various ROS and finally lead to oxidative stress. The side chains (amino acid residues) of the proteins can also be attacked by free radicals. The reaction of the oxidation of aliphatic side chains is primarily hydrogen abstraction, and the production of peroxides, alcohols, and carbonyls (Dean et al, 1997). Therefore, the protein carbonyl group test is an important biomarker for protein oxidation.

Oxidative damage to DNA: ROS can also damage DNA. A hydroxyl free radical modifies ribose phosphates, pyrimidine nucleosides, and nucleotides and is reactive with the sugar phosphate backbone of DNA to break strands. Hydroxylation of deoxy-guanosine residue produces 8-hydroxydeoxyguanosine, which can be used as a marker of oxidative DNA damage.

1.1.3. Blood-Brain Barrier. The brain microvascular endothelial cells, situated at the interface of the blood and the brain, perform the essential functions of shielding the brain from toxic substances in the blood stream, transporting micronutrients and macronutrients, leukocyte trafficking, and osmoregulation (Banks et al., 2006; Persidsky et al., 1997). Due to the unique regulatory function of the BBB, these endothelial cells possess several modifications (tight junctions), which are important for maintaining the integrity of these membranes. Loss of BBB integrity has been reported to be critical in the development and progression of neurological diseases like Alzheimers's (Fiala et al.,

2002), human immunodeficiency virus-1 (HIV-1) encephalitis (Dallasta et al., 1999), multiple sclerosis (Bar-Or et al., 2003), stroke (Ilzecka, 1996), and traumatic brain injury (Morganti-Kossmann et al., 2002).

1.1.4. Antioxidant System. Antioxidants are molecules or compounds that act as free radical scavengers. Most antioxidants are electron donors and react with the free radicals to form innocuous end products such as water. These antioxidants bind and inactivate the free radicals. Thus, antioxidants protect against oxidative stress and prevent damage to cells. By definition, oxidative stress results when free radical formation is unbalanced in proportion to the protective antioxidants. There are many examples of antioxidants:

- Intracellular enzymes: superoxide dismutase (SOD), glutathione peroxidase
- Endogenous molecules: glutathione (GSH), sufhydryl groups, alpha lipoic acid, CoQ 10, thioredoxin
- Essential nutrients: vitamin C, vitamin E, selenium, N-acetyl cysteine (NAC)
- Dietary compounds: bioflavonoids, proanthocyanidans

All cells have intracellular antioxidants (such as superoxide dismutase and glutathione) which are very important for protecting all cells from oxidative stress at all times. Glutathione (GSH) is an essential intracellular antioxidant. GSH has been found to be low in many disease states indicating that oxidative stress and inadequate antioxidant activity "keep up" with the free radicals. Maintaining and improving GSH levels may be important in these illnesses.

1.1.5. Introduction of Diesel Exhaust Particles. Diesel engine exhaust (DEE) is a complex mixture of organic and inorganic gases (NOx, SOx, CO), and particulate

matters (PMs). Diesel exhaust particles (DEPs), a by-product of DEE, are one of the major components of airborne particulate matter in the urban environment. They are composed of carbon, heavy carbohydrates, hydrated sulfuric acid, polycyclic aromatic hydrocarbons (PAHs) and their derivatives: quinones, semi-quinones, and trace amounts of transition metals such as iron, copper, chromium, and nickel (Bai et al., 2001; Vouk et al., 1983; Hartz et al., 2008). DEPs have mean diameters of 0.2 μm or less, which render them easily respirable and capable of being deposited in the airways and the alveoli. DEPs can pass through the respiratory tract to extra pulmonary tissues and have the potential to translocate to other tissues, including the brain through the blood-brain barrier (BBB) (Oberdorster et al., 2002, 2004; Elder et al., 2006; Sugamata et al., 2006). It is believed that they can translocate to the brain via two routes, either through translocation along the olfactory nerve or by crossing of the lung-blood barrier and the BBB (Oberdorster et al., 2005; Peters et al., 2006).

Translocation to and accumulation of ultrafine particles in the brain (Oberdorster et al., 2004) are a concern owing to their potential neurotoxic consequences. Epidemiological studies have demonstrated a positive association between particulate matter and a number of diseases that affect the respiratory and cardiovascular systems, as well as the central nervous system (CNS) (Dockery et al.,1993; Pope et al., 1995; Sarnat et al., 2001; Nel et al., 1998; Diaz-Sanchez, 1997; Li et al., 1996). Even though the adverse effects of DEPs on the lungs and cardiovascular system are well-known and are linked to oxidative stress, limited information is available on the effect of DEPs on the CNS.

In the last few years, there has been a body of evidence that ultra-fine particulate matter may cause neurodegenerative diseases like stroke, Parkinson's, and Alzheimer's (Hirtz et al., 2007). Histological evidences indicate neurodegeneration in both canine and human brains exposed to high ambient PM levels. In addition, *in vivo* studies in mice have demonstrated oxidative stress, toxicity, and inflammation in brain tissue upon inhalation of particulate matter (Peters et al., 2006; Campbell et al., 2005; Elder et al., 2006; Kleinman et al., 2008; Veronesi et al., 2005; Oberdorster et al., 2004, 2005; Block et al., 2004; Hartz et al., 2008). This is further supported by *in vitro* studies that reported neurotoxic effects to specific brain cells and BBB disruption upon exposure to diesel engine exhaust particles (Block et al., 2004; Hartz et al., 2008; Long et al., 2007). In addition, free radical activity on the PM particle's surface has the potential to disrupt the tight junctions and facilitate particle translocation by damaging the BBB (Peters et al., 2006). Chemical compounds of DEPs such as quinones, polycyclic aromatic hydrocarbons, and transition metals may induce reactive oxygen species (ROS) due to their ability to disrupt electron transfer in the inner mitochondrial membrane.

Translocation and accumulation of DEPs in the brain raise concerns about serious health consequences since free radical production and oxidative stress are implicated in the pathogenesis of different neurodegenerative disorders. The need for investigation of DEPs role in CNS damage is pressing because of rapidly increasing air pollution worldwide. In lieu of studies supporting the role of DEPs in oxidative stress-induced damage, the role of DEPs in inducing oxidative stress in HBMVEC cells and disrupting the integrity and function of the BBB was evaluated.

1.1.6. Introduction of Carbon Nanotubes. Carbon nanotubes (CNTs) are nanomaterials that were first discovered by Sumio Iijima in 1991. The reason that this type of material is so-called "nanotube" is because the diameter of a nanotube is on the order of a nanometer and its length can be up to several centimeters. The special hollow cylindrical structures of CNTs gives them extraordinary mechanical, electrical, thermal, optical, and chemical properties. Potential applications of CNTs include conductive plastics, antifouling paint, gas storage, micro- and nano-electronics, ultra-capacitors, batteries with improved lifetimes and extra strong fibers, etc. CNTs can be synthesized via arc discharge, laser ablation, high pressure carbon monoxide (HiPco), and chemical vapor deposition (CVD).

There are two types of CNTs, one is single-walled carbon nanotubes (SWCNTs) and the other is multi-walled carbon nanotubes (MWNTs) (Figure 1.2.). SWCNTs can be conceptualized as a layer of graphite with the thickness of a single atom and rolled up into a seamless cylinder. The graphene sheet can be wrapped in many different ways which can be represented by chiral vector (n, m). As shown in Figure 1.3., n and m are the number of unit vectors on two directions in the honeycomb crystal lattice of the graphite sheet. When m = 0, the nanotubes are so-called "zigzag"; when n = m, the nanotubes are called "armchair"; the rest of the carbon nanotubes are called "chiral". MWNTs are usually composed of multiple layers of graphite, arranged in concentric cylinders.

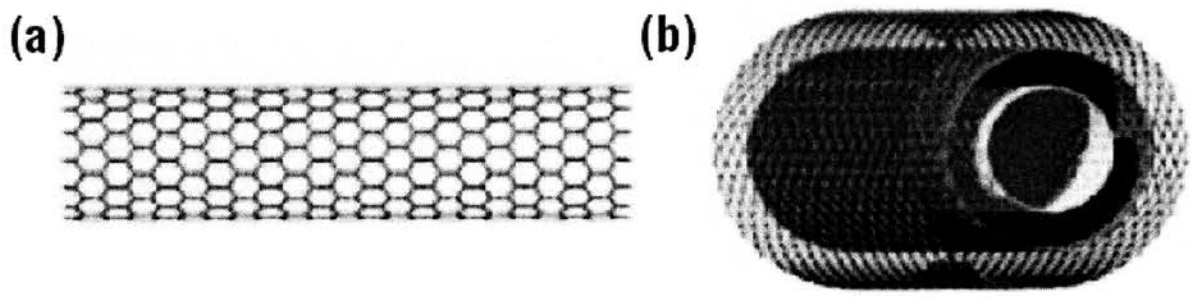

Figure 1.2. Structures of (a) SWCNT and (b) MWCNT.
(http://www.nanotechnologies.qc.ca/category/project/nanotubes)

From its first discovery in the 1990s until now, both single-walled and multi-walled carbon nanotubes have been successfully applied in many areas. SWCNTs can behave like either a semiconductor or a metal depending on their diameter and the chiral vector of the graphene sheet, while MWNTs are mainly used for their electrical conductivity which is approximately 1.85×10^3 S/cm (Ando et al. 1999). For example, Liu et al. (1999) reported using SWCNTs to store hydrogen at room temperature; Kymakis et al. (2002) demonstrated a photovoltaic device based on SWCNTs conjugated with polymeric materials; Kang et al. (2007) developed well-aligned arrays of SWCNTs as a thin film of semiconductor used for integration into transistors and some other classes of electronic devices; Feazell et al. (2007) designed an anticancer drug delivery system via conjugating a platinum (IV) complex with surface functionalized SWCNTs. Jonge et al. (2002) reported MWNTs with rigid structures can generate a high brightness electron beam; Tsai et al. (2005) made a glucose biosensor by the combination of MWNTs, a nafion cation exchanger, and glucose oxidase to form an electroanalytical nanobiocomposite film, in which MWNTs were electrochemically active and behaved as

efficient conduits for electrons; Li et al. (2009) built up UV photovoltaic cells by attaching ZnO quantum dots onto a pretreated MWCNT film surface.

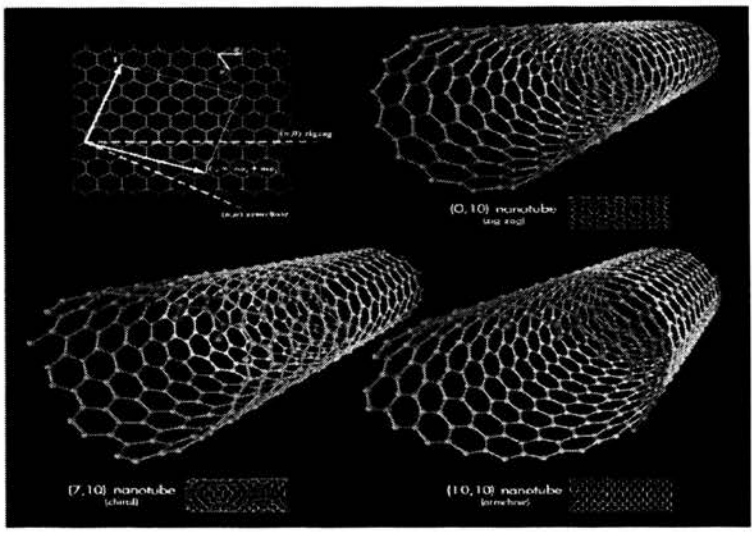

Figure 1.3. 3D structure of single wall carbon nanotubes.
(http://www.nanotechnologies.qc.ca/category/project/nanotubes)

Diagnosis and treatment of CNS disorders is extremely difficult due to the complicated environment of the CNS (Mayeux, 2003). In particular, the CNS is limited by the blood-brain barrier (BBB), which restricts the diffusion of most small molecules and almost all of the macromolecules into the CNS (de Boer and Gaillard, 2007). The BBB prevents a large amount of drugs such as antibiotics, antineoplastic agents, and CNS-active drugs from entering into the CNS (Kreuter, 2001). Current studies have suggested that nanomaterials are capable of entering the BBB following the opening of tight junctions by hyper-osmotic mannitol, which provides the possibility of delivering drugs systematically to the targeted area of the brain to treat diseases like brain tumors

and Alzheimer's disease (Singh et al., 2009; Avgoustakis et al., 2002; Beletsi et al., 1999). Owing to its unique structure and low electrical impedance at physical dimensions, CNT has become more and more popular as an ideal drug carrier applied in the CNS (Pancrazio, 2008; Malarkey and Parpura, 2007). For example, Riggio et al. (2009) built a drug delivery system by the combination of a CNT array and a thin polymer film to deliver neural growth factor. Lovat et al. (2005) reported the use of purified and nonfunctionalized MWNTs on glass that was capable of enhancing a neural signal transfer in order to support dendrite elongation and cell adhesion. Yang et al. (2010) used SWCNT to deliver acetylcholine to Alzheimer's disease brains.

Although CNTs have been considered as one of the most attractive nanomaterials, the potential toxicity of these carbon-based nanomaterials has not yet been fully understood. Jia et al. compared the cytotoxicity of SWCNTs, MWNTs, and C_{60} fullerenes on alveolar macrophages and found that SWCNTs illustrated the most cytotoxic response, while both SWCNTs and MWNTs demonstrated reduced cell viability (Jia et al. 2005). Manna et al. reported the cellular toxicity of SWCNTs on human keratinocyte cells and signaling mechanism in keratinocytes upon exposure to SWCNTs (Manna et al. 2005). Pulskamp et al. studied the toxic effects of various carbon based nanomaterials on human lung cells. They compared the adverse effects of commercial SWCNTs, MWNTs, carbon black, and quartz to that of acid-treated SWCNTs with reduced metal catalyst content. The results demonstrated that commercial CNTs may induce the generation of intracellular ROS and reduce the mitochondrial membrane potential. The purified SWCNTs presented no such effect. Therefore it was concluded that the adverse effects in

human lung cells were induced by the trace amount of metals in the commercial CNTs (Pulskamp et al. 2007).

The effect of SWCNTs on rat lung epithelial cells was analyzed by Sharma et al., who observed the generation of ROS in a dose- and time-dependent manner, the decrease of cell viability with increased concentrations of SWCNTs, the depletion of cellular glutathione levels, and the reduction of SOD-1 and SOD-2 levels (2007). Murray et al. examined the effects of unpurified and partially purified SWCNTs on murine epidermal cells (2009). They observed the production of hydroxyl radicals and a significant dose-dependent activation of AP-1 upon exposure of murine epidermal cells to unpurified SWCNTs. No significant changes in AP-1 activation were observed when introducing partially purified SWCNTs to the cells. Exposure of murine epidermal cells to both unpurified and partially purified SWCNTs resulted in a dose-dependent activation of NF-κB.

The brain microvascular endothelial cells protect the brain from toxic substances in the blood stream and are involved in transporting micronutrients and macronutrients, leukocyte trafficking, and osmoregulation (Banks et al., 2006; Persidsky et al., 1997). Due to the unique regulatory function of the BBB, these endothelial cells possess several modifications (tight junctions). Disruption of tight junction (TJ) proteins is known to play an important role in many disorders. The TJ is organized by the interactions between many transmembrane proteins, including occluding/claudin-5 and intracellular zonula occludens. Persidsky et al. showed that TJ impairment of brain microvascular endothelial cells paralleled with diminished immunostaining for occludin. Loss of BBB integrity has been reported to be critical in the development and progression of neurological diseases

like Alzheimers's (Fiala et al., 2002), human immunodeficiency virus-1 (HIV-1) encephalitis (Dallasta et al., 1999), multiple sclerosis (Bar-Or et al., 2003), stroke (Ilzecka, 1996), and traumatic brain injury (Morganti-Kossmann et al., 2002).

1.2. PROJECT SUMMARY

Induction of oxidative stress by nanoparticles have been reported *in vitro* and *in vivo*; however, most of those studies focus on lung tissue or lung epithelial cells, because that is the main tissue damage (Sharma, et al., 2007; Banerjee, et al., 2009). Recently, more and more studies show that ROS generation and oxidative damage, which induce oxidative stress (Curtin et al., 2002), are related to neurodegenerative disease.

Polyunsaturated fatty acids can be oxidized to hydroperoxides that decompose in the presence of metals to hydrocarbons and aldehydes such as MDA when exposed to ROS. This lipid peroxidation can cause severe impairment of membrane function through increased membrane permeability and membrane protein oxidation. DNA oxidation can lead to strand breakage and consequent mutation or cell death.

Glutathione (GSH) is the principal intracellular thiol responsible for scavenging ROS and maintaining the oxidative balance in tissues. Thiol supplementation to maintain cell redox balance has been studied .

The purpose in this study is to analyze how SWCNTs and DEPs induce oxidative stress and cytotoxicity on immortalized human brain microvascular endothelial cells (HBMVEC). Various experiments were designed to investigate and determine cytotoxicity and oxdative stress parameters by using BBB cell models.

2. DIESEL EXHAUST PARTICLES INDUCED OXIDATIVE STRESS IN HUMAN BRAIN ENDOTHELIAL CELLS

Diesel exhaust particles (DEPs), a prominent and persistent air pollutant, have been associated with an increased incidence of cardiovascular and respiratory diseases. However, there have been no studies to indicate that DEPs can affect the blood-brain barrier (BBB) function, which might lead to neurodegenerative diseases. DEPs contain a large portion of the polynuclear aromatic hydrocarbons (PAHs) found in diesel exhaust. In the current study, immortalized human brain endothelial cells (HBMVEC) as a BBB model was used to study whether DEPs can induce oxidative stress. Studies have shown that DEPs significantly decreased the levels of intracellular glutathione (GSH) and glutathione peroxidase (GPx). Malondialdehyde (MDA) levels increased dramatically after DEPs treatment, and generation of reactive oxygen species (ROS) increased after DEPs exposure as well. In order to determine whether DEPs-induced oxidative stress in BBB cells alters BBB integrity, permeability and trans-endothelial electrical resistance (TEER) tests were performed. Cells exposed to DEPs (50ug/ml) showed significant increases in cell permeability and significant decreases in trans-endothelial electric resistance compared to those of control. These results strongly suggest that DEPs induce oxidative stress in human brain endothelial cells and disrupt the integrity of the BBB. It was concluded that DEPs-induced oxidative damage may contribute to the increased incidences of neurodegenerative diseases. Therefore, an antioxidant should be recommended in the areas with excessive DEPs exposure.

2.1. EXPERIMENTAL DESIGN

2.1.1. Thiol Levels after DEPs Treatment of HBMVEC Cells. The purpose of these studies was to determine the levels of GSH at different concentrations of DEPs treatment of the cells. The data from these studies helped us decide whether different concentrations of DEPs changed the GSH level accordingly.

HBMVEC cells were seeded at a density of 6×10^6 per flask (25 cm^2), with 5 ml of media. After the cells had been attached, the culture flasks were divided into four groups (in triplicate). Cells were then treated with different concentration of DEPs (10μg/ml, 25 μg /ml, 50 μg /ml), and harvested at 24 hours after DEPs treatment. GSH and CYS levels were measured in the cells collected.

2.1.2. Cytotoxicity Studies. The WST-1 assay was used to conduct cytotoxicity studies. MTS tetrazolium compound was used as the reaction agent since it can react with NADH or NADPH in living cells and form a WST formazan product that can be detected at 490 nm. Because the production of formazan is proportional to the number of living cells, the intensity of the produced color could be a good indication of the viability of the cells. In other words, the higher the absorbance at 490 nm of a MTS formazan product, the higher the cell viability.

2.1.3. Oxidative Stress Studies. In these studies, cells were dosed in the presence of DEPs and then measured the cellular levels of oxidative markers such as ROS, GSH, and MDA. The activities of some antioxidant enzymes (such as glutathione peroxidase (GPx), glutathione reductase (GR) and catalase (CAT)) were also measured following treatment. The aim of this study was to determine if DEPs treatments given to the cells could induce oxidative stress.

HBMVEC cells were seeded at a density of 6×10^6 per flask (25 cm^2), with 5 ml of media. After the cells had been attached, culture flasks were divided into the following four groups (in triplicate). The control group was incubated in 5 ml of media solution without any DEPs; the other groups were incubated in 5 ml of a medium solution containing 10, 25, and 50 μg/ml DEPs, and the flasks were put into an incubator (37 °C, 5% CO_2) for 24 hours. Cell pellets were then collected by centrifuging the cell suspension in a conical tube (1000 RPM for 5 min). The following oxidative stress parameters were determined.

1. GSH levels for thiol status--principal intracellular thiol responsible for scavenging free radicals.
2. Malondialdehyde (MDA) levels to detect lipid peroxidation.
3. Activities of some antioxidant enzymes: catalase (CAT), glutathione peroxidase (GPx).

2.1.4. Functional Endpoint Assay. Dextran permeability and trans-endothelial electrical resistance (TEER) were performed for both the control group and treatment groups to assess the integration of the BBB.

2.1.5. Mitochondrial Damage Studies. JC-1 mitochondrial membrane potential assay kit from Invitrogen were used to test mitochondrial damage, A BD-C6 flow cytometry was used and all cells were detected in both FL1(530nm) and FL2 (585nm) channel.

2.2. MATERIALS AND METHODS

2.2.1. Materials. DEPs were purchased from the National Institute of Standards and Technology (NIST), (Gaithersburg, MD, USA). N-(1-pyrenyl)-maleimide (NPM) was obtained from Sigma-Aldrich (St. Louis, MO). High performance liquid chromatography (HPLC) grade solvents were purchased from Fisher Scientific (Fair Lawn, NJ). All other chemicals were bought from Sigma-Aldrich (St. Louis, MO).

2.2.2. Culture of Human Brain Microvascular Endothelial Cells. As an *in vitro* BBB model, immortalized human brain microvascular endothelial cells (HBMVEC), a gift from Dr. Pierre Courard, were seeded in 25 cm^2 tissue culture flasks coated with type 1 rat tail collagen (Sigma-Aldrich, St. Louis, MO) and maintained in an EBM-2 medium in humidified 5% CO_2/95% air at 37 °C. The culture medium was changed twice a week and endothelial cells at passages 28–34 were used in this study. A serum-free and growth-factor-free medium was used in the experiments. All assays were performed in triplicate and each experiment was repeated three times. EBM-2 medium (Lonza, Walkersville, MD) was supplemented with VEGF, IGF-1, EGF, basic FGF, hydrocortisone, ascorbate, gentamycin, and 2.5% fetal bovine serum (FBS), as recommended by the manufacturer; this fully supplemented medium is designated as Microvascular Endothelial Cell Medium-2 (EGM-2 MV, herein referred to as EGM-2 medium).

2.2.3. Cell Viability Assay. HBMVEC cells were treated with DEPs for 24 h, after which, the medium were discarded and WST-1 assay KIT (Clontech Laboratories, Inc. CA) was used to determine cell viability relative to the control group. Briefly, the cells were seeded in a 96-well tissue culture plate, at a density of approximately 5000

cells/well, for a day. The media were then discarded, and the cells were treated with DEPs (10, 25, 50μg/ml) in serum-free media for 24 h, then cells were washed three times with PBS, and 10 μl of WST-1 were added to each well for 30 min at 37 °C. The absorbance was measured at 450 nm, using a microplate reader (FLUOstar, BMG Labtechnologies, Durham, NC, USA).

2.2.4. Intracellular ROS Measurement. Intracellular ROS generation was measured using a well-characterized probe, 2',7'-dichlorofluorescin diacetate (DCFH-DA) (Wang and Joseph, 1999). DCFH-DA was hydrolyzed by esterases to dichlorofluorescin (DCFH), which was trapped within the cell. This nonfluorescent molecule was then oxidized to fluorescent dichlorofluorescin (DCF) by the action of cellular oxidants. A DCFH-DA stock solution (in methanol) of 10 mM was diluted 500-fold in HBSS without serum or other additive to yield a 20 μM working solution. Cells were washed twice with HBSS and then incubated with a DCFH-DA working solution for 1 h in a dark environment (37 °C incubator). Varying concentrations of DEPs (10, 25, 50 μg/ml) were used to treat cells for 24 h and then fluorescence was determined at 485 nm excitation and 520 nm emission, using a microplate reader (FLUOstar, BMG Labtechnologies, Durham, NC, USA).

2.2.5. Determination of Glutathione (GSH). Intracellular endothelial cell GSH content was determined by reverse phase HPLC, according to the method developed in our laboratory (Ridnour et al., 1999). HBMVEC cell samples were homogenized in serine borate buffer (SBB). Twenty microliters of this homogenate were added to 230 μl of HPLC grade water and 750 μl of NPM (1 mM in acetonitrile). The resulting solutions were incubated at room temperature for 5 min. The reaction was stopped by adding 5 μl

of 2 N HCl. The samples were then filtered through a 0.45 μm filter (Advantec MFS, Inc. Dulin, CA, USA) and injected onto the HPLC system. An aliquot of 5 μl of the sample was injected for analysis using a Thermo Finnigan TM Spectra SYSTEM SCM1000 Vacuum Membrane Degasser, Finnigan TM SpectraSYSTEM P2000 Gradient Pump, Finnigan TM SpectraSYSTEM AS3000 Autosampler, and Finnigan^{TM} SpectraSYSTEM FL3000 Fluorescence Detector (λex=330 nm and λem=376 nm). The HPLC column was a Reliasil ODS-1 C_{18} column (Column Engineering, Ontario, CA, USA). The mobile phase was 70% acetonitrile and 30% water and was adjusted to a pH of 2.5 through the addition of 1 ml/L of both acetic and o-phosphoric acids. The N-(1-pyrenyl)-maleimide derivatives were eluted from the column isocratically at a flow rate of 1 ml/min.

2.2.6. Determination of Malondialdehyde (MDA). MDA content was determined as described by Draper et al. (1993). Briefly, the cell pellets were homogenized in serine borate buffer (SBB). To 0.350 ml of cell homogenate, 0.550 ml of 5% trichloroacetic acid (TCA) and 0.100 ml of 500 ppm butylated hydroxytoluene (BHT) in methanol were added. The samples were then heated in a boiling water bath for 30 min. After cooling on ice, the samples were centrifuged. The supernatant fractions were mixed 1:1 with saturated thiobarbituric acid (TBA). The samples were again heated in a boiling water bath for 30 min. After cooling on ice, 0.50 ml of each sample was extracted with 1 ml of n-butanol and centrifuged to facilitate the separation phases. The resulting organic layers were first filtered through a 0.45 μm filter and then analyzed using the Shimadzu HPLC system with a fluorescence detector. Excitation wavelength and emission wavelength were set at 515 nm and 550 nm, respectively. The column was 100×4.6 mm i.d. C_{18} column (3 μm packing material, Astec, Bellefonte, PA). Twenty

microliter samples were injected for analysis. The mobile phase consisted of 69.4% 50 mM sodium phosphate buffer (pH 7.0), 30% acetonitrile, and 0.6% THF. The flow rate of the mobile phase was 1.0 ml/min. The concentrations of the TBA-MDA complex in the mixture were determined by using the calibration curve obtained from a malondialdehyde bis(dimethyl acetal) standard solution.

2.2.7. Glutathione Peroxidase (GPx) Activity Assay. GPx protects mammals against oxidative damage by catalyzing the reduction of a variety of ROOH, or H_2O_2, using GSH as the reducing substance. The GPx 340™ assay (a test kit from OxisResearch) was used as an indirect measure of the activity of GPx. Oxidized glutathione (GSSG), produced upon reduction of organic peroxide by GPx, is recycled to its reduced state by the enzyme glutathione reductase (GR). The oxidation of NADPH to $NADP^+$ is accompanied by a decrease in absorbance at 340 nm (A340), providing a spectrophotometric means for monitoring GPx enzyme activity. The molar extinction coefficient for NADPH is 6220 $M^{-1}cm^{-1}$ at 340 nm. To measure the activity of GPx, tissue homogenate was added to a solution containing glutathione, glutathione reductase, and NADPH. The enzyme reaction was initiated by adding the substrate, tert-butyl hydroperoxide, and the absorbance was recorded at A340. The rate of decrease in the A340 is directly proportional to the GPx activity in the sample.

2.2.8. Fluorescent Mitochondria Potential Staining. HBMVEC cells were plated in 6-well plates at initial densities of 10^4 in 1ml medium and were incubated for 72 h before addition of DEPs. Fresh medium containing different concentration of DEPs were added to each well and the cells were incubated for 24 h. All cell–material combinations were set up in triplicate. At the end of the incubation, JC-1 stain (100 μL;

Molecuar Probes/Invitrogen) at twofold working concentration was added to each well and incubated for 20 min at 37 °C. Cells were rinsed, mounted in fresh PBS, and analyzed by BD-C6 fluorescence microscopy. A stock solution of JC-1 was prepared in dimethyl sulfoxide (DMSO) at 2.5 mg mL^{-1} and kept at −20 °C. The working concentration of JC-1 for HCMVEC cells was 3 μg mL^{-1}.

2.2.9. Dextran Permeability Study. HBMVEC cells were seeded onto collagen-coated inserts with a pore size of 0.4 μm at densities of 1.5×10^4/well, and allowed to culture until a monolayer formed. The cell monolayer was then treated with varying concentrations of DEPs (10 μg/ml, 25 μg/ml, and 50 μg/ml) for 24 h. After this, the medium was replaced with 150 μl of FITC labeled dextran, and the insert was transferred to a fresh plate well, containing 500 μl of serum-free medium. The plates were incubated for 30 min at room temperature, and 100 μl of the plate well solution were removed and transferred to a 96-well plate. Fluorescence was read with a 485 nm excitation and 530 nm emission wavelengths using a microplate reader (FLUOstar, BMG Labtechnologies, Durham, NC, USA).

2.2.10. Trans-Endothelial Electric Resistance (TEER) Measurement. Trans-endothelial electrical resistance (TEER) measurement by EVOM voltohmmeter (World Precision Instrument, Sarasota, FL, USA) assessed the tightness of the HBMVEC monolayer. HBMVEC cells were seeded onto collagen-coated inserts with a pore size of 0.4 μm at densities of 15×10^3/well, and allowed to culture until a monolayer formed (4-7 days). The cell monolayer was then treated with 10, 25, or 50 μg/ml DEPs for 24 h. After this, the media was replaced with 150 μl of fresh medium. The insert containing the cell monolayer was then transferred to a fresh plate containing 500 μl of serum-free

medium. The TEER reading was recorded immediately and TEER values were calculated as: Resistance×0.32 cm^2 (insert surface area). Thus, resistance is proportional to the effective membrane.

2.2.11. Determination of Protein. Protein levels of the cell samples were measured by the Bradford method (Bradford, 1976). Bovine serum albumin was used as the protein standard.

2.2.12. Statistical Analysis. All reported values were represented as mean ± S.D. of triplicates. Statistical analysis was performed using the GraphPad Prism software (GraphPad, San Diego, CA). Statistical significance was calculated using unpaired two-tailed student's t test. Values of $p<0.05$ were considered significant.

2.3. RESULTS

2.3.1. Effect of DEPs on Cell Viability. A dose-dependent decrease in cell viability was observed in HBMVEC cells upon exposure to DEPs for 24 h (Fig. 2.1) which was confirmed using a WST-1 assay. Cell viability decreased by about 14% in the presence of 10 μg/ml of DEPs which further decreased upon increasing the DEPs concentration to 25 μg/ml. However, no significant increase in cell death was observed upon the further increase in concentration of DEPs to 50 μg/ml.

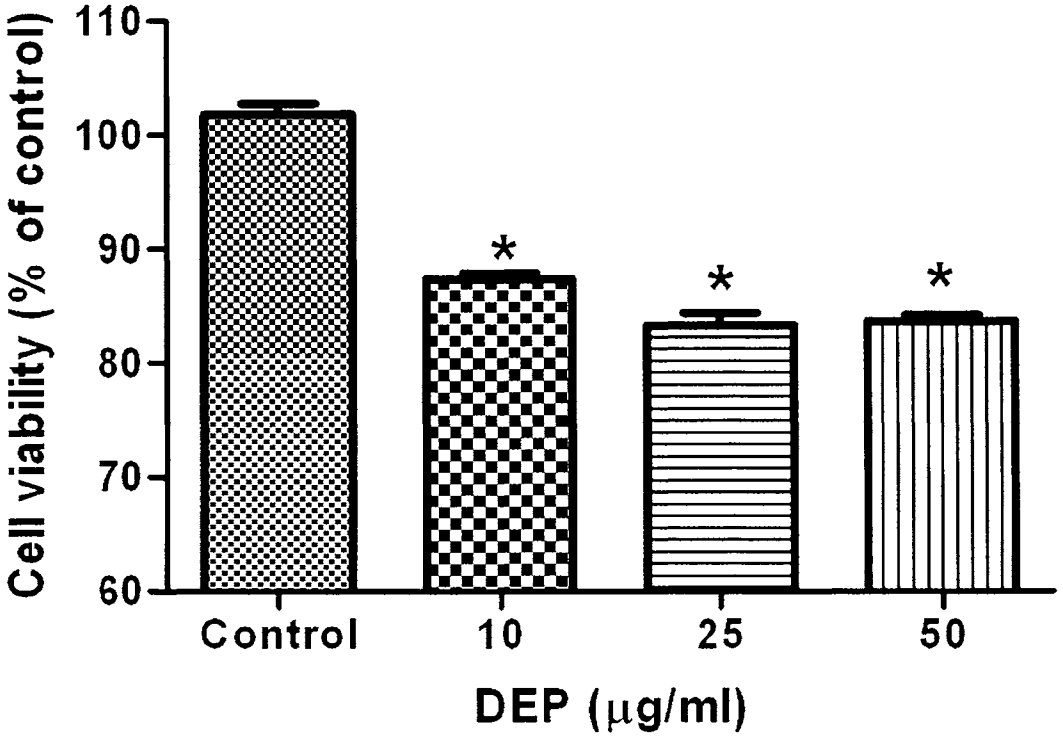

Fig. 2.1. Cytotoxicity of DEPs on HBMVEC cells. Cells were treated with various concentrations of DEPs (10, 25, and 50 μg/ml). After 24 h of treatment, the cell viability was quantified by a WST-1 assay. Values represent Mean ± SD. (*) refers to significant differences from the control with $p<0.001$. The graph is representative of three independent experiments.

2.3.2. Effect of DEPs on Intracellular ROS Levels. To substantiate the hypothesis that DEPs were causing HBMVEC cell death through oxidative stress, ROS levels were measured after the exposure of cells to DEPs for 3 h. An increase in the production of ROS in HBMVEC cells, ranging from 140% to 400%, was seen with exposure to DEPs (Fig. 2.2). These data indicated that DEPs exposure to HBMVEC cells caused a dose-dependent increase in ROS, leading to severe oxidative stress and cell death.

2.3.3. Effect of DEPs on Intracellular GSH and GPx Activity. To further elucidate the mechanism by which DEPs induce cell death and damage, their effects on GSH and the critical antioxidant enzyme, glutathione peroxidase (GPx) was investigated. GSH is one of the major intracellular thiol antioxidants in a cell. GSH levels were measured in HBMVEC cells exposed to DEPs. DEPs decreased the GSH levels in HBMVEC cells in a dose-dependent manner (Fig. 2.3). A lower dose of DEPs at 10 μg/ml did not decrease the GSH level significantly, but treatment with 25 μg/ml and 50 μg/ml of DEPs for 24 h showed marked decreases in the GSH level (~25% and 40% decreases, respectively, as compared to that of the control). This indicated that DEPs induced oxidative stress via depletion of GSH within the cells. Since GPx activity is important in cell's defense against oxidative stress, its role was further evaluated by measuring its activity in each of the treatment and control groups. The results demonstrated that exposure to DEPs caused a dramatic decline in GPx activity (Table 2.1).

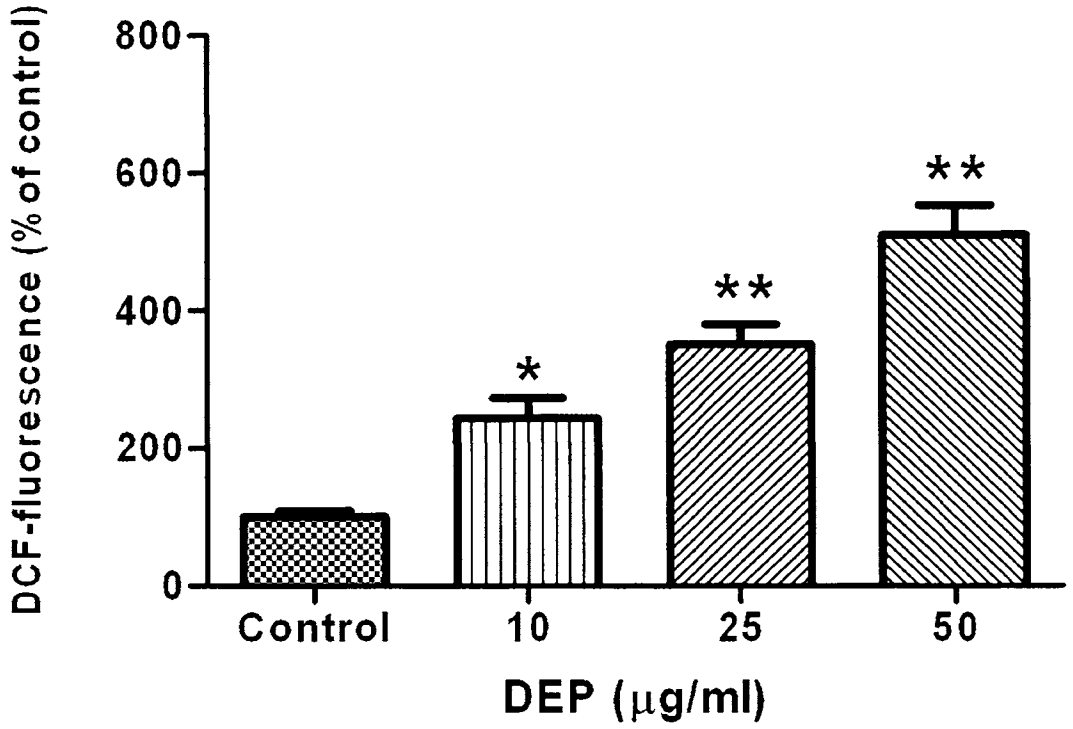

Fig. 2.2. Effect of DEPs-induced intracellular ROS levels. After treatment with various concentrations of DEPs (10, 25, and 50 μg/ml) for 24 h, the intracellular ROS levels increased, as determined by the evaluation of the DCF fluorescence. Values represent Mean ± SD. (*) and (**) refers to significant differences from the control with $p<0.001$ and $p<0.005$, respectively. The graph is representative of three independent experiments.

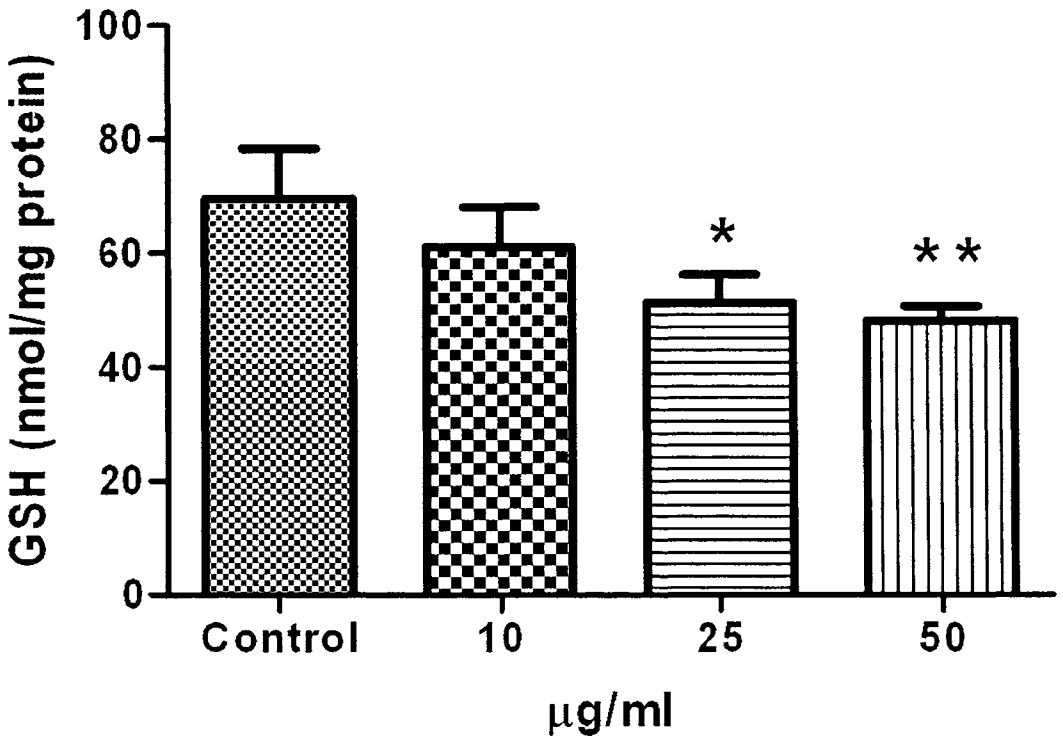

Fig. 2.3. Effect of DEPs on intracellular GSH levels in HBMVEC cells. GSH levels were measured after 24 hours of treatment with indicated concentrations of DEPs (10, 25, and 50 µg/ml). Values represent Mean ± SD. (*) and (**) refers to significant differences from the control with $p<0.01$ and $p<0.005$, respectively. The graph is representative of three independent experiments.

Table 2.1. Effects of DEPs on the activity of GPx and MDA levels.

Groups	GPx (mU/mg protein)	MDA (nmol/100 mg protein)
Control	89.6 ± 2.7	95.63 ± 5.05
10 μg/ml DEPs	76.7 ± 3.6*	109.4 ± 6.87*
25 μg/ml DEPs	72.2 ± 2.9**	154.9 ± 10.01**
50 μg/ml DEPs	61.4 ± 4.1**	192.9 ± 4.23**

'*' Significantly different from the control group at $p < 0.05$
'**' Significantly different from the control group at $p < 0.01$. All the experiments were performed in quadruplets, and the values reported are Mean ± SD.

2.3.4. Effect of DEPs on Lipid Peroxidation Byproduct MDA. MDA levels were determined in cells exposed to DEPs for 24 h. Cells treated with10 μg/ml, 25 μg/ml, and 50 μg/ml DEPs had nearly 114%, 162%, and 202% increases in MDA levels, respectively, of that of the control (Table 2.1).

2.3.5. TEER and Cell Permeability Assay. The cell permeability assay and TEER were especially important in this study because they mimic the integrity of the BBB. Permeability studies showed that exposure to DEPs increased permeability by approximately 15-40% with an increase in the concentration of DEPs from 10 μg/ml to 50 μg/ml (Fig. 2.4). To further evaluate the cellular integrity of the HBMVEC cells, trans-endothelial electrical resistance (TEER) was measured. Measurement of TEER provided information on tight junction existence and stability. Reductions in TEER reflected early cell damage. It was observed that HBMVEC exposure to DEPs significantly decreased TEER, compared to controls (Fig. 2.5). As in the permeability study, TEER results also indicated a compromised BBB. Exposure to DEPs resulted in a decrease in TEER in a concentration-dependent manner. A decrease of about 50% in the TEER value was observed in the case of exposure to 50 μg/ml of DEPs.

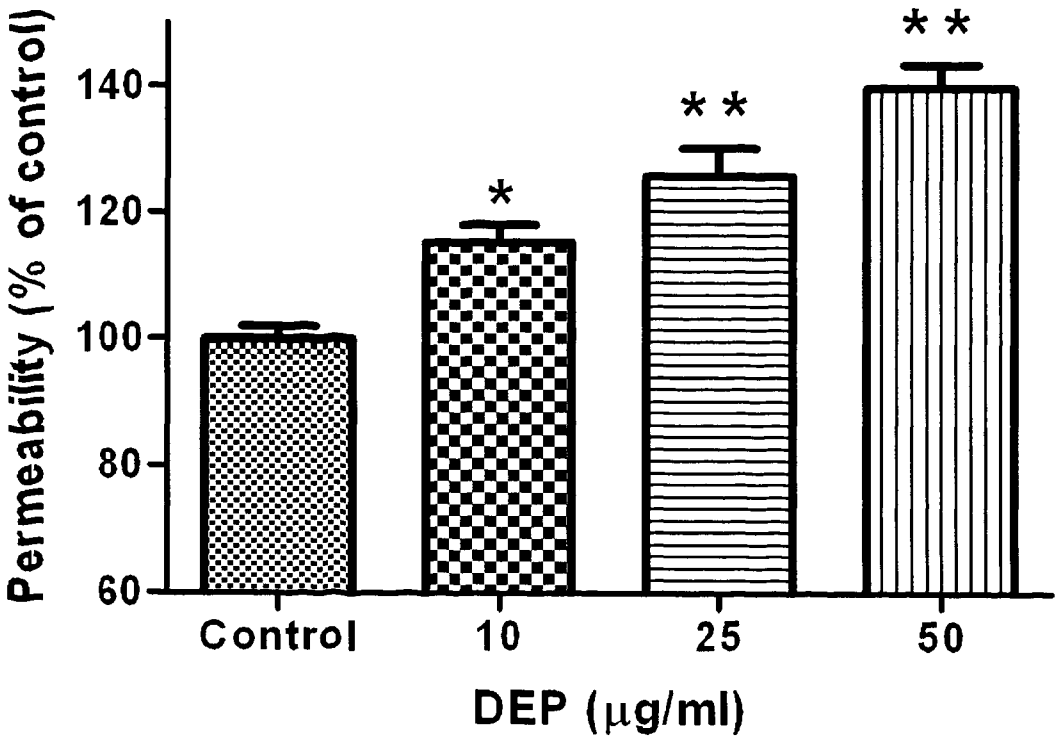

Fig. 2.4. Effects of DEPs on FITC-Dextran permeability in HBMVEC cells. HBMVEC cells were seeded onto a collagen-coated insert with a pore size of 0.4 μm at a density of 15×10^3 cells/well and allowed to grow until a monolayer was formed. The cell monolayer was then treated with indicated concentrations of DEPs for 24 h. Fluorescence was read with a 485 nm and 530 nm filter set. Values represent Mean ± SD. (*) and (**) refers to significant differences from the control with $p<0.05$ and $p<0.01$, respectively. The graph is representative of three independent experiments.

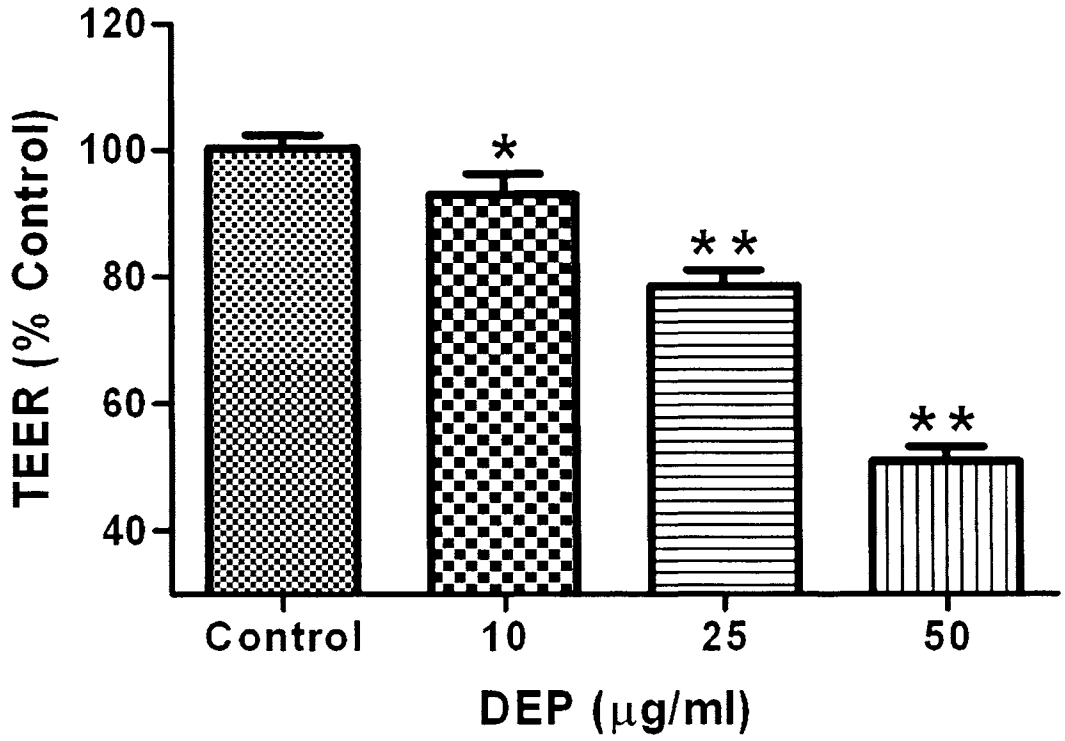

Fig. 2.5. Effects of DEPs on TEER in HBMVEC cells. HBMVEC cells were seeded onto a collagen-coated insert with a pore size of 0.4 μm at a density of 15×10^3/well, and allowed to culture until a monolayer formed. The cell monolayer was then treated with indicated concentrations of DEPs for 24 h. Cells treated with DEPs decreased TEER values as compared to the control group. Values represent Mean ± SD. (*) and (**) refers to significant differences from the control with $p<0.05$ and $p<0.01$, respectively. The graph is representative of three independent experiments.

2.3.6. Dissipation of Mitochondrial Membrane Potential ($\Delta\Psi m$). One important intracellular target of DEPs is mitochondria, which is a major source of ROS inside cells. Any disruption in mitochondrial permeability and function can be assessed by measuring the changes in mitochondrial membrane potential ($\Delta\Psi m$). The decrease in $\Delta\Psi m$ was demonstrated by using membrane permeable potentiometric dye, JC-1. JC-1 exhibits potential-dependent accumulation in mitochondria, indicated by a fluorescence emission shift from green (~529nm) to red (~590nm). Cells with mitochondrial dysfunction show primarily green fluorescence, whereas healthy cells are differentiated with red and green fluorescence. As shown in Figure 2.6 a dose-dependent increase in green fluorescence was seen in treated groups. Increases in the green fluorescence across treated groups indicated that DEPs treatment dissipated $\Delta\Psi m$ in the HBMVEC cells. These results indicate that DEPs treatment depolarizes the mitochondria membrane potential, disrupting the mitochondrial function, and resulting in cell death.

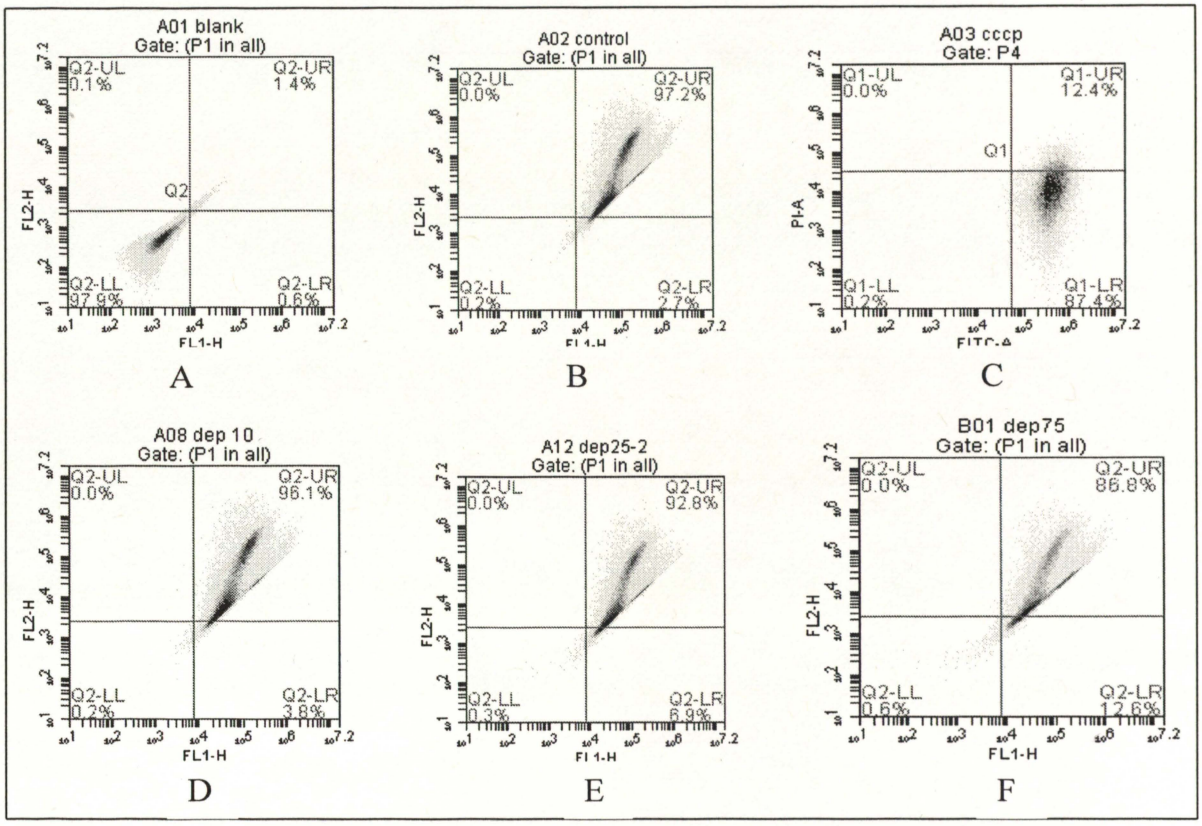

Fig. 2.6. Effects of DEPs on mitochondrial membrane damage in HBMVEC cells. (A) Blank, (B) Control, (C) Positive Control, (D) 10μg/ml DEPs Treatment, (E) 25μg/ml DEPs Treatment, and (F) 50μg/ml DEPs Treatment. HBMVEC cells were seeded onto a collagen-coated 6 wells plate at a density of $15X10^3$/well, and allowed to culture until 85% of full. Cells were treated with various concentrations of DEPs (10μg/ml, 25μg/ml, and 50μg/ml) for 24 h. The cells were collected and then incubated with JC-1 dye (1 μg/ml) in PBS for 20 min at 37^0C. The cells were then washed and resuspended in 500μl of PBS containing 1% FBS for analysis of $\Delta\Psi m$. In this figure, 10,000 cells were analyze by gating. A dose-dependent increase in green fluorescence in lower right (LR) corner was seen in treated groups. Increases in the green fluorescence from 3.8% to 12.6% across treated groups indicated that DEPs treatment dissipated $\Delta\Psi m$ in the HBMVEC cells.

2.4. DISCUSSIONS

The brain microvascular endothelial cells, situated at the interface of the blood and the brain, perform the essential functions of shielding the brain from toxic substances in the blood stream, transporting micro and macro nutrients, leukocyte trafficking, and osmoregulation (Banks et al., 2006; Persidsky et al., 1997). These endothelial cells possess several modifications (tight junctions), which are important for maintaining the integrity of these membranes. Loss of BBB integrity has been reported to be critical in the development and progression of neurological diseases like Alzheimer's (Fiala et al., 2002), human immunodeficiency virus-1 (HIV-1) encephalitis (Dallasta et al., 1999), multiple sclerosis (Bar-Or et al., 2003), stroke (Ilzecka, 1996), and traumatic brain injury (Morganti-Kossmann et al., 2002). In conjunction with reports that DEPs can pass through the BBB and accumulate in the brain, DEPs may play a key role in neurotoxicities.

Although the role of oxidative stress in DEPs-induced toxicity is well-known, little is known about how DEPs-induced oxidative stress affects the BBB. In this study, the oxidative stress parameters were determined in the HBMVEC cells exposed to DEPs, and measured GSH, lipid peroxidation byproduct (MDA), levels of ROS formation, and the activity of the antioxidant enzyme GPx. The role of DEPs in inducing oxidative stress and disrupting the permeability of the BBB *in vitro* was also investigated.

Mitocondrial damage is a key event in DEPs-induced cytotoxicity. The initial response to DEPs is a decrease in mitochondrial membrane potential and increased free radical production, followed by cytochrome c release and inner membrane damage, which include the initiation of apoptosis and decreased ATP production. Results showed

that a higher concentration of DEPs decreased the membrane potential more than lower concentrations of DEPs did.

Results from this study showed that HBMVEC cells treated with DEPs experienced a significant decrease in cell viability and GSH levels, which indicated oxidative stress. Glutathione (GSH, γ-glutamyl-cysteinyl-glycine), an intracellular thiol, is one of the important factors that is critical for maintaining the integrity of the BBB (Agarwal and Shukla, 1999). Even though the mechanism by which GSH depletion leads to the dysfunction of the BBB is not known, GSH has been reported to be a direct scavenger of ROS, leading to reduction in oxidative stress (Yamamoto and Zhu, 1998). In addition, GSH depletion also leads to a loss in protein sulfhydryls, which are believed to be essential for membrane functions such as enzyme activities and transport systems (Agarwal and Shukla, 1999). Results from this study showed that HBMVEC cells treated with DEPs experienced a significant decrease in cell viability and GSH levels, indicating that the increases in oxidative stress due to decreases in GSH levels were responsible for reduced cell viability. Decreases in GSH levels in normal human bronchial epithelial cells and in the GSH/GSSG ratio in the macrophage cell line upon exposure to DEPs have been previously reported (Li et al., 2002; Xiao et al., 2003). A possible explanation for the decrease in GSH levels is the reduced activity of the enzymes involved in GSH synthesis and/or oxidation of GSH to GSSG under oxidative stress. In conditions of severe oxidative stress, the cells' ability to reduce GSSG to GSH is overcome, leading to GSSG accumulation within the cytosol. To prevent a shift in a cell's redox equilibrium, GSSG is actively exported out of the cell or reacted with the protein sulfhydryl group, producing mixed disulfide. Under such circumstances, GSH is not regenerated; thus,

depletion of cellular GSH indicates that the cells are undergoing oxidative stress (DeLeve and Kaplowitz, 1991). GSH functions as a direct scavenger of ROS and as a cofactor in its metabolic detoxification; therefore, a decrease in GSH is suggestive of oxidative stress (Foga et al.,1997).

Further, depletion of intracellular GSH has been reported to increase production of ROS in cells (Penugonda et al., 2005). To investigate this, ROS levels were measured using a peroxide-sensitive dye, DCF. DEPs-treated cells were found to have significant increases in ROS accumulation, as compared to that of the controls. Increases in ROS levels have been observed in previous studies (Hartz et al., 2008; Block et al., 2004; Li et al., 2002) upon DEPs exposure. This indicates that low levels of GSH may render individuals susceptible to the deleterious effects of exposure to inhaled toxicants and may also perpetuate inflammatory responses.

An important target of oxidative damage is brain microvessel endothelial cells because they are rich in polyunsaturated fatty acids (Tayarani et al., 1987). The double bonds in these fatty acids undergo lipid peroxidation in the presence of free radicals and form stable by-products, such as malondialdehyde (MDA), which are used as markers of lipid peroxidation (Belghmi et al., 1988; Janero, 1990). HBMVEC cells that were exposed to DEPs had increased levels of MDA, compared to those of the controls, indicating increased lipid peroxidation in the BBB cells. Lipid peroxidation is one of the key mechanisms by which ROS induce cell death. It has been postulated that radicals attack membrane lipids and initiate a chain of events leading to lipid peroxidation (Thornalley et al., 1983; Comporti 1987; Masaki et al., 1989). Concomitant reduction of GSH levels (a substrate for glutathione peroxidase) might have hampered the

decomposition of lipid peroxides in DEPs-treated cells, thus increasing the MDA levels. Lipid peroxidation is deleterious as it impacts the cellular functions negatively, resulting in cell death, thereby lowering cell viability. ROS damage the cell membranes through lipid peroxidation and the production of lipid aldehydes such as MDA and 4-hydroxynonenal. An increased level of MDA is not only a marker of oxidative stress but also an indicator of elevated toxicity.

Antioxidant enzymes are involved in the detoxification of lethal peroxides inside the cells. A significant reduction in the activity of GPx, observed after DEPs exposure, may have been partially due to diminished GSH levels that GPx needs as a substrate. Decreased GPx activity, due to METH, in human brain microvascular endothelial cell culture was reported in a previous study (Zhang et al., 2009). Decreased activity of GPx noted in DEPs-treated cells observed in this study indicates that the cells were overwhelmed by ROS and that GPx levels were inadequate to combat ROS-mediated damage. A significant increase in MDA levels also supports this hypothesis. If an increase in antioxidant enzyme activities was observed, MDA levels would not increase. In other words, enzymes would scavenge ROS before they could attack macromolecules, including DNA, proteins, and lipids.

Under physiological conditions, the integrity of the BBB is protected from oxidative stress because the BBB has high levels of antioxidant enzymes (Plateel et al., 1995). Oxidative stress is one of the important mechanisms responsible for the disruption of the BBB. This disruption allows the passage of toxic substances into the brain, leading to development and progression of various neurological diseases (Dallasta et al.,1999; Fiala et al., 2002; Bar-Or et al., 2003). It was, therefore, crucial to determine if DEPs

altered the BBB permeability. DEPs induced a decrease in TEER, verifying its ability to disrupt cellular homeostasis and BBB integrity under severe oxidative stress conditions. Increased permeability of HBMVEC cells in this study is also supported by a similar increase in the case of human aortic endothelial cells (HAEC) upon exposure to similar concentrations of DEPs (Li et al., 2010). Decreased TEER values are also in accordance with those reported by Lehmann et al. (2009). All of these results collectively indicate that DEPs induced oxidative stress in HBMVEC cells and altered the permeability of BBB.

2.5. CONCLUSION

Data from the present study indicate that DEPs cause oxidative stress to BBB cells, as demonstrated by decreased intracellular GSH levels, increased MDA levels and intracellular ROS production, and decreased GPx activity. In addition, DEPs treatment also altered the integrity of the BBB by increasing the permeability of the cells. Although brain endothelial cells possess high levels of antioxidant defense mechanisms, such as GSH, exposure to DEPs may render the BBB susceptible to toxic damage and change its specific functions. It is believed that the damaging effect of DEPs would be more than predicted by these data as the volatile and semivolatile fractions were absent from the resuspended DEPs. Considering the ability of DEPs to disrupt the BBB, further studies should be conducted to determine the role of DEPs in inducing neurotoxicities and also to investigate and establish their role in the onset of neurodegenerative diseases like Parkinson's and Alzheimer's, which have been linked to air pollution.

3. SINGLE WALL CARBON NANOTUBE INDUCED OXIDATIVE STRESS IN HUMAN BRAIN ENDOTHELIAL CELLS

3.1. EXPERIMENTAL DESIGN

Nanotechnology is an emerging field for research and development to produce nanomaterials applied in a broad range from electronics to engineered tissues. Among these materials, single wall carbon nanotubes (SWCNT) are considered as one of the most promising nanomaterials in the field of nanotechnology. Their special tubular structure gives them outstanding physicochemical, electrical, and mechanical properties, which make them very promising for a wide spectrum of uses. According to previous studies, nanomaterials are able to pass through the blood-brain barrier (BBB) to enter into the central nervous system (CNS). Therefore, SWCNT are a very promising drug carrier for the treatment of diseases like brain tumors and Alzheimer's disease. However, there are some potential hazardous effects that need to be evaluated before this carbon-based nanomaterial can be used in biomedicine to cure CNS diseases. For example, SWCNT can induce reactive oxygen species (ROS), cause the accumulation of peroxide products, and diminish cell viability in human epidermal keratinocytes. Therefore, immortalized human brain endothelial cells were selected to mimick BBB in this study in order to analyze the effect of the cellular toxicity and oxidative stress of single wall carbon nanotubes on BBB, while SWCNT are considered as drug delivery tools for the CNS disorders.

The purpose of this study was to analyze how SWCNT induce oxidative stress and cytotoxicity on immortalized human brain microvascular endothelial cells (HBMVEC cells). BBB cell model was used to study SWCNT because results of

previous studies in this area are incomplete and controversial. (Schrand et al., 2007; Yang et al., 2007; Pancrazio, 2008). These investigations indicated that the purity and functionality of SWCNT and MWNT do affect their toxicity. For example, Tian et al. found that refined SWCNT was much more toxic than MWNT and unrefined SWCNT in cell models (2005). While, Pulskamp et al. used purified SWCNT to compare with commercial SWCNT and MWNT, and concluded that the purified SWCNT was non-toxic while the commercial SWCNT showed a dose- and time- dependent increase in ROS and a decrease in mitochondrial membrane potential (2007). A previous study of fine and ultrafine particles revealed that both are translocated by the circulation to organs including the liver, spleen, kidneys, heart, and brain (Peters et al. 2006). Therefore, cytotoxicity and oxidative stress induced by SWCNT in the human brain endothelial cells was studied. A short SWCNT, with a diameter of 1.1 nm and a length of 1 to 3 micrometer, was chosen to be used in all experiments.

A series of experiments were performed in order to determine the oxidative stress and cellular toxicity of these two materials. These experiments measured the cytotoxicity induced by different concentrations of carbon nanotubes in human brain microvascular endothelial cells. Cell viability test, reactive oxygen species (ROS) measurements, reduced glutathione and malondialdehyde analyses, and some oxidative stress enzyme analyses including catalase and glutathione peroxidase were performed. Functional endpoint assays, like dextran permeability and trans-endothelial electrical resistance (TEER), were also performed for both the control group and treatment groups to assess the integration of the BBB.

3.2. MATERIALS AND METHODS

3.2.1. Materials. The single wall carbon nanotubes were purchased from Nanostructured & Amorphous Materials Inc. The SWCNTs possess an average outside diameter of 1.1 nm and a length of 1 to 3 μm with a specific surface area of 300 – 380 m^2/g. The purity of the SWCNTs was over 90 vol. %. The MWNTs were obtained from NanoLab Inc. and the purity of the MWNTs was greater than 95 vol. %. The MWNTs had a diameter of 30 ± 15 nm and a length ranging from 5 to 20 μm with a specific surface area of 200 – 400 m^2/g. The SWCNT were characterized via Hitachi S-570 SEM (MRC in Missouri S&T).

3.2.2. Culture of Human Brain Microvascular Endothelail Cells. Immortalized Human Brain Microvascular Endothelail Cells (HBMVEC) were used as an *in vitro* BBB model. HBMVEC (a gift from Dr. Pierre Couraud) were plated on 25 cm^2 tissue culture flasks coated with type 1 rat tail collagen (Sigma, St.Louis, MO) and maintained in EBM-2 medium in humidified 5% CO_2 95% air at 37°C. The culture medium was changed twice a week and endothelial cells at passages 28-34 were used in this study. A serum-free and growth-factor-free medium were used in the experiments. All assays were performed in triplicate and each experiment was repeated at least three times. EBM-2 medium (Lonza, Walkersville, MD), supplemented with VEGF, IGF-1, EGF, basic FGF, hydrocortisone, ascorbate, gentamycin and 2.5% fetal bovine serum (FBS) were used as recommended by the manufacturer. This fully supplemented medium was designated as microvascular Endothelial Cell Medium-2 (EGM-2 MV, herein referred to as EGM-2 medium).

Culture flasks were divided into four groups in triplicate:

1. Control group
2. 25 ug/ml SWCNT group
3. 50 ug/ml SWCNT group
4. 75 ug/ml SWCNT group

3.2.3. Cell Viability Assay. HBMVEC cells were treated with SWCNT for 24 hours, after which, the medium was discarded and WST-1 assay KIT (Clontech Laboratories, Inc. CA) was used to determine cell viability relative to the control group. Briefly, the cells were seeded in a 96-well tissue culture plate, at a density of approximately 5000 cells/well for one day. The media was then discarded, and the cells were treated with SWCNT (25, 50, 75 μg/ml) in a serum-free media for 24 hours, washed three times with PBS, and then 10 μl of WST-1 were added to each well for 30 min at 37 °C. The absorbance was measured at 450 nm, using a microplate reader (FLUOstar, BMG Labtechnologies, Durham, NC, USA).

3.2.4. Determination of Glutathione (GSH). Intracellular endothelial cell GSH content was determined by reverse phase HPLC, according to the method developed in our laboratory (Ridnour et al., 1999). HBMVEC cell samples were homogenized in serine borate buffer. Twenty microliters of this homogenate were added to 230 μl of HPLC grade water and 750 μl of NPM (1 mM in acetonitrile). The resulting solutions were incubated at room temperature for 5 min. The reaction was stopped by adding 5 μl of 2 N HCl. The samples were then filtered through a 0.45 μm filter (Advantec MFS, Inc. Dulin, CA, USA) and injected onto the HPLC system. An aliquot of 5 μl of the sample was injected for analysis using a Thermo Finnigan TM Spectra SYSTEM SCM1000

Vacuum Membrane Degasser, a Finnigan TM SpectraSYSTEM P2000 Gradient Pump, a Finnigan TM SpectraSYSTEM AS3000 Autosampler, and Finnigan^{TM} SpectraSYSTEM FL3000 Fluorescence Detector (λex=330 nm and λem=376 nm). The HPLC column was a Reliasil ODS-1 C_{18} column (Column Engineering, Ontario, CA, USA). The mobile phase was 70% acetonitrile and 30% water and was adjusted to a pH of 2.5 through the addition of 1 ml/L of both acetic and o-phosphoric acids. The N-(1-pyrenyl)-maleimide derivatives were eluted from the column isocratically at a flow rate of 1 ml/min.

3.2.5. Determination of Malondialdehyde (MDA). MDA content was determined as described by Draper et al. (1993). Briefly, the cell pellets were homogenized in SBB. A total 0.35 ml of cell homogenate, 0.55 ml of 5% trichloroacetic acid (TCA) and 0.1 ml of 500 ppm butylated hydroxytoluene (BHT) in methanol was added. The samples were heated in a boiling water bath for 30 min. After cooling on ice, the samples were centrifuged at 1000 RPM. The supernatant fractions were mixed 1:1 with saturated thiobarbituric acid (TBA). The samples were again heated in a boiling water bath for 30 min. After cooling on ice, 0.50 ml of each sample was extracted with 1 ml of n-butanol and centrifuged to facilitate the separation phases. The resulting organic layers were first filtered through a 0.45 μm filter and then analyzed using the Shimadzu HPLC system with a fluorescence detector. Excitation wavelength and emission wavelength were set at 515 nm and 550 nm, respectively. The column was 100×4.6 mm i.d. C_{18} column (3 μm packing material, Astec, Bellefonte, PA). Twenty microliter samples were injected for analysis. The mobile phase consisted of 69.4% 50 mM sodium phosphate buffer (pH 7.0), 30% acetonitrile, and 0.6% THF. The flow rate of the mobile phase is 1.0 ml/min. The concentrations of the TBA-MDA complex in the mixture were

determined by using the calibration curve obtained from a malondialdehyde bis(dimethyl acetal) standard solution.

3.2.6. Intracellular ROS Measurement. Intracellular ROS generation was measured using a well-characterized probe, 2',7'-dichlorofluorescin diacetate (DCFH-DA) (Wang and Joseph, 1999). DCFH-DA was hydrolyzed by esterase to dichlorofluorescin (DCFH), which was trapped within the cell. This nonfluorescent molecule was oxidized to fluorescent dichlorofluorescin (DCF) by the action of cellular oxidants. A DCFH-DA stock solution (in methanol) of 10 mM was diluted 500-fold in HBSS without serum or other additive to yield a 20 μM working solution. Cells were washed twice with PBS and then incubated with a DCFH-DA working solution for 1 hour in a dark environment (37 °C incubator). Varying concentrations of SWCNT (25, 50, 75 μg/ml) were used to treat cells for 24 hours and then fluorescence was determined at 485 nm excitation and 520 nm emission, using a microplate reader (FLUOstar, BMG Labtechnologies, Durham, NC, USA).

3.2.7. Catalase (CAT) Activity Assay. Catalase activity was measured according to the method described by Aebi (1984). Briefly, the activity of catalase was measured spectrophotometrically (240 nm) in the supernatant of the total tissue homogenate, following the exponential disappearance of hydrogen peroxide (H_2O_2, 10mM). The catalase activity was calculated from $A_{60s} = A_{initial}e^{-kt}$, where k, was the rate constant, $A_{initial}$, was the initial absorbance and A_{60s} is the absorbance at 60s.

3.2.8. Permeability Study. HBMVEC cells were seeded onto collagen-coated inserts with a pore size of 0.4 μm at densities of 15 x 10^3 / well, and allowed to culture until a monolayer formed. The cell monolayer was treated with different concentrations

of SWCNT for 24 hours. After this, the medium were replaced with 150 µl of FITC labeled dextran, and transfered the insert to a fresh plate well, containing 500 µl of serum-free medium. The plates were incubated for 30 min at room temperature, and 100 µl of the plate well solution was removed and transferred to a 96-well plate. Fluorescence was read with a 485 nm excitation and 530 nm emission, using a microplate reader (FLOURstar, BMG Labtechnologies, Durham, NC, USA).

3.2.9. Trans-Endothelial Electric Resistance (TEER) Measurement. Trans endothelial electrical resistance (TEER) measurement by a EVOM voltohmmeter (World Precision Instrument, Sarasota, FL, USA) assess the tightness of the HBMVEC monolayer. HBMVEC cells were seeded onto collagen-coated inserts with a pore size of 0.4 µm at densities of 15×10^3 / well, and allowed to culture until a monolayer formed (4-7 days). The cell monolayer was treated with different concentrations of SWCNT for 24 hours. After this, the media was replaced with 150 µl of fresh medium. The insert containing the cell monolayer was transferred in to a fresh plate containing 500 µl of serum-free medium. The TEER reading was recorded immediately. And TEER values were calculated as: Resistance × 0.32 cm^2 (insert surface area). Thus, the resistance was proportional to the effective membrane.

3.2.10. Determination of Protein. Protein levels were determined by the Bradford method with Coomassie Blue (Bio-Rad) (Bradford, 1976). Concentrated Coomassie Blue (Bio-Rad) was diluted 1:5 (v/v) with distilled water. Then, 2.5 ml of the diluted reagent was added to 0.05 ml of a bovine serum albumin standard solution, which contained 10 to 100 mg of a 1 mg/ml stock solution. The mixture was incubated at room temperature for 5 to 10 min and the absorbance was measured at 595 nm. The

homogenized tissue samples in serine-borate buffer were subjected to appropriate dilutions, and 0.05 ml of each sample was used for the protein assay.

3.2.11. Statistical Analysis. Data is given as the Mean ± SD. The one-way analysis of variance (ANOVA) and student t-tests were used to analyze the significance of the differences between the control and experimental groups. Values of $p < 0.05$ were considered as significant.

3.3. RESULTS

3.3.1. Characterization of Single Wall Carbon Nanotubes. SWCNTs were visualized by SEM as shown in Fig. 3.1. The material consisted of large agglomerates forming bundles or ropes, however, the single wall carbon nanotubes were clearly visible. The agglomerates were tightly bound together, even when the particle suspensions in water or a medium were sonified piror to use.

3.3.2. Effect of SWCNTs on Cell Viability. A concentration-dependent decrease in cell viability was observed in HBMVEC cells upon exposure to SWCNTs for 24 hours (Fig. 3.2), which was confirmed using a WST-1 assay. Cell viability decreased by about 7.4% in the presence of 25 μg/ml of SWCNTs which further decreased to 28.3% upon increasing the SWCNTs concentration to 100 μg/ml. However, no significant increase in cell death was observed upon the further increase in concentration of SWCNTs above 100 μg/ml.

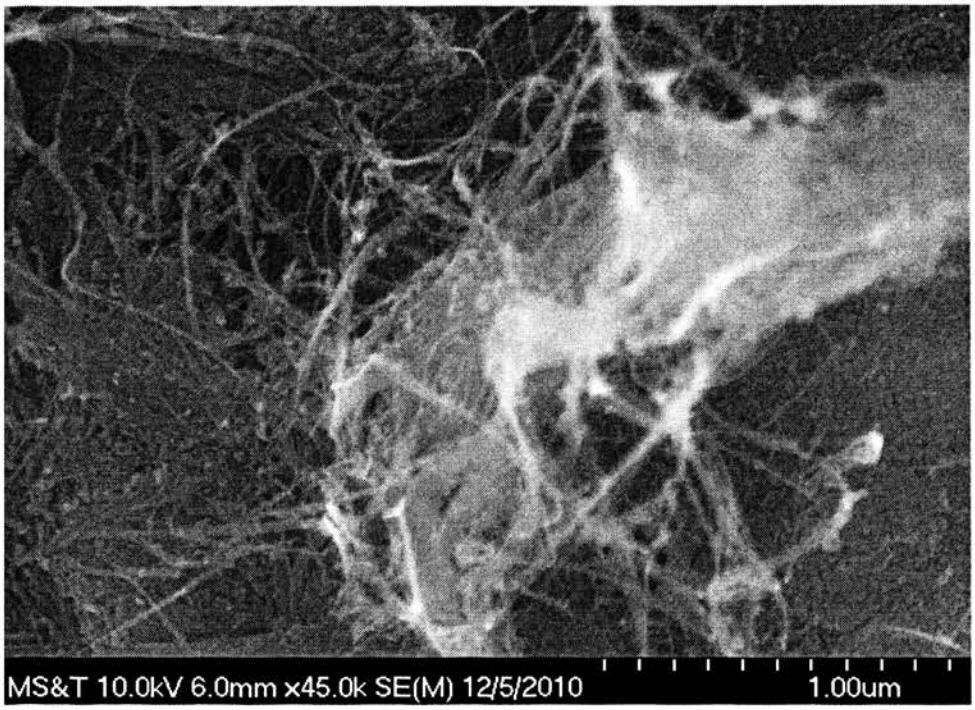

(a)

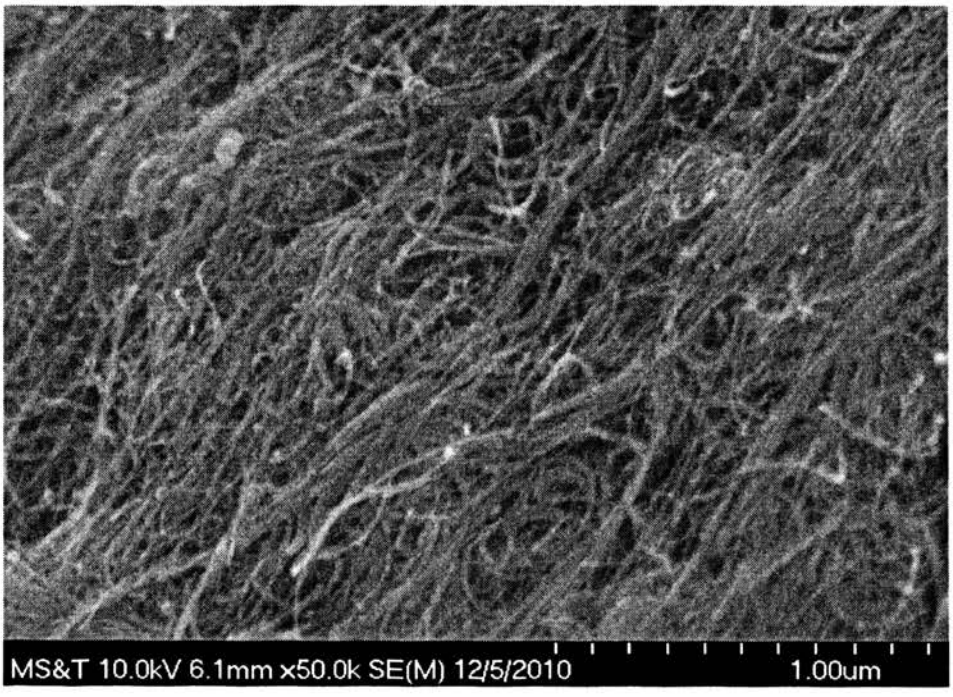

(b)

Fig. 3.1. SEM images of (a) SWCNTs and (b) MWCNTs.

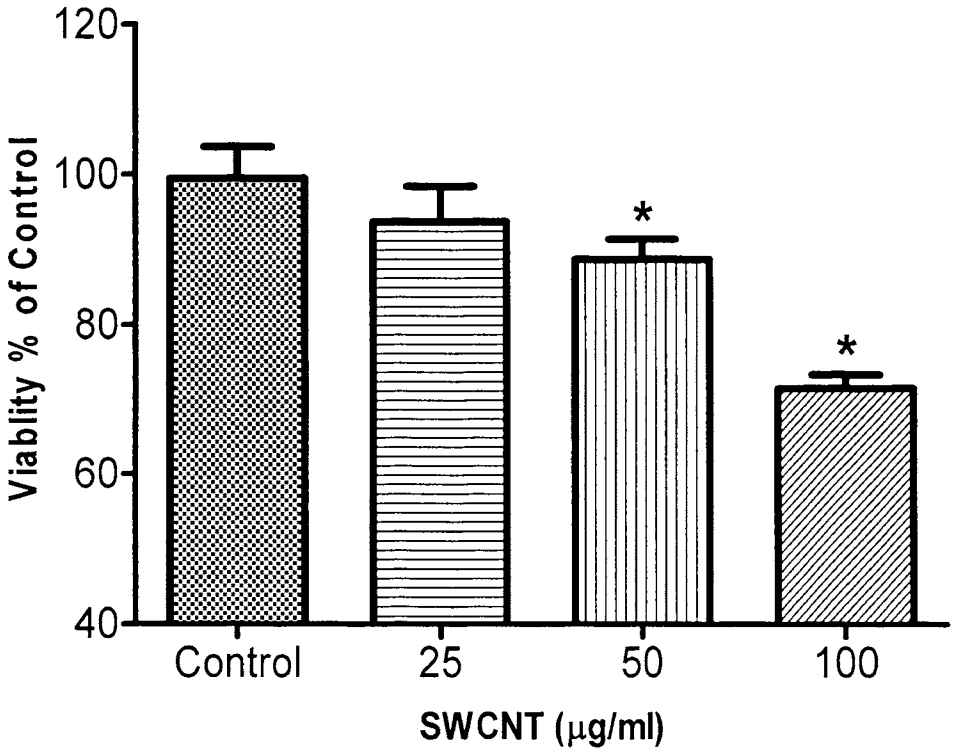

Fig. 3.2. Cytotoxicity of SWCNTs on HBMVEC cells. Cells were treated with indicated concentrations of SWCNT. After 24 hours of treatment, the cell viability was quantified by a WST-1 assay. Values represent Mean ± SD. (*) refers to significant differences from the control with $p<0.01$. The graph is representative of three independent experiments.

3.3.3. Effect of SWCNTs on Intracellular GSH and CAT Activity. To further elucidate the mechanism by which SWCNT induce cell death and damage, their effects on GSH and the critical antioxidant enzyme, catalase (CAT) were investigated. GSH is one of the major intracellular thiol antioxidants in a cell. GSH levels were measured in HBMVEC cells exposed to SWCNTs. SWCNTs decreased the GSH levels in HBMVEC cells in a dose-dependent manner (Fig. 3.3). A lower dose of SWCNTs at 10 μg/ml did not decrease the GSH level significantly, but treatment with 25 μg/ml and 50 μg/ml of SWCNT for 3 h showed marked decreases in the GSH levels (~25% and 40% decreases, respectively, as compared to that of the control). This indicated that SWCNTs induced oxidative stress via depletion of GSH within the cells. Since CAT activity is important in a cell's defense against oxidative stress, its role was further evaluated by measuring its activity in each of the treatment and control groups. The results demonstrated that exposure to SWCNT caused a dramatic decline in CAT activity (Fig. 3.4).

3.3.4. Effect of SWCNTs on Lipid Peroxidation Byproduct MDA. MDA levels were determined in cells exposed to SWCNTs for 24 hours. Cells treated with 25 μg/ml, 50 μg/ml, and 75 μg/ml SWCNTs had nearly 114%, 162%, and 202% increases in MDA levels, respectively, to that of the control (Table 3.1). Unavailability of GSH as a substrate for GPx stalls the process of lipid peroxide decomposition, thus building up the levels of MDA.

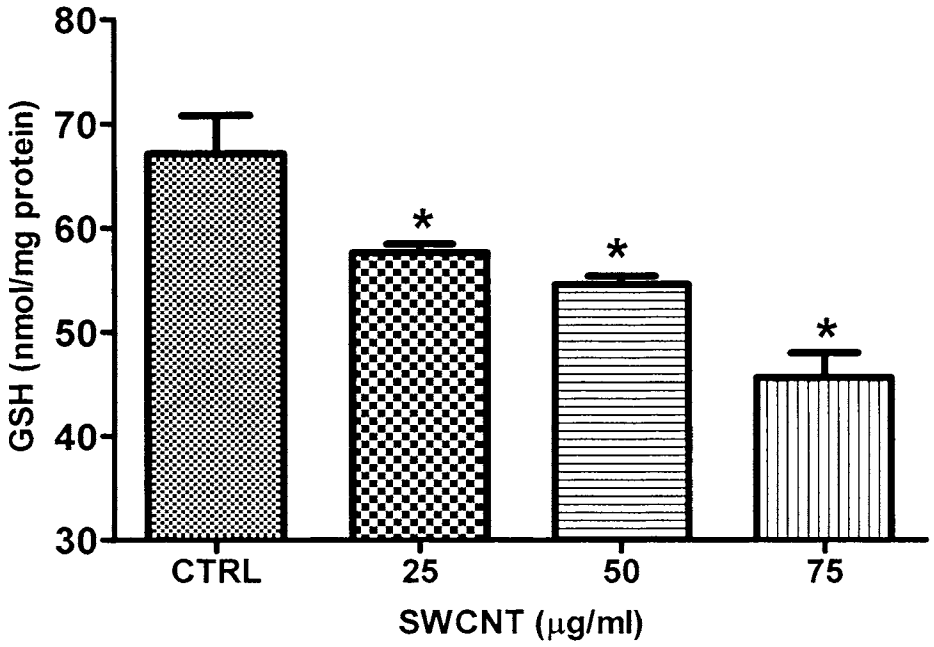

Fig. 3.3. Effects of SWCNTs on intracellular GSH levels in HBMVEC cells. GSH levels were measured by HPLC after 24 hours of treatment with various concentrations of SWCNT (25 μg/ml, 50 μg/ml and 75 μg/ml). Values represent Mean ± SD. (*) refers to significant differences from the control with $p<0.01$. The graph is representative of three independent experiments.

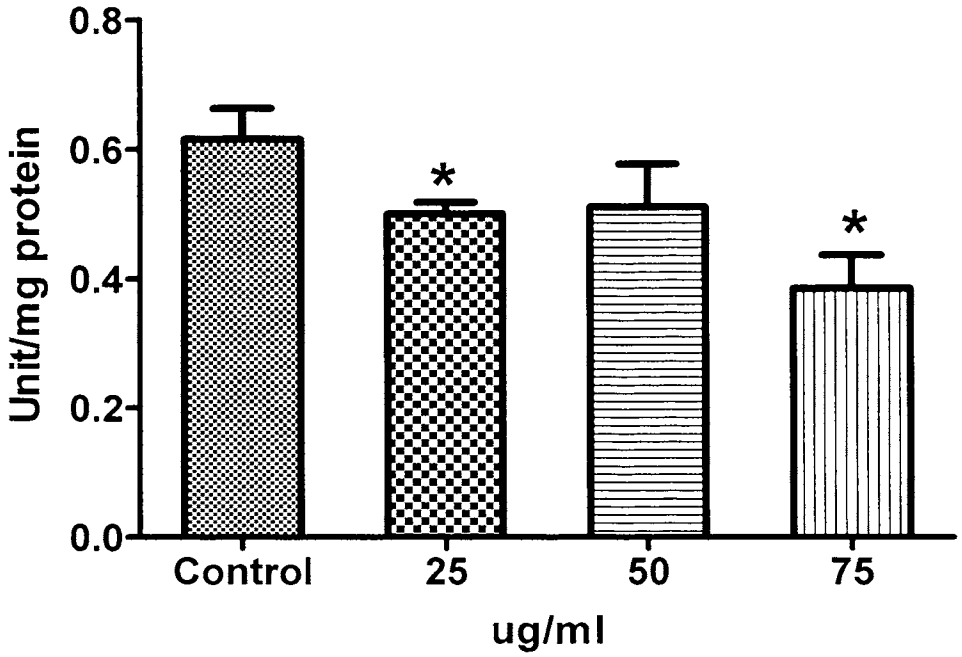

Fig. 3.4. Effects of SWCNTs-induced CAT activity. After treatment with various concentrations of SWCNT (25 μg/ml, 50 μg/ml and 75 μg/ml) for 24 hours, the CAT activity was determined. CAT levels were decreased significantly in the presence of 25 and 75 μg/ml concentrations of SWCNT. Values represent Mean ± SD. (*) refers to significant differences from the control with $p<0.01$. The graph is representative of three independent experiments.

Table 3.1 Effects of SWCNTs on intracellular MDA levels in HBMVEC cells.

Groups	**MDA (nmol/100 mg protein)**
Control	99.5 ± 6.15
25 μg/ml SWCNT	113.4 ± 6.77
50 μg/ml SWCNT	144.2 ± 10.10*
75 μg/ml SWCNT	202.1 ± 5.33**

MDA levels were measured by HPLC after 24 hours of treatment with various concentrations of SWCNTs (25, 50 and 75 μg/ml). Values represent Mean ± SD. (*) and (**) refers to significant differences from the control with $p<0.05$ and $p<0.01$, respectively. The graph is representative of three independent experiments.

3.3.5. Effect of SWCNTs on Intracellular ROS Levels. To substantiate the hypothesis that SWCNT were causing HBMVEC cell death through oxidative stress, ROS levels were measured after the exposure of cells to SWCNTs for 3 hours. An increase in the production of ROS in HBMVEC cells (ranging from 360% to 668%) was seen with an increase in the concentration of SWCNTs from 25 μg/ml to 100 μg/ml (Fig. 3.5). These data indicated that SWCNTs exposure to HBMVEC cells caused a concentration-dependent increase in ROS, leading to severe oxidative stress and cell death.

3.3.6. TEER and Cell Permeability Assay. The cell permeability assay and TEER were especially important in this study because they simulated the integrity of the BBB. Permeability studies showed that exposure to SWCNTs increased permeability by approximately 15-40% with an increase in the concentration of SWCNTs from 25 μg/ml to 75 μg/ml (Fig. 3.6). To further evaluate the cellular integrity of the HBMVEC cells, trans-epithelial electrical resistance (TEER) was measured. Measurement of TEER provided information on tight junction existence and stability. Reductions in TEER reflected early cell damage. It was observed that HBMVEC exposure to SWCNTs significantly decreased TEER, compared to controls (Fig. 3.7). As in the permeability study, TEER results also indicated a compromised BBB. Exposure to SWCNT resulted in a decrease in TEER in a concentration-dependent manner. A decrease of about 50% in the TEER value was observed in the case of exposure to 75 μg/ml of SWCNTs.

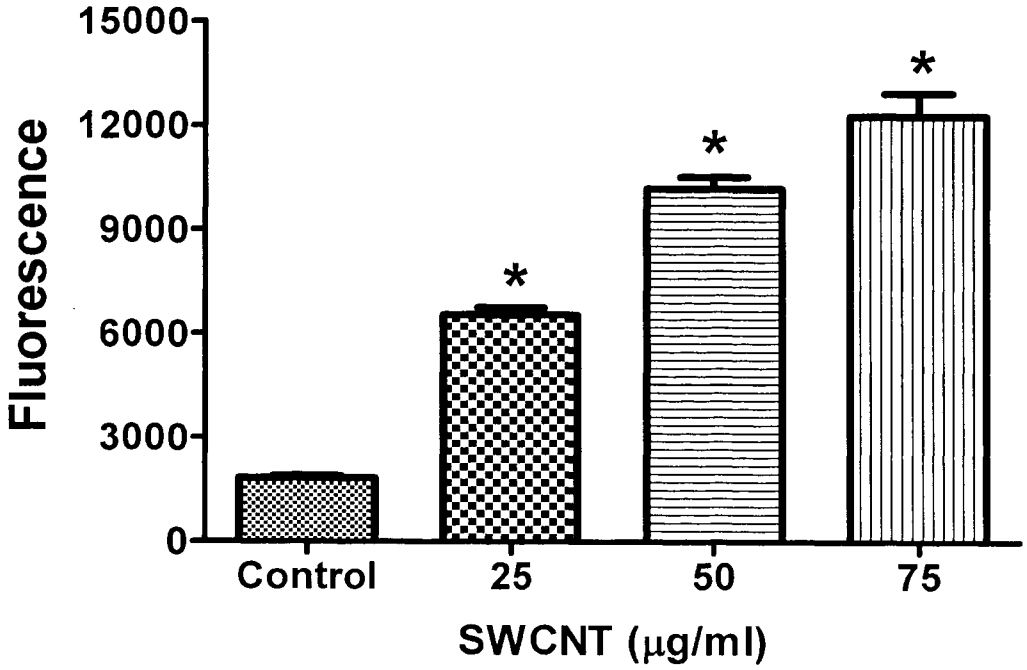

Fig. 3.5. Effects of SWCNTs-induced intracellular ROS levels. After treatment with various concentrations of SWCNTs (25 μg/ml, 50 μg/ml and 75 μg/ml) for 24 hours, the intracellular ROS levels were increased, as determined by the evaluation of the DCF fluorescence. Values represent Mean ± SD. (*) refers to significant differences from the control with $p<0.01$. The graph is representative of three independent experiments.

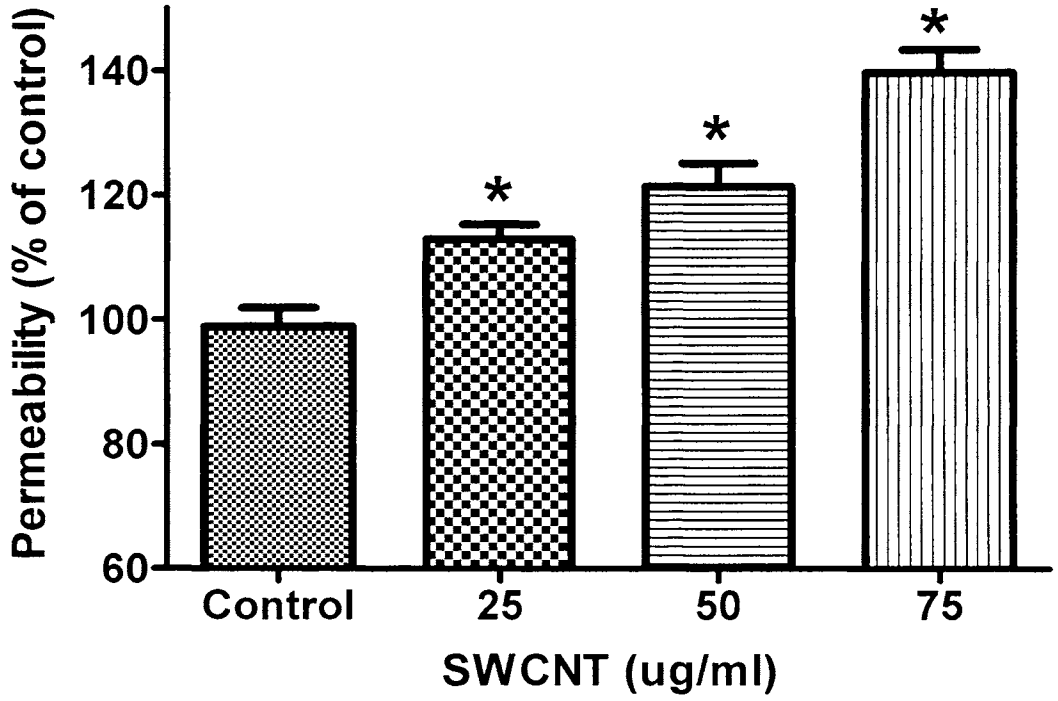

Fig. 3.6. Effects of SWCNTs on FITC-Dextran permeability in HBMVEC cells. HBMVEC cells were seeded onto a collagen-coated insert with a pore size of 0.4 μm at a density of 15×10^3 cells/well and allowed to grow until a monolayer was formed. The cell monolayer was then treated with various concentrations of SWCNTs (25 μg/ml, 50 μg/ml and 75 μg/ml) for 24 hours. Fluorescence was read with a 485 nm and 530 nm filter set. Values represent Mean ± SD. (*) refers to significant differences from the control with $p<0.01$. The graph is representative of three independent experiments.

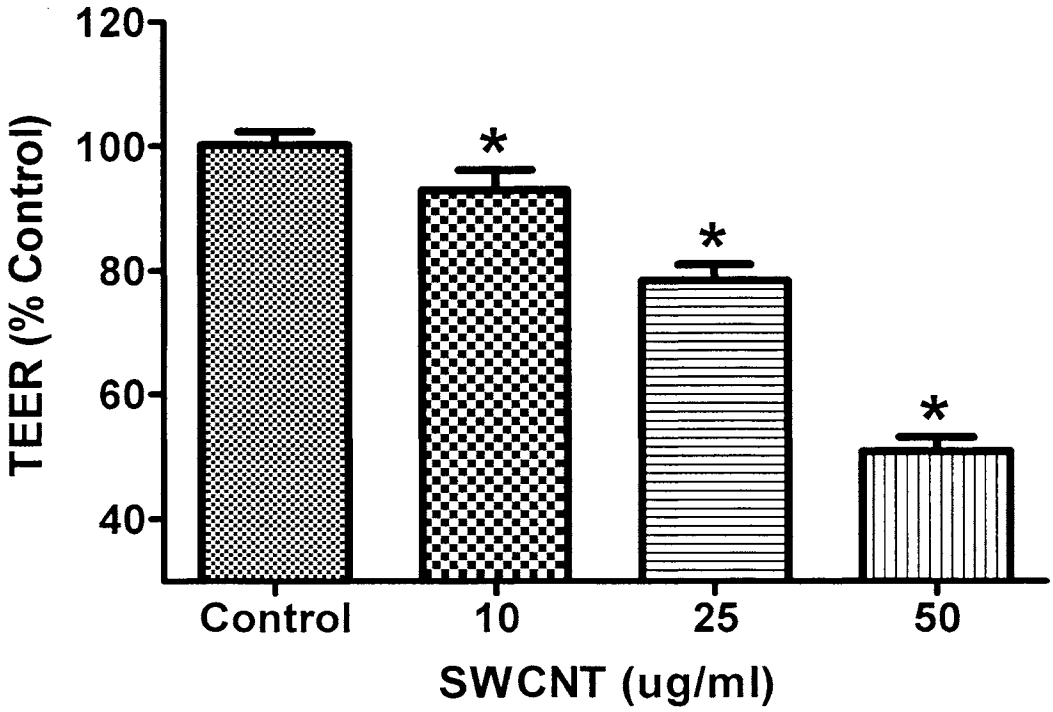

Fig. 3.7. Effects of SWCNTs on TEER in HBMVEC cells. HBMVEC cells were seeded onto a collagen-coated insert with a pore size of 0.4 μm at a density of 15×10^3/well, and allowed to culture until a monolayer formed. The cell monolayer was then treated with various concentrations of SWCNT (25 μg/ml, 50 μg/ml and 75μg/ml) for 24 hours. Cells treated with SWCNTs had decreased TEER values as compared to the control group. Values represent Mean ± SD. (*) refers to significant differences from the control with $p<0.05$. The graph is representative of three independent experiments.

3.4. DISCUSSIONS

Single wall carbon nanotubes (SWCNTs) are newly developed allotrope of carbon with extraordinary mechanical and electrical properties which offer possibilities for the development of new nano-electronics. A previous study showed single wall carbon nanotubes induced oxidative stress in rat lung epithelial cells (Sharma et.al., 2009). Translocation to and accumulation of nanoparticles in the brain (Oberdorster et al., 2004) are a concern owing to their potential neurotoxic consequences. Epidemiological studies have demonstrated a positive association between particulate matter and a number of diseases that affect the respiratory and cardiovascular systems, as well as the central nervous system (CNS) (Dockery et al.,1993; Pope et al., 1995; Sarnat et al., 2001; Nel et al., 1998; Diaz-Sanchez, 1997; Li et al., 1996). Even though the adverse effects of nanoparticle on the lungs and cardiovascular system are well-known and are linked to oxidative stress, limited information is available on the effect of SWCNT on CNS.

Manufacturing of SWCNT relies heavily on the use of catalytic metal. Transition metal, e.g. iron, cobalt, and nickel, are known to induce formation of reactive oxygen species (ROS) and subsequently cause oxidative stress.

In this study, the oxidative stress parameters were determined in the HBMEC cells exposed to different concentration of single wall carbon nanotubes and measured GSH, lipid peroxidation byproduct (MDA), levels of ROS formation, and the activity of the antioxidant enzyme catalase (CAT). The possibility of SWCNT to change the permeability of the BBB *in vitro* was also evaluated.

The BBB, composed primarily of the brain microvascular endothelial cells, forms a tight seal due to the presence of well developed tight junctions (TJ) that restrict the

entrance of circulating molecules and immune cells into the brain (Pardridge, 1997). This barrier exists between blood and brain interstitial fluid and tightly regulates the entry of compounds into the brain. The BBB helps to maintain the homeostatic environment of the brain, supplies the brain's nutritive needs, and plays a role in communication between the brain and peripheral tissues (Pardridge, 1988).

Exposure of BBB cells to SWCNT resulted in cellular oxidative stress as demonstrated by significant increases in ROS levels and decreases in cell viability and GSH levels. Depletion of reduced glutathione results in the decreased antioxidant capacity of the cell, accumulation of ROS, and ultimately apoptotic cell death. These results are in accordance with the previously reported increases in ROS and decreases in GSH levels in lung epithelial cells in response to SWCNT (Sharma, et al. 2007).

Brain microvessel endothelial cells are the main target of oxidative damage as they are rich in polyunsaturated fatty acids (PUFA). This increases the susceptibility of the BBB to lipid peroxidation. Increased MDA levels in HBMEC cells, exposed to SWCNT, further demonstrated that there was an increase in free radical formation. Concomitant reduction of GSH levels (a substrate for glutathione peroxidase) might have hampered the decomposition of lipid peroxides in SWCNT-treated cells resulting in an increase in MDA levels.

The antioxidant enzyme catalase (CAT) is involved in the detoxification of hydrogen peroxide (H_2O_2), a reactive oxygen species, which is a toxic product of both normal aerobic metabolism and pathogenic ROS production. This enzyme catalyzes the conversion of two molecules of H_2O_2 to molecular oxygen and two molecules of water. Decreases in the activity of CAT were noted in SWCNT-treated cells, as compared to

activity in controls, indicating that the cells were overwhelmed by ROS and antioxidant enzymes were somewhat inadequate to combat ROS mediated damage.

Loss of BBB integrity has been reported to be critical in the development and progression of neurological diseases like Alzheimers's (Fiala et al., 2002), human immunodeficiency virus-1 (HIV-1) encephalitis (Dallasta et al., 1999), multiple sclerosis (Bar-Or et al., 2003; Opendenakkar et al., 2003), stroke (Ilzecka et al., 1996), and traumatic brain injury (Morganti-Kossmann et al., 2002). Further, studies by Mahajan et al. and Bowyer and Ali have shown that METH causes disruption of the BBB by modulation of the tight junction expression and Rho-A activation. An increase in permeability of the BBB (as evidenced by measurements of TEER and a dextran permeability assay) in HBMVEC cells treated with SWCNT was observed. In addition, studies by Haorah et al., 2005, have shown that an increase in oxidative stress activates myosin light chain kinase, resulting in the enhanced phosphorylation of Rho protein in brain microvascular endothelial cells, leading to loss of tight junction integrity.

3.5. CONCLUSION

Studies showed that SWCNT significantly decreased the levels of intracellular glutathione (GSH) and glutathione peroxidase (GPx). Malondialdehyde (MDA) levels increased dramatically after SWCNT treatment, and generation of reactive oxygen species (ROS) increased after SWCNT exposure as well. In order to determine whether SWCNT-induced oxidative stress in BBB cells alters BBB integrity, permeability and trans-endothelial electrical resistance (TEER) tests were performed. Cells exposed to CNT showed significant increases in cell permeability and significant decreases in trans-

endothelial electrical resistance compared to those of control. These results strongly suggested that CNT induced oxidative stress in human brain endothelial cells and disrupted the integrity of the BBB. Results showed that SWCNT-induced oxidative damage may contribute to the increased incidences of neurodegenerative diseases. Therefore, a complete evaluation of nanoparticle`s toxicity is necessary before their use.

APPENDIX

N-acetylcysteine Amide Protects Against Methamphetamine-Induced Tissue Damage in CD-1 Mice

Xinsheng Zhang, (M.S.), Shakila Tobwala, (Ph.D.), Nuran Ercal, (M.D., Ph.D.)*

Department of Chemistry, Missouri University of Science and Technology, Rolla, MO 65409, USA

Running title: N-acetylcysteine amide protects against methamphetamine-induced toxicity

*Corresponding Author
Address: Department of Chemistry
Missouri University of Science and Technology
400 West 11th Street
142 Schrenk Hall
Rolla, MO 65409
Phone: 573-341-6950
Fax: 573-341-6033
Email: nercal@mst.edu

ABSTRACT

Methamphetamine (METH), a highly addictive drug used worldwide, induces oxidative stress in various animal organs, especially the brain. This study evaluated oxidative damage caused by METH to tissues in CD-1 mice and identified a therapeutic drug that could protect against METH-induced toxicity. Male CD-1 mice were pretreated with a novel thiol antioxidant, N-acetylcysteine amide (NACA), (250 mg/kg body weight) or saline. Following this, METH (10 mg/kg body weight) or saline i.p. injections were administered every 2 hours over an 8-hour period. Animals were sacrificed 24 hours after the last exposure. NACA-treated animals exposed to METH experienced significantly lower oxidative stress in their kidneys, livers, and brains than the untreated group, as indicated by their levels of glutathione (GSH), malondialdehyde (MDA), and protein carbonyl and their catalase (CAT) and glutathione peroxidase (GPx) activity. This suggests that METH induces oxidative stress in various organs and that a combination of NACA as a neuro or tissue protective agent, in conjunction with current treatment, might effectively treat METH abusers.

Keywords: *Methamphetamine, oxidative stress, antioxidant, reactive oxygen species, N-acetylcysteine amide*

1. Introduction

Methamphetamine (METH) is a potent addictive psychostimulant, being abused by approximately 35 million people worldwide.[1, 2] It has been reported that approximately 5.8% of Americans, aged 12 years or older, have used METH at least once in their lifetime.[3] A dramatic increase in METH-related emergency department visits is alarming, with >50% involving young adults aged 18–34 years.[4] The relative ease of METH's availability, coupled with its toxicity, has resulted in increased numbers of associated medical complications and fatalities.[4, 5] Chronic use and acute METH intoxication can cause substantial medical consequences, including kidney [rhabdomyolosis, myoglobinuria, acute renal failure[6-13]], liver [acute hepatic failure[14-17] centrilobular liver damage[18]], lungs [pulmonary edema, shortness of breath[19]], cardiovascular [tachycardia, atrioventricular arrhythmias, myocardial ischemia, hypertension[19-21]], cerebrovascular [hemorrhages, strokes, seizures[22-24]], and psychiatric problems [psychosis, persecutory delusions, persistent visual and auditory hallucinations, depression, anxiety, aggressiveness, social isolation, psychomotor dysfunction, [23, 25, 26] suicidal ideation [27-29]].

The adverse effects of METH on the central nervous system (CNS) are well recognized and neuropathological changes in the brains of METH abusers are associated with neuropsychiatric problems.[26] METH toxicity occurs via dopamine-dependent reactive oxygen species (ROS) production and oxidative stress.[30] The generation of ROS and nitric oxide has been implicated in METH-induced neurotoxicity.[31-35] When ROS production overwhelms the antioxidant defense mechanism, it leads to a condition known as oxidative stress. Involvement of ROS in METH toxicity is supported by several studies which reported decreased glutathione levels, reduced levels and activities of antioxidant

enzymes, and increased lipid peroxidation and protein carbonylation, all hallmarks of oxidative stress. [36-46]

Even though the adverse effects of METH on the brain are well-known and are linked to oxidative stress, little information is available about the oxidative stress induced by METH in other organs. Some studies have indicated that METH exposure induces oxidative stress in a rat's retina and adversely affects the dopaminergic system of the retina as well,[47] particularly during CNS development. Tokunaga et al.[48] studied changes in renal function and found that repeated METH administration induced oxidative DNA injury to the kidney, as a chronic or sub-acute influence.

Under physiological conditions, tissues are protected against oxidative stress by antioxidant enzymes and small antioxidant molecules, particularly glutathione (GSH). GSH, a well-known intracellular thiol antioxidant, has been shown to protect cells from various forms of oxidative injury.[49] However, since GSH cannot be transported directly into the tissue cells, the need arises for other compounds that can easily pass into cells and increase intracellular GSH levels. One such compound, known to increase intracellular GSH levels in cells, is the low molecular weight thiol antioxidant, N-acetylcysteine amide (NACA). NACA has been shown to be more effective than its parent compound, N-acetylcysteine (NAC), because the neutral carboxyl group of NACA increases its ability to permeate cell membranes and the blood-brain barrier (BBB). This allows NACA to be administered at a lower dose than NAC and prevents many side effects that are generally associated with NAC toxicity. [50-54]

New treatment challenges have arisen with the increased use of METH.[55] However, there are currently no pharmacological treatments for the wide range of symptoms

associated with METH-related problems, possibly because of the lack of understanding of METH-induced toxicity. We previously reported that METH causes oxidative stress to BBB cells and also alters the integrity of the BBB by increasing the permeability of the cells.[36] These toxic effects of METH were reversed, however, by pretreatment of the cells with NACA. This antioxidant restored the levels of GSH, and scavenged the ROS produced by treatment with METH, thereby maintaining the permeability of the BBB. Considering the ability of NACA to protect BBB cells from METH-induced oxidative stress, the effectiveness of this antioxidant was evaluated as a treatment option for multiorgan oxidative damage caused by METH abuse.

The purpose of the present study was to discover an adjunctive therapeutic drug to prevent or protect against oxidative damage to various organs in METH abusers. To accomplish this, we measured several oxidative stress parameters to determine if METH induces oxidative stress in organs other than the brain and if this damage could be prevented by the use of a novel antioxidant, NACA. Observations overall indicated that METH induced oxidative cell damage by increasing lipid peroxidation and decreasing levels of intracellular GSH and the antioxidant enzymes. The use of NACA prevented oxidative damage in the livers, kidneys, and brains of METH-treated animals.

2. Materials and methods

2.1. Materials

CD1 mice were purchased from Charles River Laboratories International, Inc. (Wilmington, MA). N-acetylcysteine amide (NACA) was purchased from Dr. Glenn Goldstein of David Pharmaceuticals in New York, NY. HPLC-grade acetonitrile, glacial acetic acid and o-phosphoric acid were obtained from Fisher Scientific (Pittsburgh, PA), while BioRad (Hercules, CA) furnished the Bradford reagent. The National Institute on Drug Abuse (NIDA) provided methamphetamine while all other chemicals were obtained from Sigma-Aldrich (St. Louis, MO), unless otherwise stated.

2.2. Animal study design

Male CD-1 mice (7 weeks old) were purchased from Charles River Laboratories International, Inc. (Wilmington, MA). Animals were housed in a controlled temperature (~22°C) and humidity (~55%) animal facility, with a 12-hour light and dark cycle. The animals had unlimited access to rodent chow and water, and were utilized after 1 day of acclimatization. All animal procedures were conducted under an animal protocol approved by the Institutional Animal Care and Use Committee of the Missouri University of Science and Technology. The mice were divided into four groups: (1) Control, (2) METH only, (3) NACA only, and (4) METH+NACA, so that each group contained four mice. All animals were injected (i.p) with either saline, for the control and METH groups, or NACA (250 mg/kg body weight) for the NACA and NACA+METH groups, 30 minutes before exposure to METH (10 mg/kg body weight). This was followed by four more injections of METH every 2 hours over an 8-hour period. This is one of the most commonly administered doses for acute high dose METH administration in rodents.[56]

This administration protocol provides an adequate model to study overdose pathologies. The dose of NACA (250 mg/kg body weight) was found to be optimum based on our previous studies with NACA where a range of NACA concentrations was used (250-500 mg/kg body weight). All rats were anesthetized 24 hours after the last METH injection by i.p. injection with a 40% urethane solution (0.1 mL / 10 g body weight). All mice were massed at the beginning and the end of the study. Following sacrifice, their organs were harvested, rinsed with PBS solution, and then immediately placed on dry ice. Samples were stored at a temperature of -80 °C for further analysis.

2.3. Experimental Design for Oxidative Stress Parameters

2.3.1. Determination of GSH levels

The levels of GSH in the tissues were determined by RP-HPLC, according to the method developed in our laboratory.[57] The HPLC system (Thermo Electron Corporation) consisted of a Finnigan Spectra System vacuum membrane degasser (model SCM1000), a gradient pump (model P2000), autosampler (model AS3000), and a fluorescence detector (model FL3000) with λex = 330 nm and λem = 376 nm. The HPLC column used was a Reliasil ODS-1 C_{18} column (5-μm packing material) with 250 mm×4.6 mm i.d. (Column Engineering, Ontario, CA). The mobile phase (70% acetonitrile and 30% water) was adjusted to a pH of 2 with acetic acid and o-phosphoric acid. The N-(1-pyrenyl)-maleimide (NPM) derivatives of GSH were eluted from the column isocratically at a flow rate of 1 ml/min. The tissue samples were homogenized in a serine borate buffer (100 mM Tris HCl, 10 mM borate, 5 mM serine, 1 mM diethylenetriaminepentaacetic acid), centrifuged, and 50 μl of the supernatant were added to 230 μl of HPLC grade water and 750 μl of NPM (1 mM in acetonitrile). The resulting solution was incubated at room

temperature for 5 minutes, and the reaction was stopped by adding 10 µl of 2 N HCl. The samples were then filtered through a 0.45-µm filter and injected into the HPLC system.

2.3.2. Determination of malondialdehyde (MDA)

The MDA levels were determined according to the method described by Draper et al.[58] Briefly, 550 µl of 5% tricholoroacetic acid (TCA) and 100 µl of 500 ppm butylated hydroxytoluene (BHT) in methanol were added to 350 µl of the tissue homogenates, and boiled for 30 minutes in a water bath. After cooling on ice, the mixtures were centrifuged, and the supernatant collected was mixed 1:1 with saturated thiobarbituric acid (TBA). The mixture was again heated in a water bath for 30 minutes, followed by cooling on ice. 500 µl of the mixture was extracted with 1 ml of nbutanol and centrifuged to facilitate the separation of phases. The resulting organic layers were first filtered through 0.45 µm filters and then injected into the HPLC system (Shimadzu, US), which consisted of a pump (model LC-6A), a Rheodyne injection valve and a fluorescence detector (model RF 535). The column was a 100 mm×4.6 mm i.d. C_{18} column (3 µmpacking material, Astec, Bellefonte, PA). The mobile phase used contained 69.4% sodium phosphate buffer, 30% acetonitrile, and 0.6% tetrahydrofuran. The fluorescent product was monitored at λex = 515 nm and λem = 550 nm. Malondialdehyde bis (dimethyl acetal), which gives malondialdehyde on acid treatment, was used as a standard. This method differs from commonly used TBARS assay in that it specifically determines TBA-MDA adducts by HPLC.

2.3.3. Catalase (CAT) activity assay

Catalase activity was measured according to the method described by Aebi.[59] Briefly, it was measured spectrophotometrically at a wavelength of 240 nm, in the supernatant of

the tissue homogenate, following the exponential disappearance of hydrogen peroxide (H_2O_2, 10 mM). The catalase activity was calculated from the equation $A_{60} = A_{initial}e^{-kt}$, where k represents the rate constant, $A_{initial}$ is the initial absorbance and A_{60} is the absorbance after 60 seconds have passed.

2.3.4. Glutathione Peroxidase Activity

Glutathione peroxidase (GPx) activity was determined using a glutathione peroxidase colorimetric assay kit purchased from Oxis Research (Foster City, CA). The tissue samples were homogenized in 50 mM of phosphate buffer (pH 7.4), containing 1 mM EDTA which were then centrifuged at 7500 ×g for 10 minutes. The resulting supernatant was collected to be used for the assay while the remaining debris was discarded. In brief, the assay buffer, supernatant, and NADPH reagent (containing glutathione reductase, GSH, and NADPH) were placed in a cuvette and the reaction initiated by the addition of t-butylhydroperoxide (tBHP). The decrease in absorbance at 340 nm was recorded for 3 minutes and the change in A_{340}/min from the initial linear portion of the curve was used to calculate the GPx enzyme activity. The GPx activity was calculated using the extinction coefficient of NADPH (6220 $M^{-1}cm^{-1}$) and expressed as units/mg of protein.

2.3.5. Determination of protein carbonyls

The amounts of protein carbonyls in each sample were determined using a modified method by Levine et al.[60] Each of the tissue samples was homogenized in a serine borate buffer (pH 7.4) and then centrifuged at 10,000 x g for 15 minutes. Next, 200 µL of supernatant containing approximately 1.5 mg of protein were added to 800 µL of 10 mM 2,4-dinitrophenylhydrazine dissolved in 2 M HCl. In parallel, 200 µL of supernatant were added to 800 µL of 2M HCl to act as a control. The resulting solutions were incubated at

room temperature in the dark for 1 hour, with vortexing every 10 minutes. Subsequently, 1 mL of 20% TCA was added to each solution, vortexed, and then placed on ice for 5 minutes. The solutions were then centrifuged for 10 minutes at 10,000 x g. The resulting pellet was washed three times with an ethanol and ethyl acetate (1:1) mixture. The samples were then left to dry for 10 minutes, after which 800 μL of 6 M guanidine solution (prepared in 20 mM potassium phosphate and adjusted to a pH of 2.3 using trifluoroacetic acid) were added. The solutions were vortexed to resuspend the proteins. The solutions were centrifuged 10,000 x g for 10 minutes and the supernatant was analyzed by spectrometry. Absorption was measured at a wavelength of 370 nm against the sample blank, and the protein carbonyl content was determined using the associated molar absorption coefficient (22,000 $M^{-1}cm^{-1}$).

2.4. Determination of protein

Protein levels of the tissue samples were measured by the Bradford method.[61] Concentrated Coomassie Blue (Bio-Rad, Hercules, CA) was diluted 1:5 (v/v) with distilled water. 20 μl of the diluted tissue homogenate were then added to 1.5 ml of this diluted dye, and absorbance was measured at 595 nm using a UV spectrophotometer (Shimadzu Scientific Instruments, Columbia, MD). Bovine serum albumin was used as the protein standard.

2.5. Statistical analysis

All reported values were represented as mean ± S.D. of quadruplets. Statistical analysis was performed using the GraphPad Prism software (GraphPad, San Diego, CA). Statistical significance was ascertained by one way analysis of variance, followed by Tukey's multiple comparison tests. Values of $p<0.05$ were considered significant.

3. Results

3.1. Effect of METH and NACA on GSH levels in different organs

Compared to the control and the NACA-only groups, the METH-treated animals had significantly lower GSH levels in the organs studied. Kidneys, livers, and brains showed a decrease in their GSH levels of approximately 64%, 54%, and 40%, respectively. However, pretreatment of the animals with NACA increased the GSH levels significantly in the METH-exposed animals, indicating that NACA was conferring protection to these animals (Fig. 1). Treatment with NACA alone was not found to have a significant impact on levels of intracellular GSH in all tissues, as compared to the control group, except in the kidneys where an increase in the GSH levels was observed.

3.2. Effect of METH and NACA on lipid peroxidation in different organs

Lipid peroxidation is an important consequence of oxidative stress, and can be estimated by measuring the levels of malondialdehyde (MDA), a stable by-product of lipid peroxidation. METH-exposed animals had about a 22%-42% increase in the MDA levels in the organs studied, as compared to the levels in the controls (Fig. 2). The kidneys were seen to be affected the most with about a 42% increase in the MDA levels. The animals in the NACA+METH group experienced significantly less lipid peroxidation than the animals did in the METH-only treated group. Treatment with NACA-only did not alter the MDA levels significantly, as compared to those of the control group.

3.3. Effects of METH and NACA on protein carbonyl levels

Animals in the METH-only group had a 1.5-2.0 fold increase in protein carbonyl levels in the organs studied, when compared to the control group. Levels of protein carbonyls in the NACA-only group were not significantly different from control levels.

However, when animals were pre-treated with NACA before exposure to METH, protein carbonyl levels within the organs were significantly lower than those in the METH-treated group (Fig. 3).

3.4. Effect of METH and NACA on antioxidant enzyme activity

3.4.1. Effect on glutathione peroxidase activity

Table 1 shows GPx activity in different organs of METH-treated animals. METH administration markedly decreased GPx activity to ~48% - 67% of that of the control. Pretreatment with NACA significantly attenuated this decrease in the activity of GPx in the METH-treated animals. NACA alone did not significantly alter the results from those of the control group.

3.4.2. Effect on catalase activity

Antioxidant enzymes like catalase (CAT) are involved in detoxification of peroxides in the body. Exposure of animals to METH increased catalase activity in the organs studied (~42% to 67% increase). Catalase activity in the kidneys (~67%) increased more than in the livers (42%) of METH-treated animals (Table 2). However, reversal in the CAT activity was observed in METH-exposed animals that had been pretreated with NACA.

4. Discussion

Methamphetamine (METH) abuse is quite prevalent worldwide due to its euphoric effects, wide availability, and relatively low cost. An acute high dose of METH causes serious consequences, including rhabdomyolysis, hyperthermia, renal and liver failure, cardiac arrhythmias, heart attacks, cerebrovascular hemorrhages, strokes, and seizures.[22-24] Multiorgan dysfunction is seen in acute overdoses, but a vast majority of human

METH abusers do not suffer from these complications. Chronic abuse of METH contributes to anxiety, depression, aggressiveness, social isolation, psychosis, mood disturbances, and psychomotor dysfunction.[23, 25, 26]

Oxidative stress is believed to play a crucial role in METH-induced toxicity in the brain and other tissues, as evidenced by findings in previous studies.[47, 48, 62, 63] In the case of the brain, it is believed that, initially, METH causes a massive release of dopamine by inhibiting monoamine oxidase activity and dopamine uptake.[64] With higher doses, however, it causes dopamine depletion by degenerating dopaminergic terminals, damaging dopaminergic neurons, and decreasing dopamine transporter numbers.[65-67] Dopamine then reacts with molecular oxygen to form ROS, such as hydrogen peroxide, superoxide, and hydroxyl free radicals resulting in a condition known as oxidative stress [67] and causes neuronal death by apoptosis.[68] Although the precise mechanisms by which METH elicits adverse effects in various organs are unclear, studies have indicated the role of sigma receptors in mediating METH effects. These receptors are a unique group of drug binding sites which are present in various organs, including, the brain, heart, and lungs.[69] Activation of these receptors by METH in peripheral organs may be involved in METH-induced peripheral organ damage. Several studies have indicated that cytotoxicity via mitochondrial dysfunction, resulting in the depletion of intracellular ATP as well as adenine nucleotide pools, is a critical factor in the pathologic effect of chemically-induced toxicity.[70, 71] Ogata et al. have reported that, incubation of hepatocytes with amphetamine-derived designer drugs, caused cell death accompanied by losses of intracellular ATP, adenine nucleotides, GSH, and mitochondrial $\Delta\Psi$, and an increase in ROS and GSSG levels, indicating that these drugs induce oxidative stress in isolated rat

hepatocytes.[72] Oxidative stress was also implicated in d -amphetamine-induced hepatotoxicity by Carvalho et al.[17] Kubo et al. have implicated oxidative damage in the kidneys of METH abusers. Immunohistochemical analysis revealed the presence of 8-OHdG, 4-HNE, and SOD, which are oxidative stress markers in the kidneys of METH abusers.[73]

Although oxidative stress is believed to play a key role in METH-induced multiorgan dysfunction, a comparison of the oxidative effects of METH in different organs has not been sufficiently studied. Herein, we report comparative in vivo oxidative effects of METH on the brain, liver, and kidney tissues of CD-1 mice. To the best of our knowledge, we are the first to study and evaluate the potential of a novel thiol antioxidant, NACA, to prevent METH-induced oxidative stress damage to these organs. Preliminary studies in our lab demonstrated that NACA was significantly more effective than NAC at providing thiols in the plasma and liver tissue of Wistar rats, which were administered either NACA or NAC, using IP injections of 500 mg/kg of each compound. Results indicated that NACA prevented oxidative damage, possibly by scavenging existing ROS, while halting the production of further ROS, lipid peroxidation, and protein carbonylation. In addition, NACA acted by increasing levels of reduced glutathione (GSH), as well as the activity of the detoxification enzyme, glutathione peroxidase (GPx).

METH-exposed animals showed significant decreases in GSH in all of the organs tested, indicating that exposure to METH induced oxidative stress in these organs. However, NACA was capable of restoring GSH levels in these organs (Fig. 1). Significant increases in the GSH levels in the kidney tissues in the NACA only group could be attributed to the fact that activity of γ-glutamyl-cysteine synthetase in this tissue

is much higher than that in the liver and brain tissue.[74, 75] NACA might be providing cysteine as a substrate for this highly active enzyme in the kidney and thereby significantly increasing GSH levels, even in the absence of any oxidative stress. Our results are in line with the results previously reported by Achat-Mendes et al.,[76] Acikgoz et al.,[77] and Kim et al.[78] In addition, Moszczynska et al.[38] reported a modest decrease in total GSH concentration after METH administration. However, Flora et al.[79] and Harold et al.[37] reported increases in the total GSH levels immediately after METH administration, possibly due to the cell's initial defense mechanism against oxidative stress, as the levels were measured within a few hours of METH administration. Increases in the GSH content can be explained by an upregulation of γ-glutamyl-cysteine synthetase in response to oxidative stress. In addition, total GSH (GSH + GSSG) levels may not reflect individual changes in GSH and GSSG. We believe that reduced GSH is a better indicator of oxidative stress; therefore, we determined the reduced GSH levels in the afore mentioned organs.

A possible explanation for a decrease in GSH levels is the reduced activity of the enzymes involved in GSH synthesis and/or the oxidation of GSH to GSSG under oxidative stress. An alternative explanation could be an increase in extracellular levels of glutamate which, in turn, might inhibit the uptake of cystine via the glutamate-cystine exchange system, thereby reducing GSH synthesis. The protective effect of NACA is probably mediated by the ability of the NACA to increase GSH biosynthesis by reducing extracellular cystine to cysteine, and/or by supplying the sulfydryl groups that can stimulate GSH biosynthesis, or by conversion of GSSG to GSH by non-enzymatic thiol disulfide exchange.[80]

Free radicals attack lipids, especially polyunsaturated fatty acids, in the cell membranes and lead to the formation of by-products like MDA.[81] Our studies indicate that exposure to METH induced a significant increase in MDA levels in various organs of these animals, as compared to the NACA-treated group, thereby pointing to the role of this antioxidant in protecting animals from METH-induced damage. Our results are in accordance with the previously reported increases in lipid peroxidation in response to METH.[42, 45-47, 79, 82, 83] Concomitant reduction of GSH levels (a substrate for glutathione peroxidase) might have hampered the decomposition of lipid peroxides in METH-treated animals. NACA was able to prevent lipid peroxidation by supplying an adequate amount of GSH as a substrate for glutathione peroxidase to effectively decompose lipid peroxides in the mice, thereby reducing MDA levels.

It is well established that proteins, like lipids and DNA, are oxidized by ROS. Oxidative damage to tissue proteins is an important factor in METH-induced organ toxicities. Increased protein carbonylation is a reliable parameter of oxidative stress, as it lacks interference from other non-protein substances,[60] and measures carbonylation of various protein residues, including lysine and arginine.[84] Our results showed that protein carbonyls significantly increased in METH-treated animals, but such increases were prevented by NACA (Fig. 3). These results are in line with those reported by Gluck et al..[46]

Antioxidant enzymes are involved in the detoxification of lethal peroxides inside the cells. A significant reduction in the activity of GPx, observed after METH administration, may have been partially due to diminished GSH levels that GPx needs as a substrate. We previously reported decreased GPx activity, due to METH, in human brain microvascular

endothelial cell culture [36]. Our results are also in accordance with the previously reported decrease in GPx activity after METH administration in brain tissue.[40, 42, 78] In contrast, the increased GPx activity in rat brains, observed by Flora et al.[79] after METH administration, could have been due to the enhanced levels of cellular glutathione observed in their study. On the other hand, no change in GPX activity in rat brains was reported by Moszczynska et al.[38] in response to METH.

Increased catalase activity was observed in animals injected with METH. NACA pretreatment, yet again, reversed catalase activity in the METH + NACA group. Changes in catalase activity had been observed in various tissues that were undergoing oxidative stress. Increased catalase activity in METH-treated animals could be an adaptive response to the higher levels of H_2O_2 generated by inhibition of GPx. Almeida et al.[40] and Melo et al.[47] reported no change in catalase activity when exposed to METH, whereas Jayanthi et al.[42] observed a decrease in catalase activity after METH exposure. We believe that the response of this antioxidant enzyme to oxidative agents is tissue/organ specific and has an adaptive character. Increased catalase activity in METH-treated animals could be an adaptive response to the higher levels of H_2O_2 generated by inhibition of GPx. The possible mechanism for the restored catalase activity in METH-exposed mice, when treated with NACA, may be the scavenging of free radicals by NACA or by providing more GSH, which is a substrate for GPx. However, further investigation is needed to confirm this theory.

Depletion of GSH by METH initiates a myriad of events. There is an initial increase in free radicals that overwhelms the scavenging ability of the GSH-dependent enzymes (glutathione peroxidase), which leads to oxidation of lipids and proteins. Riviere et al.[85]

studied the disposition of METH and its metabolite amphetamine and reported the rank order of (+)-METH tissue accumulation after i.v. dosing was kidney >spleen >brain > liver >heart > serum, with terminal elimination half-life values ranging from 53 to 66 minutes. In another study, Volkow et al.[86] studied METH distribution and accumulation in the human body via Positron Emission Tomography and reported that the liver, brain, and kidney had relatively higher uptakes of the drug. It was distributed through most organs. They reported that the rank order of uptake was lungs, liver > brain > kidneys. METH's clearance was fastest in the heart and lungs; slowest in the brain, liver, and stomach; and intermediate in the kidneys, spleen, and pancreas. Our results indicated maximum oxidative stress in the kidneys followed by the liver and brain.

Despite different results reported by the two groups, a high accumulation of METH in most body organs is likely to contribute to the medical complications associated with METH abuse and, therefore, treatment of METH abusers should focus on multi-organ damage. The multiple roles of NACA in preventing METH-induced toxicity include scavenging of free radicals (directly and indirectly) by providing GSH, and chelating Cu^{2+}, ultimately preventing catalyzation of ROS formation, providing cysteine for GSH synthesis, non-enzymatic reduction of the preexisting toxic GSSG into GSH, and stimulating cytosolic enzymes involved in glutathione regeneration. Studies have shown protective effects of NACA against radiation-induced toxicity, HIV-protein-induced oxidative stress, allergic airway disease, pollutant-induced lung disease, and lead-induced death.[51, 52, 87-89]

We believe that NACA also prevents METH-induced oxidative stress by scavenging free radicals. This hypothesis is supported by studies in which edaravone (3-methyl-1-

phenyl-2-pyrazolin-5-one), a potent scavenger of hydroxyl radicals, prevented METH-induced neurotoxicity.[90, 91] This is also supported by studies in which antioxidants like NAC, L-carnitine, ascorbic acid, ethanol, mannitol, selenium, and melatonin attenuated the neurotoxicity after METH administration. [31, 92-96]

Currently, no medications are available to safely reverse life-threatening METH overdoses quickly. Medications that could help METH users recover rapidly from the toxic effects of chronic use are highly desirable for compliance to the current treatment regimen. Findings from this study will aid in developing potentially effective adjunctive therapy with existing METH treatment for addressing oxidative stress induced organ damage and accompanying psychiatric problems. Based on encouraging results from the use of NAC and other antioxidants, we believe that NACA would be more effective in treating METH-induced toxicities because of its better permeability across membranes and low toxicity profile. Combining NACA with current treatment medications, as a neuro- and tissue-protective agent, might be an effective approach to treating METH abusers. Additional studies are needed to further delineate and clarify strategies that might improve treatment of METH-induced toxicity. In any case, our future studies will focus on the antioxidant effects of NACA on acute METH intoxication.

NACA might also be beneficial in reducing drug cravings. These cravings are believed to be caused by glutamate dysfunction within the accumbens nucleus.[97] A mixed disulfide exchange via NACA can result in formation of cystine, which would help restore the extracellular glutamate concentration in the accumbens nucleus by stimulating the inhibitory metabotropic glutamate receptors and, thereby, reducing synaptic release of

glutamate.[97-99] On the other hand, a recent study of NAC plus naltrexone did not show significant improvement in the reduction of cravings.[100]

In summary, data from the present study indicated oxidative stress in the livers, kidneys, and brains of METH-treated animals, with the kidneys being affected the most. Administration of NACA, however, resulted in a significant reduction in the oxidative stress induced by METH, thereby suggesting a therapeutic potential for this novel antioxidant as a tissue- and neuro-protectant against METH toxicity. Further investigation could help determine NACA's efficacy in METH-abuse treatment and an evaluation of the histology of these organs in METH-treated animals would provide additional information on its therapeutic potential.

Abbreviations:

BBB- blood-brain barrier; CNS- central nervous system; GSH- glutathione; GPx- glutathione peroxidase; H_2DCFDA- 2', 7' –dichlorofluorescein diacetate; MDA- malondialdehyde; METH- methamphetamine; NACA- N-acetylcysteine amide; NAC- N-acetylcysteine; NPM- N-(1-pyrenyl)-maleimide; PBS- phosphate buffered saline; ROS- reactive oxygen species.

Acknowledgments

The authors appreciate the editorial efforts of Barbara Harris and Youyou Zheng.

Funding Acknowledgement

This work was supported by the NIDA, NIH [grant number 1 R15DA023409-01A2].

Declaration of Conflicting Interests

None.

References

1. Office of Applied Studies. Primary Methamphetamine/ Amphetamine Treatment Admissions: 1992–2002. The DASIS Report. 2004. Available from: http://www.oas.samhsa.gov/facts.cfm.

2. Office of Applied Studies. Treatment Episode Data Set (TEDS) Highlights - 2004: National Admissions to Substance Abuse Treatment Services Rockville, MD: Substance Abuse and Mental Health Services Administration; 2006. DHHS Publication No. SMA 06-4140, Drug and Alcohol Services Information System Series S-31, Available from: http://www.oas.samhsa.gov/dasis.htm#teds4.

3. Office of Applied Studies. The NSDUH Report: Methamphetamine Use. Rockville, MD: Substance Abuse and Mental Health Services Administration; 2007.

4. Office of Applied Studies. Emergency Department Trends From Drug Abuse Warning Network, Final Estimates 1995-2002. Rockville, MD: Substance Abuse and Mental Health Services Administration; 2003. DHHS Publication No. SMA 03-3780, DAWN Series D-24.

5. Gonzales R, Mooney L, Rawson RA. The methamphetamine problem in the United States. Annu Rev Publ Health. 2010;31:385-98.

6. Karch SB, Stephens BG, Ho CH. Methamphetamine-related deaths in San Francisco: demographic, pathologic, and toxicologic profiles. J Forensic Sci. 1999;44:359-68.

7. Richards JR. Rhabdomyolysis and drugs of abuse. J Emerg Med. 2000;19:51-6.

8. Kendrick WC, Hull AR, Knochel JP. Rhabdomyolysis and shock after intravenous amphetamine administration. Ann Intern Med. 1977;86:381-7.

9. Richards JR, Johnson EB, Stark RW, Derlet RW. Methamphetamine abuse and rhabdomyolysis in the ED: a 5-year study. Am J Emerg Med. 1999;17:681-5.

10. Terada Y, Shinohara S, Matui N, Ida T. Amphetamine-induced myoglobinuric acute renal failure. Jpn J Med. 1988;27:305-8.

11. Holt S and Moore K. Pathogenesis of renal failure in rhabdomyolysis: the role of myoglobin. Exp Nephrol. 2000;8:72-6.

12. Ramcharan S, Meenhorst PL, Otten JM, Koks CH, de Boer D, Maes RA, Beijnen JH. Survival after massive ecstasy overdose. Journal of toxicology. Clin Toxicol. 1998;36:727-31.

13. Lan KC, Lin YF, Yu FC, Lin CS, Chu P. Clinical manifestations and prognostic features of acute methamphetamine intoxication. J Formos Med Assoc. 1998;97:528-33.

14. Jones AL, Simpson KJ. Review article: mechanisms and management of hepatotoxicity in ecstasy (MDMA) and amphetamine intoxications. Aliment Pharm Ther. 1999;13:129-33.

15. Hall AP, Henry JA. Acute toxic effects of 'Ecstasy' (MDMA) and related compounds: overview of pathophysiology and clinical management. Brit J Anaesth. 2006;96:678-85.

16. Jones AL, Jarvie DR, McDermid G, Proudfoot AT. Hepatocellular damage following amphetamine intoxication. J Toxicol-Clin Toxic. 1994;32:435-44.

17. Carvalho F, Remião F, Soares ME, Catarino R, Queiroz G, Bastos ML. d-Amphetamine-induced hepatotoxicity: possible contribution of catecholamines and hyperthermia to the effect studied in isolated rat hepatocytes. Arch Toxicol. 1997;71:429-36.

18. Zalis EG, Lundberg GD, Knutson RA. The pathophysiology of acute amphetamine poisoning with pathologic correlation. J Pharm Exp Ther. 1967;158:115-27.

19. Mooney LJ, Glasner-Edwards S, Rawson RA, Ling W. Medical effects of methamphetamine use. In: Roll JM, Rawson, R.A., Ling, W., Shoptaw, S., editor. Methamphetamine Addiction: From Basic Science to Treatment. New York: The Guilford Press; 2009. p. 117-42.

20. Yu Q, Larson D, Watson RR. Heart disease, methamphetamine and AIDS. Life Sci. 2003;73:129-40.

21. Derlet RW, Horowitz BZ. Cardiotoxic drugs. Emerg Med Clin N Am. 1995;13:771-91.

22. Albertson TE, Derlet RW, Van Hoozen BE. Methamphetamine and the expanding complications of amphetamines. Western J Med. 1999;170:214-9.

23. Darke S, Kaye S, McKetin R, Duflou J. Major physical and psychological harms of methamphetamine use. Drug Alcohol Rev. 2008;27:253-62.

24. Perez JAJ, Arsura EL, Strategos S. Methamphetamine-related stroke: four cases. J Emerg Med. 1999;17:469-71.

25. Homer BD, Solomon TM, Moeller RW, Mascia A, DeRaleau L, Halkitis PN. Methamphetamine abuse and impairment of social functioning: a review of the underlying neurophysiological causes and behavioral implications. Psychol Bull. 2008;134:301-10.

26. Scott JC, Woods SP, Matt GE, Meyer RA, Heaton RK, Atkinson JH, Grant I. Neurocognitive effects of methamphetamine: a critical review and meta-analysis. Neuropsychol Rev. 2007;17:275-97.

27. Zweben JE, Cohen JB, Christian D, Galloway GP, Salinardi M, Parent D, Iguchi M. Psychiatric symptoms in methamphetamine users. Am J Addiction. 2004;13:181-90.

28. Glasner-Edwards S, Marinelli-Casey P, Hillhouse M, Ang A, Mooney LJ, Rawson R. Depression among methamphetamine users: association with outcomes from the Methamphetamine Treatment Project at 3-year follow-up. J Nerv Ment Dis. 2009;197:225-31.

29. Meredith CW, Jaffe C, Ang-Lee K, Saxon AJ. Implications of chronic methamphetamine use: a literature review. Harvard Rev Psychiat. 2005;13:141-54.

30. Cubells JF, Rayport S, Rajendran G, Sulzer D. Methamphetamine neurotoxicity involves vacuolation of endocytic organelles and dopamine-dependent intracellular oxidative stress. J Neurosci. 1994;14:2260-71.

31. De Vito MJ, Wagner GC. Methamphetamine-induced neuronal damage: a possible role for free radicals. Neuropharmacology. 1989;28:1145-50.

32. Itzhak Y, Ali SF. The neuronal nitric oxide synthase inhibitor, 7-nitroindazole, protects against methamphetamine-induced neurotoxicity in vivo. J Neurochem. 1996;67:1770-3.

33. Itzhak Y, Gandia C, Huang PL, Ali SF. Resistance of neuronal nitric oxide synthase-deficient mice to methamphetamine-induced dopaminergic neurotoxicity. J Pharmacol Exp Ther. 1998;284:1040-7.

34. Wagner GC, Ricaurte GA, Seiden LS, Schuster CR, Miller RJ, Westley J. Long-lasting depletions of striatal dopamine and loss of dopamine uptake sites following repeated administration of methamphetamine. Brain Res. 1980;181:151-60.

35. Kita T, Wagner GC, Nakashima T. Current research on methamphetamine-induced neurotoxicity: animal models of monoamine disruption. J Pharmacol Sci. 2003;92:178-95.

36. Zhang X, Banerjee A, Banks WA, Ercal N. N-Acetylcysteine amide protects against methamphetamine-induced oxidative stress and neurotoxicity in immortalized human brain endothelial cells. Brain Res. 2009;1275:87-95.

37. Harold C, Wallace T, Friedman R, Gudelsky G, Yamamoto B. Methamphetamine selectively alters brain glutathione. Eur J Pharmacol. 2000;400:99-102.

38. Moszczynska A, Turenne S, Kish SJ. Rat striatal levels of the antioxidant glutathione are decreased following binge administration of methamphetamine. Neurosci Lett. 1998;255:49-52.

39. Chen H, Lee Y, Huang C, Liu H, Liao W, Lai W, Lin Y, Huang N. Methamphetamine downregulates peroxiredoxins in rat pheochromocytoma cells. Biochem Bioph Res Co. 2007;354:96-101.

40. D'Almeida V, Camarini R, Azzalis LA, Mattei R, Junqueira VB, Carlini EA. Antioxidant defense in rat brain after chronic treatment with anorectic drugs. Toxicol Lett. 1995;81:101-5.

41. Iwazaki T, McGregor IS, Matsumoto I. Protein expression profile in the striatum of acute methamphetamine-treated rats. Brain Res. 2006;1097:19-25.

42. Jayanthi S, Ladenheim B, Cadet JL. . Methamphetamine-induced changes in antioxidant enzymes and lipid peroxidation in copper/zinc-superoxide dismutase transgenic mice. Ann NY Acad Sci. 1998;844:92-102.

43. Kobeissy FH, Warren MW, Ottens AK, Sadasivan S, Zhang Z, Gold MS, Wang KKW. Psychoproteomic analysis of rat cortex following acute methamphetamine exposure. J Proteome Res. 2008;7:1971-83.

44. Li X, Wang H, Qiu P, Luo H. Proteomic profiling of proteins associated with methamphetamine-induced neurotoxicity in different regions of rat brain. Neurochem Int. 2008;52:256-64.

45. Açikgöz O, Gönenç S, Kayatekin BM, Uysal N, Pekçetin C, Semin I, Güre A. Methamphetamine causes lipid peroxidation and an increase in superoxide dismutase activity in the rat striatum. Brain Res. 1998;813:200-2.

46. Gluck MR, Moy LY, Jayatilleke E, Hogan KA, Manzino L, Sonsalla PK. Parallel increases in lipid and protein oxidative markers in several mouse brain regions after methamphetamine treatment. J Neurochem. 2001;79:152-60.

47. Melo P, Rodrigues LG, Pinazo-Durán MD, Tavares MA. Methamphetamine and lipid peroxidation in the rat retina. Birth Defects Res A. 2005;73:455-60.

48. Tokunaga I, Kubo S, Ishigami A, Gotohda T, Kitamura O. Changes in renal function and oxidative damage in methamphetamine-treated rat. Legal Medicine (Tokyo, Japan). 2006;8(16-21).

49. Shan XQ, Aw TY, Jones DP. Glutathione-dependent protection against oxidative injury. Pharmacol Therapeut. 1990;47:61-71.

50. Penugonda S, Mare S, Goldstein G, Banks WA, Ercal N. Effects of N-acetylcysteine amide (NACA), a novel thiol antioxidant against glutamate-induced cytotoxicity in neuronal cell line PC12. Brain Res. 2005;1056:132-8.

51. Wu W, Abraham L, Ogony J, Matthews R, Goldstein G, Ercal N. Effects of N-acetylcysteine amide (NACA), a thiol antioxidant on radiation-induced cytotoxicity in Chinese hamster ovary cells. Life Sci. 2008;82:1122-30.

52. Price TO, Uras F, Banks WA, Ercal N. A novel antioxidant N-acetylcysteine amide prevents gp120- and Tat-induced oxidative stress in brain endothelial cells. Exp Neurol. 2006;201:193-202.

53. Amer J, Atlas D, Fibach E. N-acetylcysteine amide (AD4) attenuates oxidative stress in beta-thalassemia blood cells. Biochim Biophys Acta. 2008;1780:249-55.

54. Grinberg L, Fibach E, Amer J, Atlas D. N-acetylcysteine amide, a novel cell-permeating thiol, restores cellular glutathione and protects human red blood cells from oxidative stress. Free Radical Bio Med. 2005;38:136-45.

55. Shrem MT, Halkitis PN. Methamphetamine abuse in the United States: contextual, psychological and sociological considerations. J Health Psychol. 2008;13:669-79.

56. Madden LJ, Flynn CT, Zandonatti MA, May M, Parsons LH, Katner SN, Henriksen SJ, Fox HS. Modelling Human Methamphetamine Exposure in Nonhuman Primates: Chronic Dosing in the Rhesus Macaque Leads to behavioral and Physiological Abnormalities. Neuropsychopharmacol. 2005; 30: 350–359.

57. Winters RA, Zukowski J, Ercal N, Matthews RH, Spitz DR. Analysis of glutathione, glutathione disulfide, cysteine, homocysteine, and other biological thiols by high-performance liquid chromatography following derivatization by n-(1-pyrenyl)maleimide. Anal Biochem. 1995;227:14-21.

58. Draper HH, Squires EJ, Mahmoodi H, Wu J, Agarwal S, Hadley M. A comparative evaluation of thiobarbituric acid methods for the determination of malondialdehyde in biological materials. Free Radical Bio Med. 1993;15:353-63.

59. Aebi H. Catalase in vitro. Method Enzymol. 1984;105:121-6.

60. Levine RL, Garland D, Oliver CN, Amici A, Climent I, Lenz AG, Ahn BW, Shaltiel S, Stadtman ER. Determination of carbonyl content in oxidatively modified proteins. Method Enzymol. 1990;186:464-78.

61. Bradford MM. A rapid and sensitive method for the quantitation of microgram quantities of protein utilizing the principle of protein-dye binding. Anal Biochem. 1976;72:248-54.

62. Burrows KB, Yamamoto BK. Methamphetamine neurotoxicity. Roles for glutamate, oxidative processes and metabolic stress. In: Herman BH, editor. Glutamate and Addiction New Jersey: Humana Press Inc. ; 2003. p. 211-27.

63. Stephans SE, Yamamoto BK. Methamphetamine-induced neurotoxicity: roles for glutamate and dopamine efflux. Synapse. 1994;17:203-9.

64. Melo P, Pinazo-Durán MD, Salgado-Borges J, Tavares MA. . Correlation of axon size and myelin occupancy in rats prenatally exposed to methamphetamine. Brain Res. 2008;1222:61-8.

65. Giros B, Jaber M, Jones SR, Wightman RM, Caron MG. Hyperlocomotion and indifference to cocaine and amphetamine in mice lacking the dopamine transporter. Nature. 1996;379:606-12.

66. Golembiowska K, Zylewska A. Agonists of A1 and A2A adenosine receptors attenuate methamphetamine-induced overflow of dopamine in rat striatum. Brain Res. 1998;806:202-9.

67. Graham DG. Oxidative pathways for catecholamines in the genesis of neuromelanin and cytotoxic quinones. Mol Pharmacol. 1978;14:633-43.

68. Stumm G, Schlegel J, Schäfer T, Würz C, Mennel HD, Krieg JC, Vedder H. Amphetamines induce apoptosis and regulation of bcl-x splice variants in neocortical neurons. FASEB J. 1999;13:1065-72.

69. Matsumoto RR, Liu Y, Lerner M, Howard E.W, Brackett D.J. Sigma receptors: potential medications development target for anti-cocaine agents. Eur J Pharmacol. 2003; 469: 1-12.

70. Bellomo G, Mirabelli F, Richelmi P, Malorni W, Iosi F, Orrenius S. The cytoskeleton as a target in quinone toxicity. Free Radic Res Commun. 1990; 8:391–399.

71. Nicotera P, Bellomo G, Orrenius S. Calcium-mediated mechanisms in chemically induced cell death. Ann Rev Pharmacol Toxicol. 1992; 32:447–470.

72. Nakagawa Y, Suzuki T, Tayama S, Ishii H, Ogata A. Cytotoxic effects of 3,4-ethylenedioxy-*N*-alkylamphetamines, MDMA and its analogues, on isolated rat hepatocytes. Arch Toxicol. 2009; 83:69–80.

73. Ishigami A, Tokunaga I, Gotohda T, Kubo S. Immunohistochemical study of myoglobin and oxidative injury related markers in the kidney of methamphetamine abusers. Legal Med. 2003; 5: 42–48.

74. Orlowski M, Meister A. Isolation of highly purified gamma-glutamylcysteine synthetase from rat kidney. Biochem. 1971;10:372-80.

75. Palekar AG, Tate SS, Meister A. Decrease in glutathione levels of kidney and liver after injection of methionine sulfoximine into rats. Biochem Bioph Res Co. 1975;62:651-7.

76. Achat-Mendes C, Anderson KL, Itzhak Y. Impairment in consolidation of learned place preference following dopaminergic neurotoxicity in mice is ameliorated by N-acetylcysteine but not D1 and D2 dopamine receptor agonists. Neuropsychopharmacol. 2007;32:531-41.

77. Açikgöz O, Gönenç S, Gezer S, Kayatekin BM, Uysal N, Semin I, Gure A. Methamphetamine causes depletion of glutathione and an increase in oxidized glutathione in the rat striatum and prefrontal cortex. Neurotox Res. 2001;3:277-80.

78. Kim HC, Jhoo WK, Choi DY, Im DH, Shin EJ, Suh JH, Floyd RA, Bing G. Protection of methamphetamine nigrostriatal toxicity by dietary selenium. Brain Res. 1999;851(76-86).

79. Flora G, Lee YW, Nath A, Maragos W, Hennig B, Toborek M. Methamphetamine-induced TNF-alpha gene expression and activation of AP-1 in discrete regions of mouse brain: potential role of reactive oxygen intermediates and lipid peroxidation. Neuromol Med. 2002;2:71-85.

80. Issels RD, Nagele A, Eckert KG, Wilmanns W. Promotion of cystine uptake and its utilization for glutathione biosynthesis induced by cysteamine and N-acetylcysteine. Biochem Pharmacol. 1988;37:881-8.

81. Karbownik M, Reiter RJ. Antioxidative effects of melatonin in protection against cellular damage caused by ionizing radiation. Proceedings of the Society for Experimental Biology and Medicine Society for Experimental Biology and Medicine (New York, NY). 2000;225:9-22.

82. Açikgöz O, Gönenç S, Kayatekin BM, Pekçetin C, Uysal N, Dayi A, Semin I, Güre A. The effects of single dose of methamphetamine on lipid peroxidation levels in the rat striatum and prefrontal cortex. Eur Neuropsychopharm. 2000;10:415-8.

83. Yamamoto BK, Zhu W. The effects of methamphetamine on the production of free radicals and oxidative stress. J Pharmacol Exp Ther. 1998;287:107-14.

84. Rice-Evans CA, Diplock AT, Symons MCR. Laboratory Techniques in Biochemistry and Molecular Biology: Techniques in Free Radical Research. In: Burdon RHVK, P. H., editor. Mechanisms of Radical Production. New York: Elsevier; 1991. p. 19-50.

85. Rivière GJ, Gentry WB, Owens SM. Disposition of methamphetamine and its metabolite amphetamine in brain and other tissues in rats after intravenous administration. J Pharmacol Exp Ther. 2000;292:1042-7.

86. Volkow ND, Fowler JS, Wang G, Shumay E, Telang F, Thanos PK, Alexoff D. Distribution and pharmacokinetics of methamphetamine in the human body: clinical implications. PLoS One. 2010;5:e15269.

87. Penugonda S, Mare S, Lutz P, Banks WA, Ercal N. Potentiation of lead-induced cell death in PC12 cells by glutamate: protection by N-acetylcysteine amide (NACA), a novel thiol antioxidant. Toxicol Appl Pharm. 2006;216:197-205.

88. Banerjee A, Trueblood MB, Zhang X, Manda KR, Lobo P, Whitefield PD, Hagen DE, Ercal N. N-acetylcysteineamide (NACA) prevents inflammation and oxidative stress in animals exposed to diesel engine exhaust. Toxicol Lett. 2009;187:187-93.

89. Lee KS, Kim SR, Park HS, Park SJ, Min KH, Lee KY, Choe YH, Hong SH, Han HJ, Lee YR, Kim JS, Atlas D, Lee YC. A novel thiol compound, N-acetylcysteine amide, attenuates allergic airway disease by regulating activation of NF-kappaB and hypoxia-inducible factor-1alpha. Exp Mol Med. 2007;39:756-68.

90. Kawasaki T, Ishihara K, Ago Y, Nakamura S, Itoh S, Baba A, Matsuda T. Protective effect of the radical scavenger edaravone against methamphetamine-induced dopaminergic neurotoxicity in mouse striatum. Eur J Pharmacol. 2006;542:92-9.

91. Banno M, Mizuno T, Kato H, Zhang G, Kawanokuchi J, Wang J, Kuno R, Jin S, Takeuchi H, Suzumura A. The radical scavenger edaravone prevents oxidative neurotoxicity induced by peroxynitrite and activated microglia. Neuropharmacol. 2005;48:283-90.

92. Wagner GC, Carelli RM, Jarvis MF. Pretreatment with ascorbic acid attenuates the neurotoxic effects of methamphetamine in rats. Res Commun Chem Path. 1985;47:221-8.

93. Fukami G, Hashimoto K, Koike K, Okamura N, Shimizu E, Iyo M. . Effect of antioxidant N-acetyl-L-cysteine on behavioral changes and neurotoxicity in rats after administration of methamphetamine. Brain Res. 2004;1016:90-5.

94. Virmani A, Gaetani F, Imam S, Binienda Z, Ali S. Possible mechanism for the neuroprotective effects of L-carnitine on methamphetamine-evoked neurotoxicity. Ann NY Acad Sci. 2003;993:197-207.

95. Hashimoto K, Tsukada H, Nishiyama S, Fukumoto D, Kakiuchi T, Shimizu E, Iyo M. Protective effects of N-acetyl-L-cysteine on the reduction of dopamine transporters in the striatum of monkeys treated with methamphetamine. Neuropsychopharmacol. 2004;29:2018-23.

96. Imam SZ, el-Yazal J, Newport GD, Itzhak Y, Cadet JL, Slikker WJ, Ali SF. Methamphetamine-induced dopaminergic neurotoxicity: role of peroxynitrite and neuroprotective role of antioxidants and peroxynitrite decomposition catalysts. Ann NY Acad Sci. 2001;939:366-80.

97. McFarland K, Lapish CC, Kalivas PW. Prefrontal glutamate release into the core of the nucleus accumbens mediates cocaine-induced reinstatement of drug-seeking behavior. J Neurosci. 2003;23:3531-7.

98. LaRowe SD, Mardikian P, Malcolm R, Myrick H, Kalivas P, McFarland K, Saladin M, McRae A, Brady K. Safety and tolerability of N-acetylcysteine in cocaine-dependent individuals. Am J Addiction. 2006;15:105-10.

99. Grant JE, Odlaug BL, Kim SW. N-acetylcysteine, a glutamate modulator, in the treatment of trichotillomania: a double-blind, placebo-controlled study. Arch Gen Psychiat. 2009;66:756-63.

100. Grant JE, Odlaug BL, Kim SW. A double-blind, placebo-controlled study of N-acetylcysteine plus naltrexone for methamphetamine dependence. Eur Neuropsychopharmacol. 2010;20:823-8.

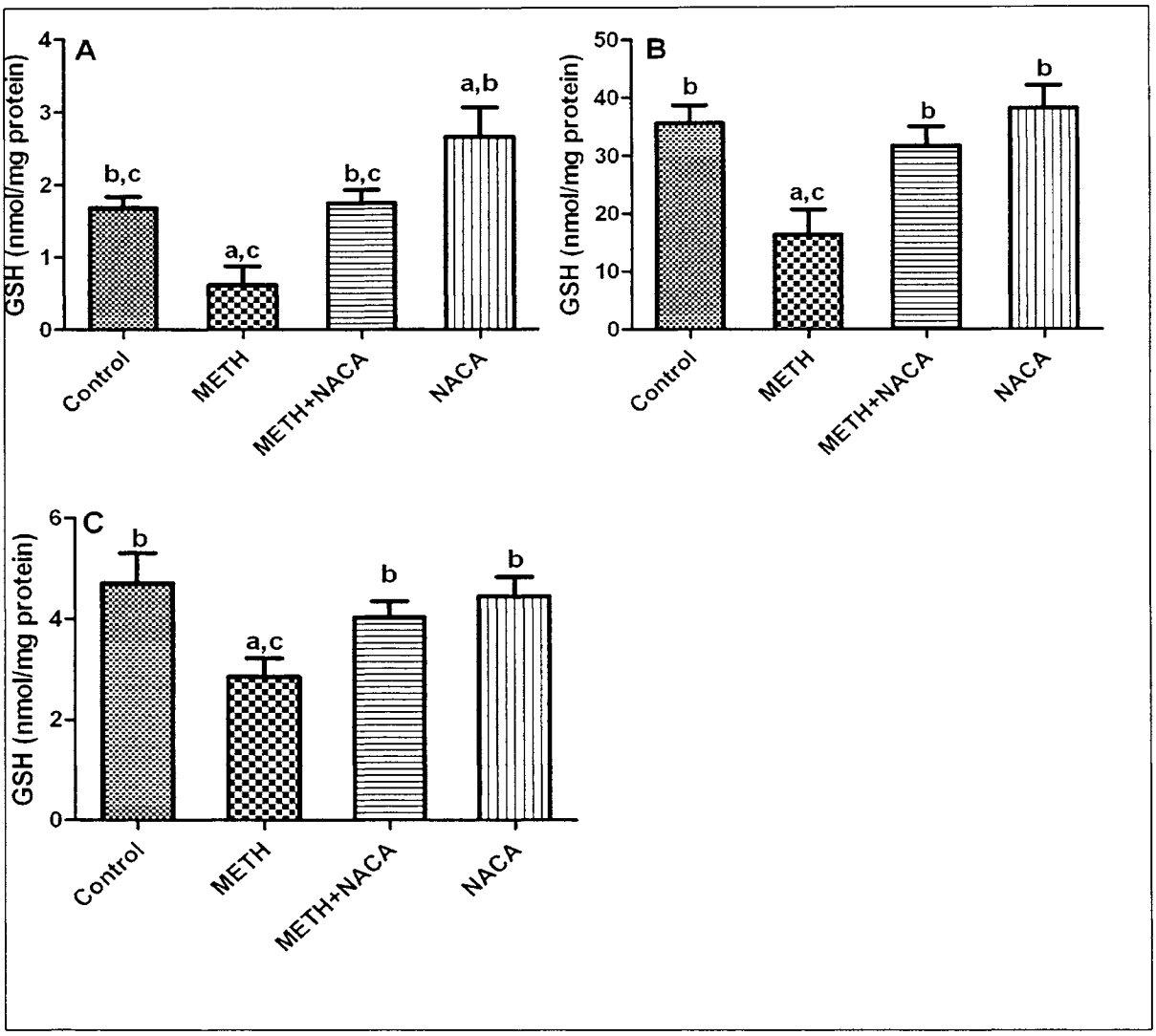

Fig. 1. Effect of METH and NACA on GSH levels in (A) kidneys, (B) livers, and (C) brains of CD-1 mice. CD-1 mice were injected (i.p) with either saline, for control and METH group, or NACA (250 mg/kg body weight) for the NACA and NACA+METH groups, 30 minutes before exposure to METH (10 mg/kg body weight). This was followed by four more injections of METH every 2 hours over an 8 hour period. Mice were sacrificed 24 hours after the last METH injection and GSH levels were measured in homogenized tissue samples. All experiments were performed in quadruplet, and the values reported are Mean ± SD (a: different from control group, b: different from METH group, c: different from NACA group, $p<0.05$).

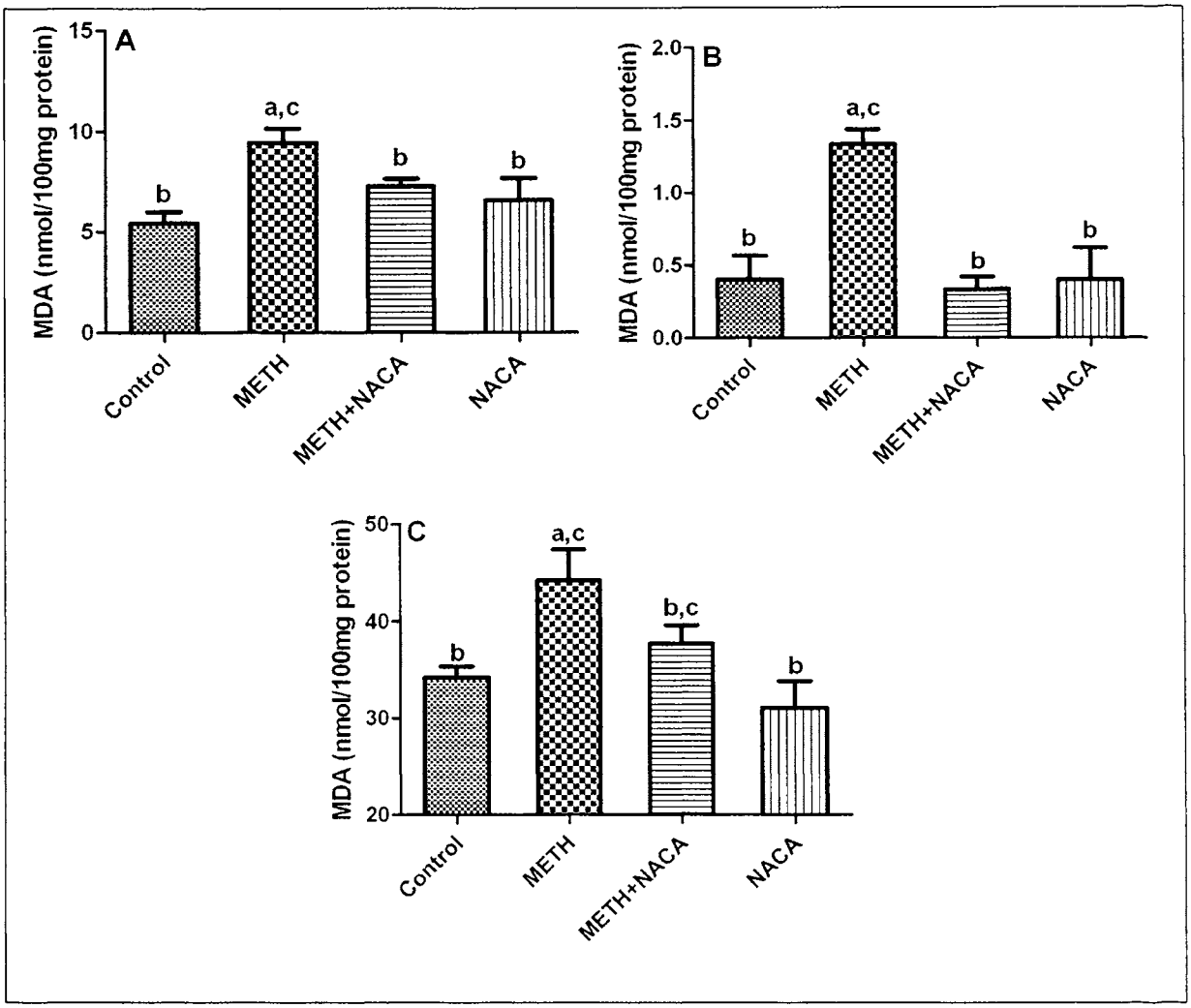

Fig. 2. Effect of METH and NACA on lipid peroxidation in (A) kidneys, (B) livers, and (C) brains of CD-1 mice. CD-1 mice were injected (i.p) with either saline, for control and METH group, or NACA (250 mg/kg body weight) for the NACA and NACA+METH groups, 30 minutes before exposure to METH (10 mg/kg body weight). This was followed by four more injections of METH every 2 hours over an 8 hour period. Mice were sacrificed 24 hours after the last METH injection and MDA levels were measured in homogenized tissue samples. All experiments were performed in quadruplet, and the values reported are Mean ± SD (a: different from control group, b: different from METH group, c: different from NACA group, $p<0.05$).

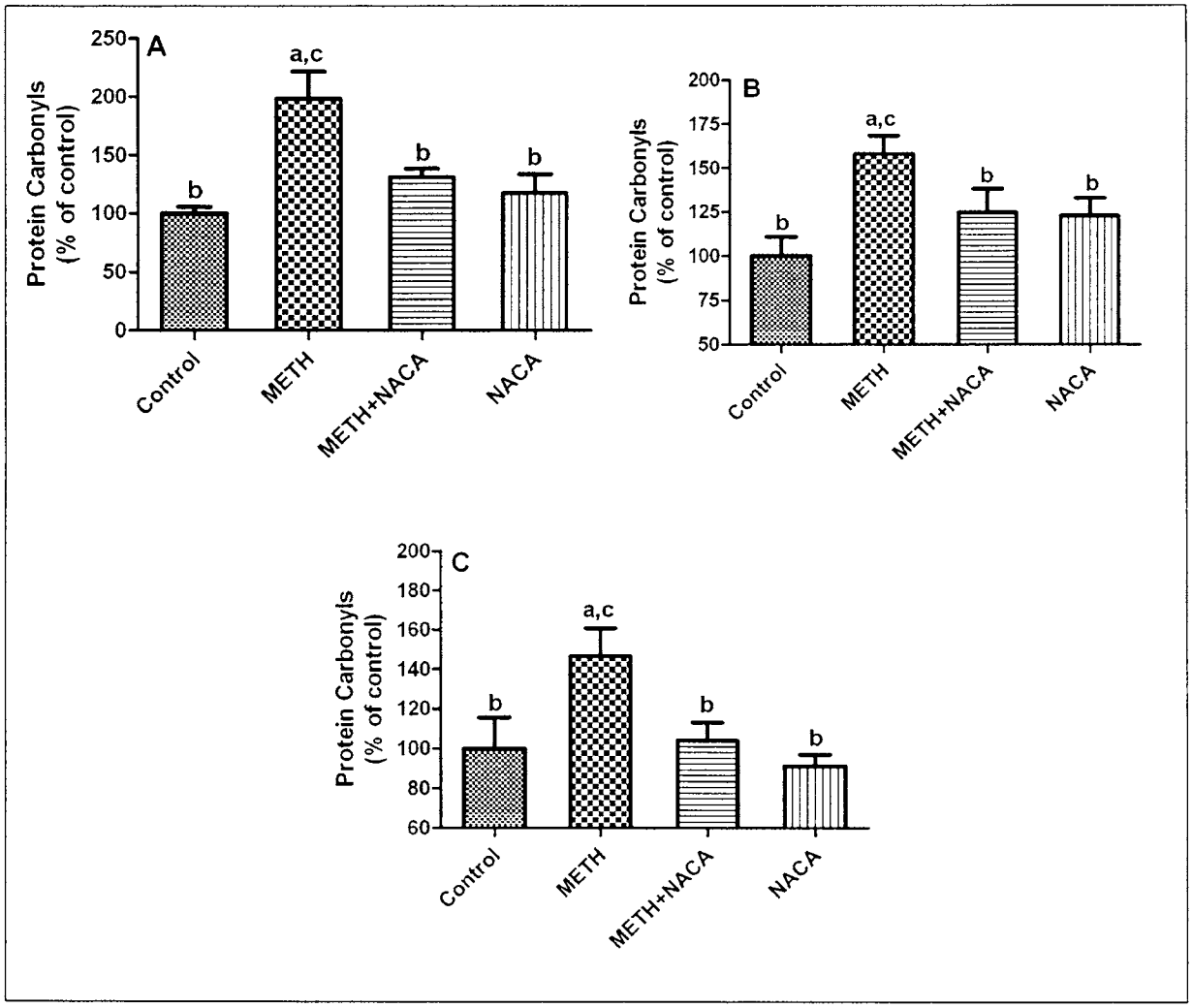

Fig. 3. Effect of METH and NACA on protein carbonyl levels in (A) kidneys, (B) livers, and (C) brains of CD-1 mice. Protein carbonyl levels were measured in homogenized tissue samples for control, METH-only, NACA-only, and METH+NACA groups. The data shows that protein oxidation is significantly increased in the tissues of mice exposed to METH. Pretreatment with NACA significantly reduced the levels of protein carbonyls in mice also treated with METH to levels similar to that of the control group. All experiments were performed in quadruplet, and the values reported are Mean ± SD (a: different from control group, b: different from METH group, c: different from NACA group, $p<0.05$).

Table 1: Effects of NACA on the activities of GPx (mU/mg protein)

Groups	Kidney	Liver	Brain
Control	212.4 ± 16.1^{b}	110.9 ± 2.97^{b}	5.900 ± 0.540^{b}
METH only	102.1 ± 14.9^{ac}	74.20 ± 2.76^{ac}	3.410 ± 0.500^{ac}
NACA only	180.6 ± 18.4^{b}	125.6 ± 12.0^{b}	5.310 ± 0.330^{b}
METH+NACA	162.6 ± 12.7^{ab}	95.50 ± 14.6^{abc}	5.030 ± 0.780^{b}

'a' Significantly different from the control group at $p< 0.05$
'b' Significantly different from the METH group at $p< 0.05$
'c' Significantly different from the NACA group at $p< 0.05$
All experiments were performed in quadruplet, and the values reported are Mean ± SD.

Table 2: Effects of NACA on the activities of Catalase (mU/mg protein)

Groups	Kidney	Liver	Brain
Control	1.38 ± 0.36^{b}	6.49 ± 0.46^{b}	0.750 ± 0.11^{b}
METH-only	4.19 ± 0.71^{ac}	11.3 ± 1.8^{ac}	1.38 ± 0.25^{ac}
NACA-only	1.50 ± 0.30^{b}	3.76 ± 1.3^{b}	0.600 ± 0.15^{b}
METH+NACA	2.00 ± 0.38^{b}	4.71 ± 0.54^{b}	0.900 ± 0.22^{b}

'a' Significantly different from the control group at $p< 0.05$
'b' Significantly different from the METH group at $p< 0.05$
'c' Significantly different from the NACA group at $p< 0.05$
All experiments were performed in quadruplet, and the values reported are Mean ± SD.

BIBLIOGRAPHY

Agarwal, R., Shukla, G.S., 1999. Potential role of cerebral glutathione in the maintenance of blood-brain barrier integrity in rat. Neurochem. Res., 24, 1507-1514.

Ando, Y., Zhao X., Shimoyama, H., Sakai, G., Kaneto, K., 1999. Physical properties of multiwalled carbon nanotubes. Int. J. Inorg. Mater. 1, 77-82.

Avgoustakis, K., Beletsi, A., Panagi, Z., Klepetsanis, P., Karydas, A.G., Ithakissios, D.S., 2002. PLGA-mPEG nanoparticles of cisplatin: in vitro nanoparticle degradation, in vitro drug release and in vivo drug residence in blood properties. J Control Release 79 (1-3), 123-135.

Bai, Y., Suzuki, A.K, Sagai, M., 2001. The cytotoxic effects of diesel exhaust particles on human pulmonary artery endothelial cells in vitro: role of active oxygen species. Free Radic. Biol. Med., 30, 555-562.

Banks, W.A., Ercal, N, Price, T.O., 2006. The blood-brain barrier in neuroAIDS. Curr. HIV Res., 4, 259-266.

Banerjee, A., Trueblood, M.B., Zhang, X., Manda, K., Lobo, P., Whitefield, P.D., Hagen, D.E., Ercal, N., 2009. N-acetylcysteineamide (NACA) prevents inflammation and oxidative stress in animals exposed to diesel engine exhaust, Toxicology Letters, Volume 187, Issue 3: 187-193.

Bar-Or, A., Nuttall, R.K., Duddy, M., Alter, A., Kim, H.J., Ifergan, I., Pennington, C.J., Bourgoin, P., Edwards, D.R. and Yong, V.W., 2003. Analyses of all matrix metalloproteinase members in leukocytes emphasize monocytes as major inflammatory mediators in multiple sclerosis. Brain research. 126, 2738–2749.

Beletsi, A., Leontiadis, L., Klepetsanis, P., Ithakissios, D.S., Avgoustakis, K., 1999. Effect of preparative variables on the properties of poly(dl-lactide-co-glycolide)-methoxypoly (ethyleneglycol) copolymers related to their application in controlled drug delivery. Int. J. Pharm. 182(2), 187-197.

Belghmi, K., Nicolas, J.C., Crastes de Paulet, A., 1988. Chemiluminescent assay of lipid hydroperoxides. J. Biolumin. Chemilumin., 2, 113-119.

Block, M.L., Wu, X., Pei, Z., Li, G., Wang, T., Qin, L., Wilson, B., Yang, J., Hong, J.S., Veronesi, B., 2004. Nanometer size diesel exhaust particles are selectively toxic to dopaminergic neurons: the role of microglia, phagocytosis, and NADPH oxidase. FASEB J., 18, 1618-1620.

Block, M.L., Calderón-Garcidueñas, L., 2009. Air pollution: mechanisms of neuroinflammation and CNS disease. Trends Neurosci., 32, 506-516.

Bradford, M.M., 1976. A rapid and sensitive method for the quantitation of microgram quantities of protein utilizing the principle of protein-dye binding. Anal. Biochem., 72, 248-254.

Campbell, A., Oldham, M., Becaria, A., Bondy, S.C., Meacher, D., Sioutas, C., Misra, C., Mendez, L.B., Kleinman, M., 2005. Particulate matter in polluted air may increase biomarkers of inflammation in mouse brain. Neurotoxicology, 26, 133-140.

Cheng, C., Muller, K.H., Koziol, K.K.K., Skepper, J.N., Midgley, P.A., Welland M.E., Porter A.E. 2009. Biomaterials. 30, 4152-4160.

Comporti, M., 1987. Glutathione depleting agents and lipid peroxidation. Chem. Phys. Lipids, 45, 143-169.

Dallasta, L.M., Pisarov, L.A, Esplen, J.E, Werley, J.V, Moses, A.V, Nelson, J.A., Achim, C.L., 1999. Blood-brain barrier tight junction disruption in human immunodeficiency virus-1 encephalitis. Am. J. Pathol., 155, 1915-1927.

Dean, R.T., Fu, S., Stocker, R., and Davies, M.J., 1997. Biochemistry and pathology of radical-mediated protein oxidation. Biochem J 324: 1–18.

de Boer, A.G., Gaillard, P.J., 2007. Drug targeting to the brain. Annu. Rev. Pharmacol. Toxicol. 47, 323-355.

DeLeve, L.D., Kaplowitz, N., 1991. Glutathione metabolism and its role in hepatotoxicity. Pharmacol. Ther., 52, 287-305.

Diaz-Sanchez, D., Tsien, A., Fleming, J., Saxon, A., 1997. Combined diesel exhaust particulate and ragweed allergen challenge markedly enhances human in vivo nasal ragweed-specific IgE and skews cytokine production to a T helper cell 2-type pattern. J. Immunol., 158, 2406-2413.

Dockery, D.W., Pope, C.A., Xu, X., Spengler, J.D., Ware, J.H., Fay, M.E., Ferris, B.G.J., Speizer, F.E., 1993. An association between air pollution and mortality in six U.S. cities. N. Engl. J. Med., 329, 1753-1759.

Draper, H.H., Squires, E.J., Mahmoodi, H., Wu, J., Agarwal, S., Hadley, M., 1993. A comparative evaluation of thiobarbituric acid methods for the determination of malondialdehyde in biological materials. Free Radic. Biol. Med., 15, 353-363.

Dringen, R., Gutterer, J.M., and Hirrlinger, J., 2000. Glutathione metabolism in brain. Metabolic interaction between astrocytes and neurons in the defense against reactive oxygen species. Eur. J. Biochem., 267: 4912–4916.

Elder, A., Gelein, R., Silva, V., Feikert, T., Opanashuk, L., Carter, J., Potter, R., Maynard, A., Ito, Y., Finkelstein, J., Oberdörster, G., 2006. Translocation of inhaled ultrafine manganese oxide particles to the central nervous system. Environ. Health Perspect., 114, 1172-1178.

Feazell R.P., Nakayama-Ratchford N., Dai H., Lippard S.J., 2007. Soluble single-walled carbon nanotubes as longboat delivery systems for platinum(IV) anticancer drug design. J. Am. Chem. Soc., 129 (127), 8438-8439.

Felix, M., Manna, S.K., Wise K., Barr, J., Ramesh, G.T., 2005. J. Biochem. Mol. Toxicol. 19, 67-77.

Fiala, M., Liu, Q.N., Sayre, J., Pop, V., Brahmandam, V., Graves, M.C., Vinters, H.V., 2002. Cyclooxygenase-2-positive macrophages infiltrate the Alzheimer's disease brain and damage the blood-brain barrier. Eur. J. Clin. Invest., 32, 360-371.

Foga, I.O., Nath, A, Hasinoff, B.B., Geiger, J.D., 1997. Antioxidants and dipyridamole inhibit HIV-1 gp120-induced free radical-based oxidative damage to human monocytoid cells. J. Acquir. Immune Defic. Syndr. Hum. Retrovirol., 16, 223-229.

Halliwell, B., Whiteman, M., 2004. Measuring reactive species and oxidative damage in vivo and in cell culture: how should you do it and what do the results mean? Br J Pharmacol; 142: 231–55.

Halliwell, B., 2007. Biochemistry of oxidative stress. Biochem Soc Trans 35:1147-50.

Hartz, A.M.S., Bauer, B., Block, M.L., Hong, J., Miller, D.S., 2008. Diesel exhaust particles induce oxidative stress, proinflammatory signaling, and P-glycoprotein up-regulation at the blood-brain barrier. FASEB J., 22, 2723-2733.

Hirtz, D., Thurman, D.J., Gwinn-Hardy, K., Mohamed, M., Chaudhuri, A.R., Zalutsky, R., 2007. How common are the "common" neurologic disorders?. Neurology, 68, 326-337.

Iłzecka, J., 1996. The structure and function of blood-brain barrier in ischaemic brain stroke process. Ann. Univ. Mariae Curie Sklodowska Med., 51, 123-127.

Inoue, K., Yanagisawa, R., Koike, E., Nishikawa, M., Takano, H., 2010. Repeated pulmonaryexposure to single-walled carbon nanotubes exacerbates allergic inflammation of theairway: Possible role of oxidative stress. Free Radic. Biol. Med. 48*(7)*: 924–934.

Janero, D.R., 1990. Malondialdehyde and thiobarbituric acid-reactivity as diagnostic indices of lipid peroxidation and peroxidative tissue injury. Free Radic. Biol. Med., 9, 515-540.

Jia, G., Wang, H., Yan, L., Wang, X., Pei, R., Yan, T., Zhao, Y., Guo, X., 2005. Cytotoxicity of carbon nanomaterials: single-wall nanotube, multi-wall nanotube, and fullerene. Environ. Sci. Technol. 39, 1378-1383.

Jonge, N.D., Lamy, Y., Schoots, K., Oosterkamp, T.H., 2002. High brightness electron beam from a multi-walled carbon nanotube. Nature 420, 393-395.

Kam, N.W.S., Jessop, T.C., Wender, P.A., and Dai, H., 2004. Nanotube molecular transporters: internalization of carbon nanotube-protein conjugates into mammalian cells. J.AM.CHEM.SOC. 126, 6850-6851.

Kang, S.J., Kocabas, C., Ozel, T., Shim, M., Pimparkar, N., Alam, M.A., Rotkin, S.V., Rogers J.A., 2007. High-performance electronics using dense, perfectly aligned arrays of single-walled carbon nanotubes. Nature Nanotechhnology 2, 230-236.

Kleinman, M.T., Araujo, J.A., Nel, A., Sioutas, C., Campbell, A., Cong, P.Q., Li, H., Bondy, S.C., 2008. Inhaled ultrafine particulate matter affects CNS inflammatory processes and may act via MAP kinase signaling pathways. Toxicol. Lett., 178, 127-130.

Kreuter J., 2001. Nanoparticulate systems for brain delivery of drugs. Advanced Drug Delivery Reviews 47(1), 65-81.

Kymakis, E., Amaratunga, G.A.J., 2002. Single-wall carbon nanotube/conjugated polymer photovoltaic devices. Applied Physics Letters 80 (1), 112-114.

Lehmann, A.D., Blank, F., Baum, O., Gehr, P., Rothen-Rutishauser, B.M., 2009. Diesel exhaust particles modulate the tight junction protein occludin in lung cells in vitro. Part. Fibre Toxicol., 6, 26.

Li, F., Cho, S.H., Son, D.I., Kim, T.W., Lee, S-K, Cho, Y-H, Jin, S., 2009. UV photovoltaic cells based on conjugated ZnO quantum dot/multiwalled carbon nanotube heterostructures. Appl. Phys. Lett. 94, 111906.

Li, N., Wang, M., Oberley, T.D., Sempf, J.M., Nel, A.E., 2002. Comparison of the pro-oxidative and proinflammatory effects of organic diesel exhaust particle chemicals in bronchial epithelial cells and macrophages. J. Immunol., 169, 4531-4541.

Li, N., Sioutas, C., Cho, A., Schmitz, D., Misra, C., Sempf, J., 2003. Ultrafine particulate pollutants induce oxidative stress and mitochondrial damage. Environ Health Perspect. 111:455–460.

Li, R., Ning, Z., Cui, J., Yu, F., Sioutas, C., Hsiai, T., 2010. Diesel exhaust particles modulate vascular endothelial cell permeability: implication of ZO-1 expression. Toxicol. Lett., 197, 163-168.

Li, X.Y., Gilmour, P.S, Donaldson, K., MacNee, W., 1996. Free radical activity and pro-inflammatory effects of particulate air pollution (PM10) in vivo and in vitro. Thorax, 51, 1216-1222.

Liu, C., Fan, Y.Y., Liu, M., Cong, H.T., Cheng, H.M., Dresselhaus, M.S., 1999. Hydrogen storage in single-walled carbon nanotubes at room temperature. Science 286 (5442), 1127-1129.

Long, T.C., Tajuba, J., Sama, P., Saleh, N., Swartz, C., Parker, J., Hester, S., Lowry, G.V., Veronesi, B., 2007. Nanosize titanium dioxide stimulates reactive oxygen species in brain microglia and damages neurons in vitro. Environ. Health Perspect., 115, 1631-1637.

Lovat, V., Pantarotto, D., Lagostena, L., Cacciari, B., Grandolfo, M., Righi, M., Spalluto, G., Prato, M., and Ballerini, L., 2005. Carbon nanotube substrates boost neuronal electrical signaling. Nano Lett. 5(6), 1107-1110.

Magrez, A., Kasas, S., Salicio, V., Pasquier, N., Seo, J.W., Selio, M., Catsicas, S., Schwaller, B., Forro, L., 2006. Cellular toxicity of carbon-based nanomaterials. Nano Letters 6(6), 1121-1125.

Malarkey, E.B.. and Parpura, V., 2007. Applications of carbon nanotubes in neurobiology. Neurodegener. Dis. 4(4), 292-299.

Manna, S.K., Sarkar, S., Barr, J., Wise, K., Barrera, E.V., Jejelowo, O., Rice-Ficht, A.C., Ramesh, G.T., 2005. Single-walled carbon nanotube induces oxidative stress and activates nuclear transcription factor-κB in human keratinocytes. Nano letters. 5(9): 1676-16684.

Masaki, N., Kyle, M.E., Farber, J.L.,1989. tert-butyl hydroperoxide kills cultured hepatocytes by peroxidizing membrane lipids. Arch. Biochem. Biophys., 269, 390-399.

Mayeux, R., 2003. Epidemiology of neurodegeneration. Annu. Rev. Neurosci. 26, 81-104.

Morganti-Kossmann, M.C., Rancan, M., Stahel, P.F., Kossmann, T., 2002. Inflammatory responses to traumatic brain injury: an overview for the new millennium. Immune and Inflammatory Responses in the Nervous System Oxford,. UK: University Press, UK: University Press Oxford, pp. 106–126.

Muller, J., Decordier, I., Hoet, P.H., Lombaert, N., Thomassen, L., Huaux, F., Lison, D., Kirsch-Volders, M., 2008. Clastogenic and aneugenic effects of multi-wall carbon nanotubes in epithelial cells. Carcinogenesis 29(2), 427-433.

Murray, A.R., Kisin, E., Leonard, S.S., Young S.H., Kommineni, C., Kagan, V.E., Castranova, V., Shvedova, A.A., 2009. Oxidative stress and inflammatory response in dermal toxicity of single-walled carbon nanotubes. Toxicology. 257, 161-171.

Nel, A.E., Diaz-Sanchez, D., Ng, D., Hiura, T., Saxon, A., 1998. Enhancement of allergic inflammation by the interaction between diesel exhaust particles and the immune system. J. Allergy Clin. Immunol., 102, 539-554.

Oberdörster, G., Oberdörster, E., Oberdörster, J., 2005. Nanotoxicology: an emerging discipline evolving from studies of ultrafine particles. Environ. Health Perspect., 113, 823-839.

Oberdörster, G., Sharp, Z, Atudorei, V, Elder, A, Gelein, R, Kreyling, W., Cox, C., 2004. Translocation of inhaled ultrafine particles to the brain. Inhal Toxicol, 16, 437-445.

Oberdörster, G., Sharp, Z., Atudorei, V., Elder, A., Gelein, R., Lunts, A., Kreyling, W., Cox, C., 2002. Extrapulmonary translocation of ultrafine carbon particles following whole-body inhalation exposure of rats. J. Toxicol. Environ. Health A, 65, 1531-1543.

Pancrazio J.J., 2008. Neural interfaces at the nanoscale. Nanomedicine 3(6), 823-830.

Pantarotto, D., Briand, J., Prato, M., Bianco, A. Chem., Commun. 2004, 1, 16-17.

Penugonda, S., Mare, S, Goldstein, G, Banks, W.A., Ercal, N., 2005. Effects of N-acetylcysteine amide (NACA), a novel thiol antioxidant against glutamate-induced cytotoxicity in neuronal cell line PC12. Brain Res., 1056, 132-138.

Persidsky, Y., Stins, M, Way, D, Witte, M.H, Weinand, M, Kim, K.S, Bock, P, Gendelman, H.E., Fiala, M., 1997. A model for monocyte migration through the blood-brain barrier during HIV-1 encephalitis. J. Immunol., 158, 3499-3510.

Peters, A., Veronesi, B., Calderon-Garciduenas, L., Gehr, P., Chen, L.C., Geiser, M., Reed, W., Rothen-Rutishauser, B., Schurch, S., and Schulz, H.,2006. Particle and Fibre Toxico. 3: 13.

Peters, A., Veronesi, B., Calderón-Garcidueñas, L., Gehr, P., Chen, L.C., Geiser, M., Reed, W., Rothen-Rutishauser, B., Schürch, S., Schulz, H., 2006. Translocation and potential neurological effects of fine and ultrafine particles a critical update. Part. Fibre Toxicol., 3, 13.

Plateel, M., Dehouck, M.P, Torpier, G., Cecchelli, R., Teissier, E., 1995. Hypoxia increases the susceptibility to oxidant stress and the permeability of the blood-brain barrier endothelial cell monolayer. J. Neurochem., 65, 2138-2145.

Pope, C.A., Thun, M.J, Namboodiri, M.M., Dockery, D.W., Evans, J.S., Speizer, F.E., Heath, C.W.J., 1995. Particulate air pollution as a predictor of mortality in a prospective study of U.S. adults. Am. J. Respir. Crit. Care Med., 151, 669-674.

Pardridge, W.M., 1997. Drug delivery to the brain. J. Cereb. Blood Flow Metab., **17:** 713–731.

Pardridge, W.M., 1988. Recent advances in blood–brain barrier transport. Annu. Rev. Pharmacol. Toxicol., 28: 25–39.

Pulskamp, K., Worle-Knirsch, J.M., Hennrich, F., Kern, K., Krug, H.F., 2007. Human lung epithelial cells show biphasic oxidative burst after single-walled carbon nanotube contact. Carbon. 45: 2241-2249.

Pulskamp, K., Diabate, S., Harald, F., Krug, H.F. 2007. Carbon nanotubes show no sign of acute toxicity but induce intracellular reactive oxygen species in dependence on contaminants. Toxicol. Lett. 168:58-74.

Ridnour, L.A., Winters, R.A., Ercal, N., Spitz, D.R., 1999. Measurement of glutathione, glutathione disulfide, and other thiols in mammalian cell and tissue homogenates using high-performance liquid chromatography separation of N-(1-pyrenyl)maleimide derivatives. Methods Enzymol., 299, 258-267.

Riggio C., Ciofani G., Raffa V., Cuschieri A., Micera S., 2009. Combination of polymer technology and carbon nanotube array for the development of an effective drug delivery system at cellular level. Nanoscale Res. Lett. 4, 668-673.

Sarnat, J.A., Schwartz, J., Suh, H.H., 2001. Fine particulate air pollution and mortality in 20 U.S. cities. N. Engl. J. Med, 344, 1253-1254.

Schrand A.M., Dai L., Schlager J.J., Hussain S.M., Osawa E., 2007. Differential biocompatibility of carbon nanotubes and nanodiamonds. Diamond Relat. Mater. 16(12), 2118-2123.

Sharma, C.S., Sarkar, S., Periyakaruppan, A., Barr, J., Wise, K., Thomas, R., Wilson, B.L., Ramesn, G.T., 2007. Single-walled carbon nanotubes induced oxidative stress in rat lung epithelial cells. J Nanosci Nanotechnol. 7(7): 2466-2472.

Singh R., Lillard J.W. Jr., 2009. Nanoparticle-based targeted drug delivery. Experimental and Molecular Pathology 86(3), 215-223.

Sugamata, M., Ihara, T., Takano, H., Oshio, S., Takeda, K., 2006. Maternal Diesel Exhaust Exposure Damages Newborn Murine Brains. J. Health Sci., 52, 82-84.

Sun, Y. P., Fu, K. F., Lin, Y., Huang, W. J., 2002. Functionalized Carbon Nanotubes: Properties and Applications. Acc. Chem. Res., 35, 1096– 1104.

Tayarani, I., Chaudiere, J, Lefauconnier, J.M., Bourre, J.M., 1987. Enzymatic protection against peroxidative damage in isolated brain capillaries. J. Neurochem., 48, 1399-1402.

Thornalley, P.J., Trotta, R.J., Stern, A., 1983. Free radical involvement in the oxidative phenomena induced by tert-butyl hydroperoxide in erythrocytes. Biochim. Biophys. Acta, 759, 16-22.

Tian, F., Cui D., Schwarz, H., Estrada, G.G., Kobayashi, H., 2006. Cytotoxicity of single-wall carbon nanotubes on human fibroblasts. Toxicology in Vitro 20, 1202-1212.

Tansey, M.G., McCoy, M.K., Frank-Cannon, T.C., 2007. Neuroinflammatory mechanisms in Parkinson's disease: Potential environmental triggers, pathways, and targets for early therapeutic intervention, Experimental Neurology, Volume 208, 1: 1-25.

Tsai, Y.C., Li, S.C., Chen, J.M., 2005. Cast thin film biosensor design based on a nafion backbone, a multiwalled carbon nanotube conduit, and a glucose oxidase function. Langmuir 21(8), 3653-3658.

Veronesi, B., Makwana, O, Pooler, M., Chen, L.C., 2005. Effects of subchronic exposures to concentrated ambient particles. VII. Degeneration of dopaminergic neurons in Apo E-/- mice. Inhal. Toxicol., 17, 235-241.

Vouk, V.B., Piver, W.T., 1983. Metallic elements in fossil fuel combustion products: amounts and form of emissions and evaluation of carcinogenicity and mutagenicity. Environ. Health Perspect., 47, 201-225.

Wang, H., Joseph, J.A., 1999. Quantifying cellular oxidative stress by dichlorofluorescein assay using microplate reader. Free Radic. Biol. Med., 27, 612-616.

Xiao, G.G., Wang, M., Li, N., Loo, J.A., Nel, A.E., 2003. Use of proteomics to demonstrate a hierarchical oxidative stress response to diesel exhaust particle chemicals in a macrophage cell line. J. Biol. Chem., 278, 50781-50790.

Yamamoto, B.K., Zhu, W., 1998. The effects of methamphetamine on the production of free radicals and oxidative stress. J. Pharmacol. Exp. Ther., 287, 107-114.

Yang, S., Guo, W., Lin, Y., Deng, X., Wang, H., Sun, H., Liu, Y., Wang, X., Wang, W., Chen, M., Huang, Y., Sun, Y., 2007. Biodistribution of pristine sing-walled carbon nanotubes in vivo. J. Phys. Chem. C 111(48), 17761-17764.

Yang, Z., Zhang, Y., Yang, Y., Sun, L., Han, D., Li, H., Wang, C., 2010. Pharmacological and toxicological target organelles and safe use of single-walled carbon nanotubes as drug carriers in treating Alzheimer disease. Nanomed. 6(3), 427-441.

Zhou, Y.M., Zhong, C.Y., Kennedy, I.M., Leppert, V.J., Pinkerton, K.E., 2002. Toxicol. Appl. Pharmacol. 2003. 190, 157-169.

Zhang, X., Banerjee, A, Banks, W.A., Ercal, N., 2009. N-Acetylcysteine amide protects against methamphetamine-induced oxidative stress and neurotoxicity in immortalized human brain endothelial cells. Brain Res., 1275, 87-95.

VITA

Xinsheng Zhang was born on August 6th, 1977, in Hutubi, Xinjiang province, P.R China. He received his Bachelor of Medicine degree (MD) in Clinical Medicine, School of Medicine, Shihezi University, Shihezi, Xinjiang, P.R.China in 2001, and his Master of Science Degree in Pharmacology, School of Pharmaceutical Science, Shihezi University, Shihezi, Xinjiang, P.R.China in 2005. He worked as a lecturer in the Department of Pharmacology, Shihezi University from 2001 to 2005. In August 2006, he came to United States and enrolled in Department of Chemistry pursing his Ph.D. degree at the Missouri University of Science & Technology (formerly known University of Missouri-Rolla).